2006-02-02

Characterization, Functionalization and Applications of Alkyl Monolayers on Silicon Surfaces

Guilin Jiang
Brigham Young University - Provo

CHARACTERIZATION, FUNCTIONALIZATION AND APPLICATIONS OF ALKYL MONOLAYERS ON SILICON SURFACES

by

Guilin Jiang

A dissertation submitted to the faculty of

Brigham Young University

in partial fulfillment of the requirements for the degree of

Doctor of Philosophy

Department of Chemistry and Biochemistry

Brigham Young University

April 2006

BRIGHAM YOUNG UNIVERSITY

GRADUATE COMMITTEE APROVAL

of a dissertation submitted by

Guilin Jiang

This dissertation has been read by each member of the following graduate committee and by majority vote has been found to be satisfactory.

Date	Matthew R. Linford, Chair
Date	Milton L. Lee
Date	Paul B. Farnsworth
Date	Robert C. Davis
Date	Calvin H. Bartholomew

BRIGHAM YOUNG UNIVERSITY

As chair of the candidate's graduate committee, I have read the dissertation of Guilin Jiang in its final form and have found that (1) its format, citations, and bibliographical style are consistent and acceptable and fulfill university and department style requirements; (2) its illustrative materials including figures, tables, and charts are in place; and (3) the final manuscript is satisfactory to the graduate committee and is ready for submission to the university library.

_____ _____

Date

Matthew R. Linford
Chair, Graduate Committee

Accepted for the Department

_____

David V. Dearden
Graduate Coordinator

Accepted for the College

_____

Thomas W. Sederberg
Associate Dean, College of Physical and Mathematical Sciences

ABSTRACT

CHARACTERIZATION, FUNCTIONALIZATION AND APPLICATIONS OF ALKYL MONOLAYERS ON SILICON SURFACES

Guilin Jiang

Department of Chemistry and Biochemistry

Doctor of Philosophy

Investigations were performed on the stability, mechanism of formation and an application of alkyl monolayers chemomechanically prepared on silicon surfaces. A new method of surface modification, laser-activation modification of surfaces (LAMS), and multivariate analyses of time-of-flight secondary ion mass spectrometry (ToF-SIMS) images of LAMS spots were also reported.

X-ray photoelectron spectroscopy (XPS) and other data show that alkyl monolayers prepared by scribing silicon under 1-iodoalkanes and 1-alkenes were stable over extended periods of time to air, water, a boiling acid and Al Kα X-rays. The stability is attributed to direct Si-C bonding in the monolayers. The observation that the oxygen signals gradually increased and the iodine signals gradually decreased, with both finally reaching plateaus is attributed to the oxidation of exposed silicon by scribing, and the hydrolysis of Si-I bonds, respectively. In alkyl monolayers prepared with 1-alcohols, the

carbon signals decreased about 50% after two 1-h immersions in a boiling acid, suggesting unstable Si-O bonding.

In the analogous experiment of grinding silicon with alkyl halides, the expected free-radical combination and disproportionation byproducts were observed. This observation provides evidence for the mechanism previously proposed for alkyl monolayer formation on silicon by chemomechanically scribing.

Miniaturized sample supports for matrix-assisted laser desorption/ionization mass spectrometry (MALDI-MS) were made on hydrophobic silicon or glass surfaces by scribing. With these sample supports, improved MALDI-MS signal intensities and reproducibilities were achieved for a test peptide, as expected.

A new and promising method for surface modification, LAMS, was developed. XPS and ToF-SIMS analyses show that both silicon and germanium were effectively modified by LAMS with even quite inert compounds. This technique was also used to make miniaturized MALDI-MS sample supports. Compared to scribing, LAMS is faster and can be more precisely controlled.

Multivariate analyses, automated expert spectral image analysis (AXSIA) and principal component analysis (PCA), were used in interpreting ToF-SIMS images of silicon surfaces modified with 1-alkenes by LAMS. Both analyses show that modified and unmodified areas are chemically different.

ACKNOWLEDGEMENTS

This dissertation is completed under the guidance of Dr. Matthew R. Linford, my advisor, and with assistance from my graduate committee members and many other people. I would like to take this opportunity to express my deep gratitude to all of them.

First of all, I thank Dr. Matthew R. Linford for his guidance, encouragements and patience on my research and study. His help has driven me to overcome difficulties in my research and my life.

It's my honor to have Dr. Milton L. Lee, Dr. Paul B. Farnsworth, Dr. Robert C. Davis and Dr. Calvin H. Bartholomew as my graduate committee members. I sincerely appreciate their advice, suggestions, critiques and revisions to my research and this dissertation.

I also thank Dr. Craig D. Thulin, and Katie Southwick in his group, Dr. Matthew C. Asplund, Dr. Bonnie J. Tyler and Dr. Vincent S. Smentkowski for their help in my research. I thank all my colleagues, especially Dr. Travis L. Niederhauser, Yit-Yian Lua, Michael V. Lee and Li Yang. I always feel happy to work together with them.

My wife always gives me strong support and my lovely children always make me happy; care and love from my parents and sisters make me strong.

Finally, I would thank Brigham Young University, especially the Department of Chemistry and Biochemistry for offering me financial support for my graduate study.

TABLE OF CONTENTS

LIST OF FIGURES

− CHAPTER I −

INTRODUCTION

I.1 GENERAL SILICON SURFACE MODIFICATION BY ALKYL MONOLAYERS

In the past half century, silicon has played a key role in the rapid development of semiconductor and microelectronics technologies. In these areas, silicon's physical and electronic properties are of primary concern. However, because silicon reactions are important in a number of the semiconductor processing steps, and silicon surfaces have a different structure from bulk silicon and high reactivity, interest in understanding the chemical properties of silicon surfaces has also continued. Though silicon surfaces are usually passivated, either overnight degassing at high temperature or Ar^+ sputtering under ultra high vacuum at room temperature can remove their native oxide layers to produce the bare silicon surfaces. The radicals or dangling bonds on the bare silicon surfaces typically interact to form the Si(100)-2 × 1 or Si(111)-7 × 7 reconstruction.[1] These reconstructed surfaces are still very reactive because of their strained geometry and unsaturated bonding. When they are exposed in the air, oxygen molecules attack these silicon surfaces and a native silicon dioxide layer of *ca.* 15 Å gradually grows on the fresh silicon surfaces and eventually passivates them. Much thicker oxide layers can be grown onto silicon surfaces by thermo-oxidation methods used in the semiconductor industry. In the presence of reactive organic molecules, alkyl monolayers may also grow onto the reconstructed silicon surfaces based on direct Si-C bonding via free-radical mechanisms. Because of the broad range of choices in organic chemical functionalities,

the alkyl monolayers formed on silicon surfaces may then provide specific interfacial characteristics needed in many areas, such as microarray technology.[2]

Though silicon chemistry has a long history and the silicon-oxygen backbone based organic silicon compounds (silicones) are widely used, direct silicon surface functionalization by alkyl monolayers can only be tracked back to around a decade ago. In 1993, Linford and coworkers first reported that alkyl monolayers could covalently bond to hydrogen-terminated silicon surfaces.[3] Densely packed alkyl monolayers on silicon surfaces were prepared by heating the hydrogen-terminated planar silicon(100) or silicon(111) with diacyl peroxides to 90-100 °C for 1 h in a nitrogen/argon atmosphere. Stability tests of the alkyl monolayers suggested that the major linkage was through direct Si-C bonding, while approximately 30% of the monolayer that was removed under hydrolytic conditions was probably bound through Si-O bonding. A radical mechanism was proposed for alkyl monolayer formation on silicon surfaces. That is, diacyl peroxides underwent pyrolysis to produce alkyl radicals, which readily attacked surface Si-H bonds to form alkyl monolayers on silicon surfaces, as well as alkane molecules. The alkyl monolayers formed on silicon surfaces demonstrated high stability, even under some harsh conditions, such as boiling acids and bases, and concentrated aqueous HF.

Linford and coworkers subsequently reported that stable alkyl monolayers on silicon surfaces could also be prepared from 1-alkenes and 1-alkynes either by the same radical mechanism in the presence of peroxide initiators, where the monolayers were from both the 1-alkenes/1-alkynes and the initiators, or by thermal initiation.[4,5] By radical initiation, a mixture of a diacyl peroxide (10%, by weight) and an 1-alkene or 1-alkyne (90%) was first heated to 70 °C under vacuum until the diacyl peroxide fully dissolved. A

freshly prepared hydrogen-terminated silicon(111) chip and the mixture were then heated to 100 °C for 1 h in an argon environment. Alkyl monolayers on silicon surfaces made by thermal initiation were prepared by heating a degassed 1-alkene/1-alkyne together with freshly etched hydrogen-terminated silicon(111) or silicon(100) under an inert environment up to 200 °C for 1-2 h.

Meanwhile, many other methods that are usually used in organic syntheses were reported for growing alkyl monolayers on silicon surfaces. Alkyl Grignard, alkyllithium, and alkylmagnesium bromide reagents were used in preparing alkyl monolayers on silicon surfaces.[7-17] Hydrogen-terminated silicon was found to react with alkyl Grignard or alkyllithium reagents and form alkyl monolayers on the silicon surface at room temperature. While halogen-terminated silicon surfaces, made by chlorination or bromination of hydrogen-terminated silicon(111), were found to be alkylated by alkyl Grinard or alkyllithium reagents at 60-80 °C. Boukherroub and Buriak also reported Lewis acid-catalyzed alkene/alkyne monolayer formation on silicon surfaces.[8,18,19] By catalysis with Lewis acids $AlCl_3$, $EtAlCl_2$ or BH_3·THF, they prepared alkyl monolayers on hydrogen-terminated porous silicon surfaces at room temperature, or on planar hydrogen-terminated silicon(111) surfaces at 100 °C. In general, alkyl monolayer formation on silicon surfaces with an organometallic reagent or a Lewis acid required long times and/or heating. In addition, by further functionalizing alkyl monolayers, Wagner and Cicero prepared bioreactive alkyl monolayers on silicon(111) surfaces.[20,21] Terminal methyl groups of alkyl monolayers on silicon were functionalized by photo-induced chlorosulfonation, followed by a sulfonamide formation with primary or secondary amine groups, indicating the possibility of conjugating biomolecules on silicon

surfaces. Electrochemical grafting was also used in growing alkyl/aryl monolayers on silicon surfaces.[22-25] When hydrogen-terminated silicon was exposed to an alkyl/aryl halide or an alkyne containing solution, upon application of a current to the solution, dense alkyl/aryl monolayers grew on silicon surfaces at room temperature. For alkynes, cathodic electrochemical grafting or negative bias produced monolayers without reduction of C≡C bonds, while anodic electrochemical grafting or positive bias led to formation of reduced monolayers on silicon surfaces. As a common method for inducing radical reactions, UV irradiation was used to prepare alkyl monolayers on hydrogen-terminated planar silicon surfaces.[26-31] In the presence of an 1-alkene or 1-alkyne, irradiating a hydrogen-terminated planar silicon surface with a UV light (wavelength between 185-385 nm) resulted in formation of an alkyl monolayer on the silicon surface in hours, usually at room temperature, the longer the UV light wavelength, the longer the reaction time plus a slight increase in temperature. White light (wavelength 400-600 nm) was also found to induce alkyl monolayer formation on hydrogen-terminated porous silicon surfaces that were photoluminescent and wet with an alkene or alkyne.[32,33] In all the methods mentioned above, hydrogen-terminated silicon surfaces were required, because weak Si-H bonds easily broke when attacked by free radicals.[34]

Reconstructed Si(100)- 2 × 1 surfaces are extremely reactive as mentioned, and in general, only exist in a UHV environment. Under UHV conditions, alkenes, alkynes, dienes, alkyl halides and other organic compounds containing functional groups reacted easily with reconstructed silicon surfaces to form alkyl monolayers.[2] Scanning tunneling microscopy (STM) was usually used to observe those monolayers on silicon surfaces. The STM tip was also used to induce alkyl monolayer formation on hydrogen-terminated

silicon surfaces.[2] The tunneling current on the STM tip breaks Si-H bonds at room temperature under UHV and causes a reaction between silicon and an alkene on areas where the STM tip was scanned.

I.2 A NON-CONVENTIONAL METHOD: PREPARING ALKYL MONOLAYERS ON SILICON SURFACES BY CHEMOMECHANICALLY SCRIBING

Recently, Linford and coworkers developed a simple and effective technique for preparing alkyl monolayers on silicon surfaces, chemomechanically grinding/scribing silicon with reactive organic compounds.[35-44] Grinding/scribing was suggested to break Si-Si bonds and produce radicals, which instantaneously initiated alkyl monolayer formation on silicon surfaces.

In 2000 Linford first reported that alkyl monolayers could be chemomechanically formed on silicon particle surfaces, where silicon substrates were not hydrogen-terminated.[35] Instead of using sophisticated chemical or physical methods, Linford used a mechanical method, grinding silicon with 1-hexadecene, to bypass the inert silicon oxide layer, break Si-Si bonds and create reactive silicon dangling bonds or radicals, and form alkyl monolayers on silicon particle surfaces, all in one step. Obviously, that was a simple and effective way to functionalize silicon surfaces with alkyl monolayers. However, grinding is not applicable to planar silicon surfaces. To chemomechanically functionalize planar silicon surfaces, Niederhauser and coworkers in the Linford group at Brigham Young University developed an analogous method, scribing silicon surfaces in the presence of reactive organic compounds, to prepare alkyl monolayers on silicon surfaces (see Figure I.1).[36] Similar to grinding, mechanical scribing removes the

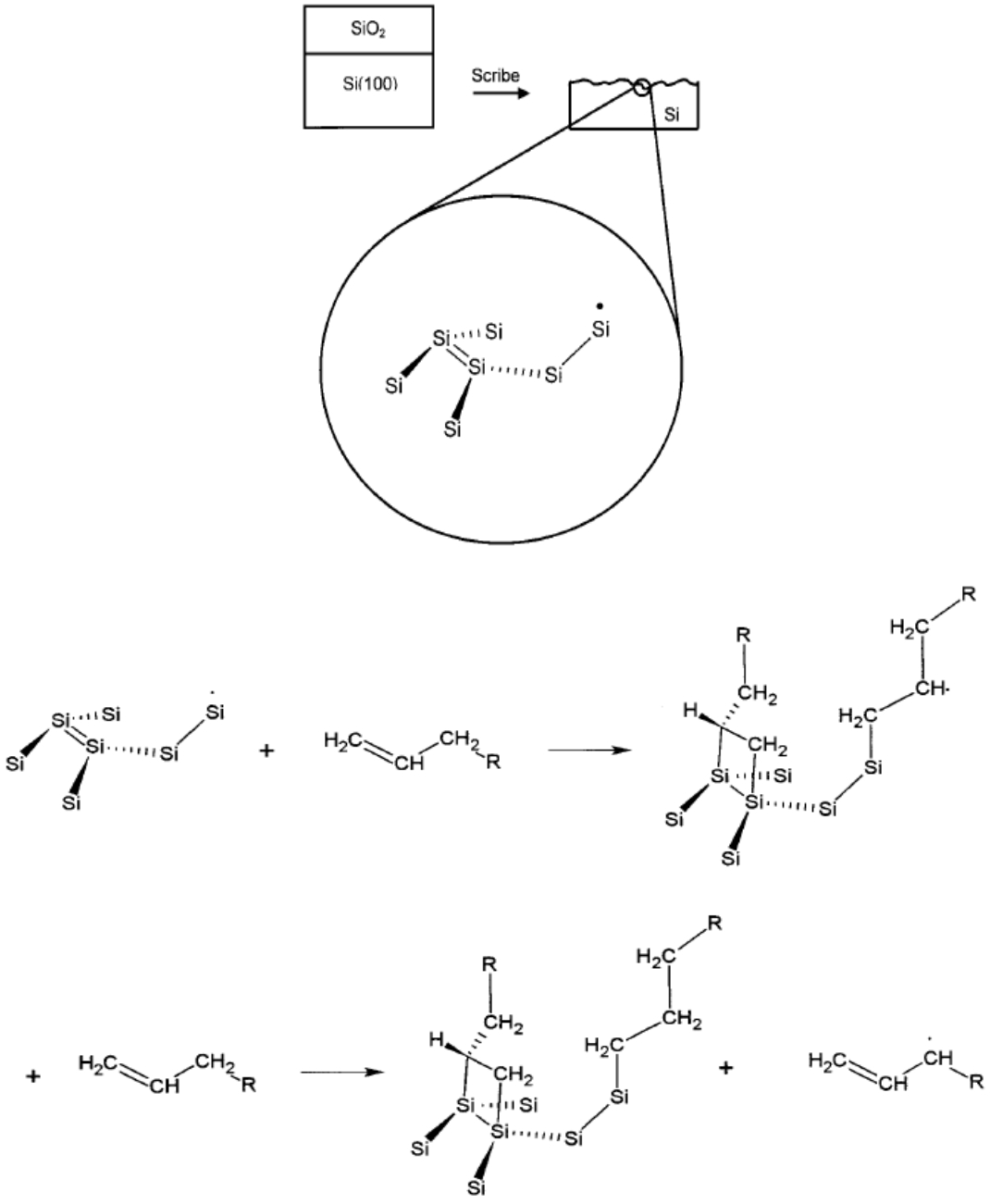

Figure I.1. Scribing silicon to produce reactive species at fracture surfaces and possible reactions of reactive species on scribed silicon with a 1-alkene. (Reproduced with permission from *Langmuir* 2001, *17*, 5889-5900. Copyright 2001 Am. Chem. Soc.)

passivation layer and is believed to create reactive species, dangling bonds and reconstructed Si=Si dimers, on a planar silicon surface. In the presence of a 1-alkene, alkyl monolayers can be formed on silicon surfaces either through dangling bonds attacking C=C bonds, or through a formal [2 + 2] cycloaddition of C=C bonds to silicon dimers. A diamond tip driven by either a scribing apparatus (see Figure I.2) developed by the Linford group, or a commercially available computer numerical controlled (CNC) milling machine was used to scribe silicon. The home-built scribing apparatus basically consists of three computer controlled orthogonally mounted translation stages that drive the diamond tip over a sample holder. The diamond tip was spring-loaded and attached to the Z-stage. The force applied to the diamond tip can be adjusted through the compression of the spring. With a new diamond tip, ~10 μm thick lines can be drawn on silicon surfaces. Patterns of patches, corrals, circles and other features can be scribed with sizes from several centimeters to ~200 μm. The experiments of scribing silicon with reactive compounds were generally performed in an open laboratory without degassing or otherwise specially treating the compounds. A piece of a clean silicon wafer was first wet with a reactive organic compound, and then a pattern was scribed on the wet area and thereby functionalized with alkyl monolayers.

With the chemomechanical scribing technique, Niederhauser and coworkers then successfully prepared alkyl monolayers on silicon surfaces with a wide variety of organic compounds, such as 1-alkenes,[36,37] 1-alkynes,[36] alcohols,[37] alkyl halides,[36,38] epoxides,[39] aldehydes,[40] acid chlorides,[41] and even gas phase compounds.[42] Wetting a silicon wafer with a gas phase compound was realized by keeping the silicon wafer in an atmosphere of the gas phase compound. Figure I.3 shows water droplets held in a pattern of corrals

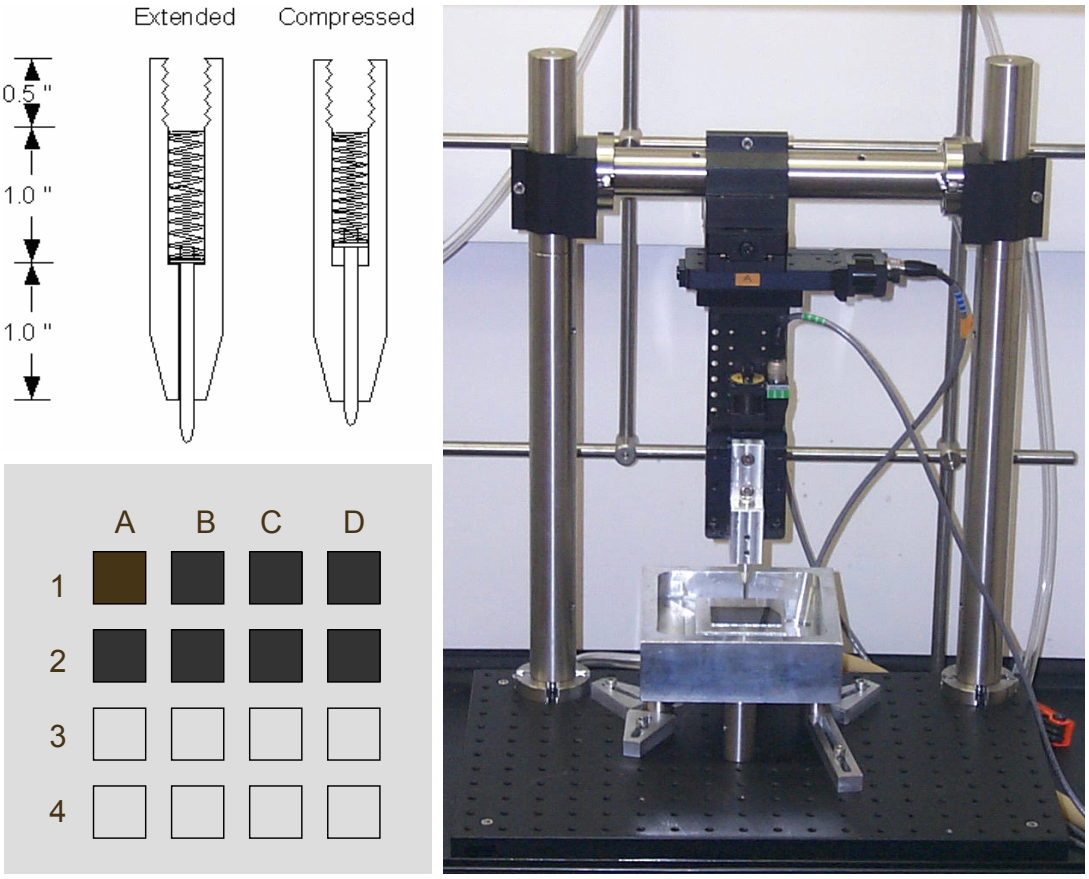

Figure I.2. The scribing apparatus developed in the Linford group, its diamond tip construction (upper left) and features that could be scribed on silicon surfaces with the apparatus.

Figure I.3. Water droplets held in a set of 28 hydrophobic corrals produced by scribing silicon(100) in the presence of 1-hexadecene. (Reprint with permission from *Langmuir* **2001**, *17*, 5889-5900. Copyright 2001 Am. Chem. Soc.)

scribed on a piece of silicon.[36] The corrals were scribed on the silicon surface in the presence of 1-hexadecene. The silicon surface was hydrophilic after cleaning. The corrals' capability of holding water droplets indicates that the sidelines of the corrals were hydrophobic because of alkyl monolayers grown on them. The XPS spectra of scribed areas on the silicon surface (Figure I.4) provide further support for silicon surface modification with alkyl monolayers by scribing.[36] Silicon scribed in the air, and then wet with 1-dodecene shows a very small carbon signal and a significant oxygen signal (Figure I.4a). On the other hand, silicon scribed while wet by 1-dodecene or 1-octyne shows significant carbon signals as well as much lower oxygen signals (Figure I.4b, c). These data indicate that the detected carbon signals were not from 1-dodecene or 1-octyne by physical adsorption, but from covalently bonded alkyl monolayers on scribed silicon surfaces. In addition, as shown in Figure I.5, both the XPS C1s/Si2p ratios and water contact angles of scribed areas increased while O1s/Si2p ratios decreased with increasing 1-alkene chain lengths.[37] That is, the longer the 1-alkene chain length, the thicker the alkyl monolayers on silicon surfaces that were obtained, and the better the protection to silicon surfaces from oxidation while they were exposed in the air.

While scribing silicon surfaces with a diamond tip is facile, it results in rough surfaces. To chemomechanically prepare alkyl monolayers on a smooth silicon surface, Lua and coworkers used a tungsten carbide ball instead of a diamond tip for scribing.[43] Compared to sharp and hard diamond tips, tungsten carbide balls are smooth and somewhat softer. When a carefully controlled, gentle force was applied to the tungsten carbide ball, it only broke weak Si-H bonds and created functionalized, smooth areas on hydrogen-terminated silicon surfaces.

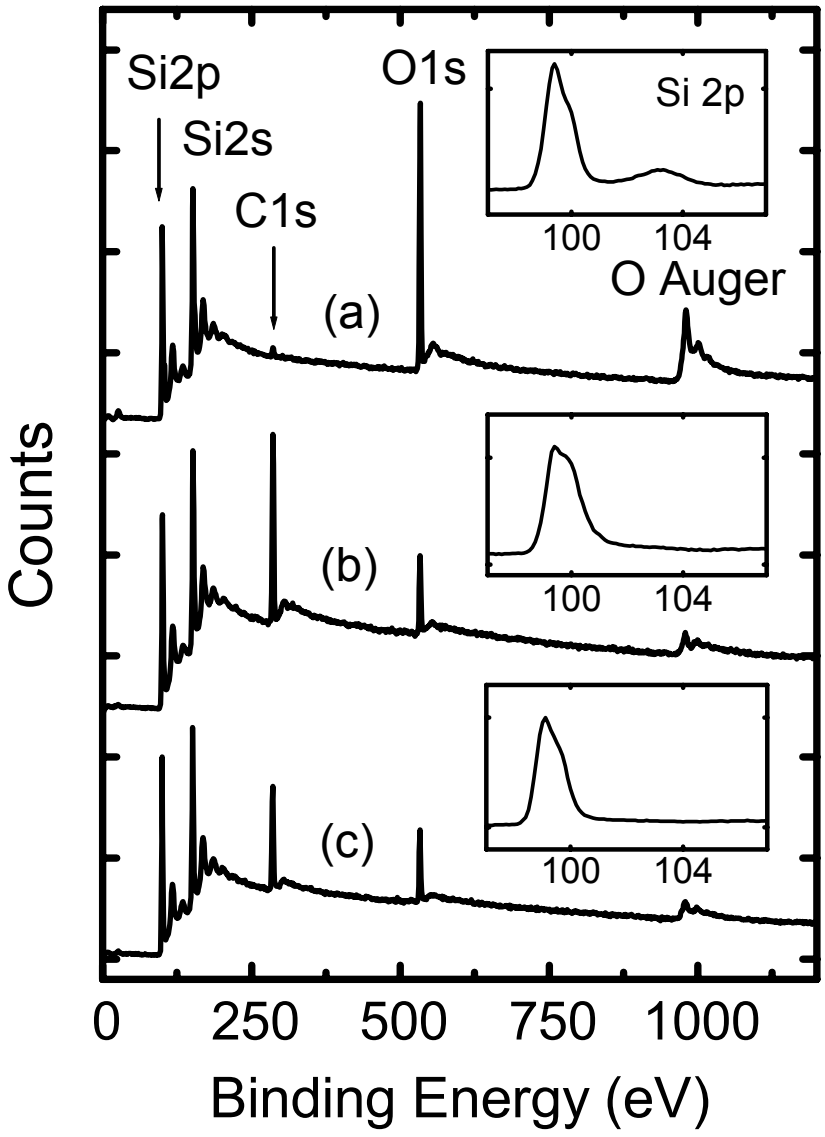

Figure I.4. XPS spectra of silicon: (a) scribed in the air and then wet with 1-dodecene; (b) scribed while wet by 1-dodecene; and (c) scribed while wet by 1-octyne. (Reprint with permission from *Langmuir* **2001**, *17*, 5889-5900. Copyright 2001 Am. Chem. Soc.)

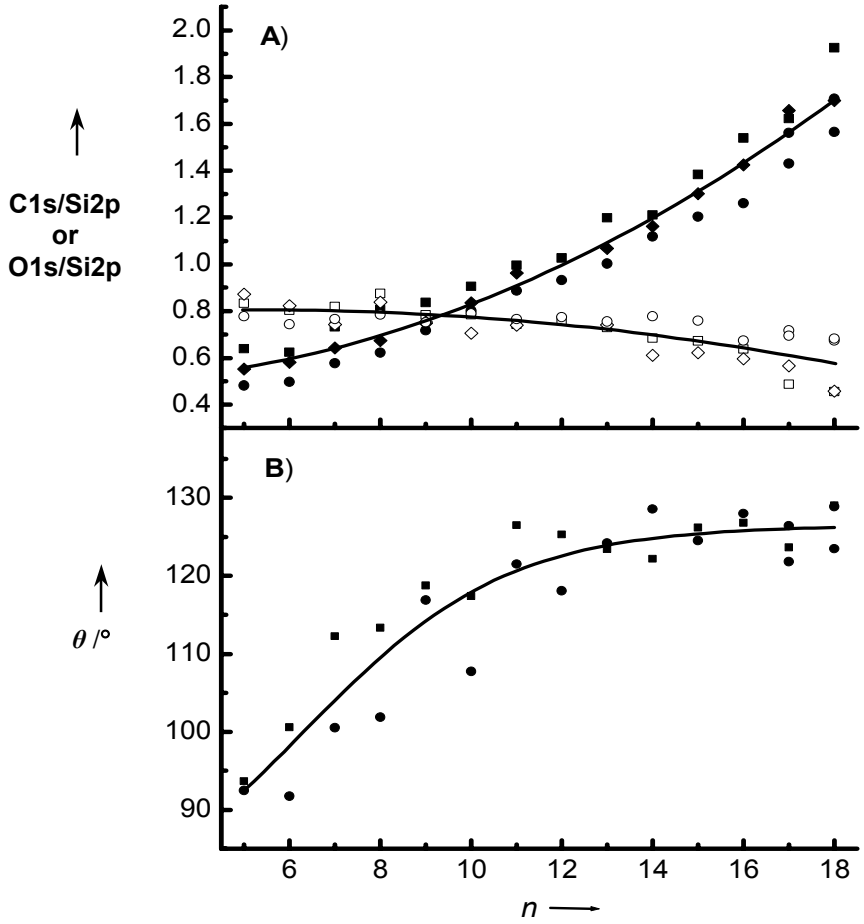

Figure I.5. XPS (C1s/Si2p: solid symbols; O1s/Si2p: open symbols) and water contact angle measurements (θ) from arrays of patches prepared from 1-alkenes of different chain lengths (n). (Reprint with permission from *Angew. Chem. Int. Ed.* **2002**, *41*(13), 2353-2356. Copyright WILEY-VCH Verlag GmbH, 69451 Weinheim, Germany, 2002)

A recent development of the chemomechanical scribing technique was using an atomic force microscope (AFM) probe to scribe nano-scale features on hydrogen-terminated silicon(111) surfaces in the presence of reactive organic compounds.[44] Silicon surfaces were wet by a 1-alkene or 1-octanol in an AFM fluid cell and then scribed by the AFM probe. Because of the extremely small size of AFM probes and only very gentle forces applied on them, features in the range of 30-100 nm were created on silicon surfaces. This development makes the chemomechanical scribing technique a useful tool in nano science and technology, such as nanoshaving[45] and nanografting.[46-49]

As mentioned, silicon surface modification with alkyl monolayers aims to provide specific interfacial characteristics for different technological areas. Thus, it is critical that alkyl monolayers be stable under different environments for further manipulations. Linford and coworkers reported that alkyl monolayers formed on silicon surfaces by free-radical initiation were very stable to long exposures to the air, boiling $CHCl_3$, boiling H_2O, boiling acidic and basic solutions, and hydrofluoric acid.[4] Sieval and Sung reported alkyl monolayers formed on silicon surfaces by thermal initiation were stable at temperatures up to 615 K in vacuum.[5,6] The stability of those alkyl monolayers on silicon surfaces was attributed to direct Si-C bonding between alkyl monolayers and silicon. Similarly, the stability of alkyl monolayers formed on silicon surfaces by chemomechanically scribing was also investigated[50] and is reported in Chapter II of this dissertation.

A free-radical mechanism was suggested for the alkyl monolayer formation on silicon surfaces by chemomechanically scribing.[38] As mentioned above, while there are many different approaches to prepare alkyl monolayers on silicon surfaces, very similar

free-radical reaction mechanisms were proposed for alkyl monolayer formation on silicon surfaces, where an activated silicon surface was a prerequisite.[3,51] Once generated, reactive silicon dangling bonds and reconstructed silicon dimers on silicon surfaces initiated the reaction between silicon and the compound that had functional groups in the immediate vicinity. Thus, almost all alkyl monolayers formed on silicon surfaces were through direct Si-C bonding. However, no direct evidence for free-radical intermediates in these proposed reactions was ever given. For the method of chemomechanically scribing, in the case of preparing alkyl monolayers on silicon surfaces from 1-haloalkanes, the suggested mechanism was that, by scribing, Si-Si bonds were broken to produce silicon dangling bonds, Si·:

$$Si\cdot + XCH_2(CH_2)_{n-1}H \rightarrow Si\text{-}X + \cdot CH_2(CH_2)_{n-1}H \quad (1)$$

$$Si\cdot + \cdot CH_2(CH_2)_{n-1}H \rightarrow Si\text{-}CH_2(CH_2)_{n-1}H \quad (2)$$

If this mechanism was correct, then the combination and/or disproportionation byproduct(s) of the free alkyl radical $\cdot CH_2(CH_2)_{n-1}H$ could also be present if not every free-radical diffused back to the surface. If observed, such species would provide evidence for the mechanism (1)-(2). Chapter III reports the observation of these species.[52]

As for applications, Lua and Owen reported the selective deposition of DNA and nanoparticles on hydrophobic corrals that were chemomechanically scribed on silicon surfaces.[43,53] When a DNA or nano-particle solution was dispensed onto the corrals, the charged DNA and the nano-particles selectively deposited onto bare or polyelectrolyte coated hydrophilic silicon surfaces, instead of alkyl monolayer modified, hydrophobic

corral sidelines. Zilch also reported an application of mechanical scribing in microcontact printing.[54] Silicon surfaces with thin features made by scribing were used as masters for stamps. However, this work was not related to alkyl monolayer functionalization of silicon surfaces. Chapter IV reports an application of chemomechanical scribing of silicon/glass surfaces in matrix-assisted laser desorption/ionization mass spectrometry (MALDI-MS).[55] Miniaturized sample supports for MALDI-MS were scribed on silicon or glass surfaces for improved signal intensity and reproducibility.

I.3 A NEW SURFACE MODIFICATION TECHNIQUE: LASER-ACTIVATION MODIFICATION OF SURFACES (LAMS)

Surface modification and surface patterning continue to be topics of much interest in research and in industry. Thus a wide variety of methods have been developed and studied. Except for the methods for the silicon surface modification already mentioned above, surfaces can also be modified by photolithography,[56] e-beam lithography,[57] microcontact printing,[58] and dip pen nanolithography.[59] In photolithography, light plays the central role. Light was also used to induce monolayer formation on and/or pattern hydrogen-terminated,[28,31,32,60-62] iodine-terminated,[63] and porous silicon.[64,65] In these latter reports, the exposure time to light ranged from a few minutes up to a few hours, where 30 minutes was typical. Chapter V reports a new surface modification technique, laser-activation modification of surfaces (LAMS), in which laser pulses were used to generate reactive species on surfaces and induce surface modification.

LAMS modified surfaces were then characterized by XPS and Time-of-flight secondary ion mass spectrometry (ToF-SIMS). As is well known, ToF-SIMS is a

powerful tool for surface analysis. Secondary ion spectra, secondary ion images or depth profiles can be easily acquired. However, unlike XPS spectra, ToF-SIMS spectra contain immense amounts of information. With typical, conventional data analysis methods, only a few characteristic peaks would be selected and compared from sample to sample. This approach usually works well for known samples. However, it runs the risk of missing important information for unknown samples since the majority of sample data is wasted. Instead, multivariate data analysis methods, such as principal component analysis (PCA) used in ToF-SIMS spectral data analysis, exploit the majority of spectral data to avoid possibly missing important information contained in the data set.[66] Similarly, automated expert spectral image analysis (AXSIA) used in ToF-SIMS image data analysis, extracts information from the mean ion image that is reconstructed from the ToF-SIMS total ion image of a sample, instead of analyzing some selected individual ion images.[67] Chapter VI reports multivaritate analyses on ToF-SIMS images of LAMS modified silicon surfaces using a series of 1-alkenes.

I.4 REFERENCES

(1) Hamers, R. J. and Wang Y. *Chem. Rev.* **1996**, *96*, 1261.

(2) Buriak, J. M. *Chem. Rev.* **2002**, *102*, 1271.

(3) Linford, M. R.; Chidsey, C. E. D. *J. Am. Chem. Soc.* **1993**, *115*(26), 12631.

(4) Linford, M. R.; Fenter, P.; Eisenberger, P. M.; Chidsey, C. E. D. *J. Am. Chem. Soc.* **1995**, *117*(11), 3145.

(5) Sieval, A. B.; Demirel, A. L.; Nissink, J. W. M.; Linford, M. R.; van der Maas, J. H.; de Jeu, W. H.; Zuilhof, H.; Sudhölter, E. J. R. *Langumir* **1998**, *14*, 1759.

(6) Sung, M. M.; Kluth, J.; Yauw, O. W.; Maboudian, R. *Langmuir* **1997**, *13*, 6164.

(7) Bansal, A.; Li, X.; Lauermann, I.; Lewis, N. S.; Yi, S. I.; Weinberg, W. H. *J. Am. Chem. Soc.* **1996**, *118*, 7225.

(8) Boukherroub, R.; Morin, S.; Bensebaa, F.; Wayner, D. D. M. *Langmuir* **1999**, *15*, 3831.

(9) Viellard, C.; Warntjes, M.; Ozanam, F.; Chazalviel, J.-N. *Proc. Electrochem. Soc.* **1996**, *95*(25), 250.

(10) Ozanam, F.; Vieillard, C.; Warntjes, M.; Dubois, T.; Pauly, M.; Chazalviel, J. N. *Can. J. Chem. Eng.* **1998**, *76*, 1020.

(11) Fide´lis, A.; Ozanam, F.; Chazalviel, J.-N. *Surf. Sci.* **2000**, *444*, L7.

(12) Song, J. H.; Sailor, M. J. *J. Am. Chem. Soc.* **1998**, *120*, 2376.

(13) Song, J. H.; Sailor, M. J. *Inorg. Chem.* **1999**, *38*, 1498.

(14) Kim, N. Y.; Laibinis, P. E. *J. Am. Chem. Soc.* **1999**, *121*, 7162.

(15) Kim, N. Y.; Laibinis, P. E. *J. Am. Chem. Soc.* **1998**, *120*, 4516.

(16) Royea, W. J.; Juang, A.; Lewis, N. S. *Appl. Phys. Lett.* **2000**, *77*, 1988.

(17) He, J.; Patitsas, S. N.; Preston, K. F.; Wolkow, R. A.; Wayner, D. D. M. *Chem. Phys. Lett.* **1998**, *286*, 508.

(18) Buriak, J. M.; Allen, M. J. *J. Am. Chem. Soc.* **1998**, *120*, 1339.

(19) Buriak, J. M.; Stewart, M. J.; Geders, T. W.; Allen, M. J.; Choi, H. C.; Smith, J.; Raftery, M. D.; Canham, L. T. *J. Am. Chem. Soc.* **1999**, 1*21*, 11491.

(20) Wagner, P.; Nock, S.; Spudich, J. A.; Volkmuth, W. D.; Chu, S.; Cicero, R. L.; Wade, C. P.; Linford, M. R.; Chidsey, C. E. D. *J. Struct. Biol.* **1997**, *119*(2), 189.

(21) Cicero, R. L.; Wagner, P.; Linford, M. R.; Hawker, C. J.; Waymouth, R. M.; Chidsey, C. E. D. *Polym. Prepr.* **1997**, *38*(1), 904.

(22) Yang, C. S.; Kauzlarich, S. M.; Wang, Y. C. *Chem. Mater.* **1999**, *11*, 3666.

(23) Henry de Villeneuve, C.; Pinson, J.; Bernard, M. C.; Allongue, P. *J. Phys. Chem. B* **1997**, *101*, 2415.

(24) Gurtner, C.; Wun, A. W.; Sailor, M. J. *Angew. Chem., Int. Ed.* **1999**, *38*, 1966.

(25) Robins, E. G.; Stewart, M. P.; Buriak, J. M. *Chem. Commun.* **1999**, 2479.

(26) Terry, J.; Linford, M. R.; Wigren, C.; Cao, R.; Pianetta, P.; Chidsey, C. E. D. *Appl. Phys. Lett.* **1997**, *71*(8), 1056.

(27) Terry, J.; Linford, M. R.; Wigren, C.; Cao, R.; Pianetta, P.; Chidsey, C. E. D. *J. Appl. Phys.* **1999**, *85*(1), 213.

(28) Effenberger F.; Go¨tz, G.; Bidlingmaier, B.; Wezstein, M. *Angew. Chem., Int. Ed.* **1998**, *37*, 2462.

(29) Burkhard, C. A.; Krieble, R. H. *J. Am. Chem. Soc.* **1947**, *69*, 2687.

(30) Cicero, R. L.; Linford, M. R.; Chidsey, C. E. D. *Langmuir* **2000**, *16*(13), 5688.

(31) Wojtyk, J. T. C.; Tomietto, M.; Boukherroub, R.; Wayner, D. D. M. *J. Am. Chem. Soc.* **2001**, *123*, 1535.

(32) Stewart, M. P.; Buriak, J. M. *Angew. Chem., Int. Ed.* **1998**, *37*, 3257.

(33) Stewart, M. P.; Buriak, J. M. *J. Am. Chem. Soc.* **2001**, *123*, 7821.

(34) Kanabus-Kaminska, J. M.; Hawari, J. A.; Griller, D.; Chatgilialoglu, C. *J. Am. Chem. Soc.* **1987**, *109*, 5267.

(35) Linford, M. R. U.S. Patent 6,132,801, 2000.

(36) Niederhauser, T. L.; Jiang, G.; Lua, Y.-Y.; Dorff, M. J.; Woolley, A. T.; Asplund, M. C.; Berges, D. A.; Linford, M. R. *Langmuir* **2001**, *17*, 5889.

(37) Niederhauser, T. L.; Lua, Y.-Y.; Jiang, G.; Davis, S. D.; Matheson, R.; Hess, D. A.; Mowat, I. A.; Linford, M. R. *Angew. Chem. Int. Ed.* **2002**, *41*(13), 2353.

(38) Niederhauser, T. L.; Lua, Y.-Y.; Sun, Y.; Jiang, G.; Strossman, G. S.; Pianetta, P.; Linford, M. R. *Chem. Mater.* **2002**, *14*, 27.

(39) Lua, Y.-Y.; Lee, M. V.; Fillmore, W. J. J.; Matheson, R.; Sathyapalan, A.; Asplund, M. C.; Fleming, S. A.; Linford, M. R. *Angew. Chem. Int. Ed.* **2003**, *42*. 4046.

(40) Lua, Y.-Y.; Fillmore, W. J. J.; Linford, M. R. *Appl. Surf. Sci.* **2004**, *231-232*, 323.

(41) Lua, Y.-Y.; Fillmore, W. J. J.; Yang, Li; Lee, M. V.; Savage, P. B.; Asplund, M. C.; Linford, M. R. *Langmuir* **2005**, *21*(6); 2093.

(42) Lee, M. V.; Linford, M. R. *Accepted by Appl. Phy. Lett.* **2005**.

(43) Lua, Y.-Y.; Niederhauser, T. L.; Wacaser, B. A.; Mowat, I. A.; Woolley, A. T.; Davis, R. C.; Fishman, H. A.; Linford, M. R. *Langmuir* **2003**, *19*(4), 985.

(44) Wacaser, B. A.; Maughan, M. J.; Mowat, I. A.; Niederhauser, T. L.; Linford, M. R.; Davis, R. C. *Appl. Phys. Lett.* **2003**, *82*(5), 808.

(45) Xu, S. and Liu, G.-Yu. *Langmuir* **1997**, *13*, 127.

(46) Xu, S.; Miller, S.; Laibinis, P. E.; Liu, G.-Yu. *Langmuir* **1999**, *15*, 7244.

(47) Schwartz, P. V. *Langmuir* **2001**, *17*, 5971.

(48) Liu, J.-Fu; Cruchon-Dupeyrat, S.; Garno, J. C.; Frommer, J.; Liu, G.-Yu. *Nano Lett.* **2002**, *2*, 937.

(49) Lee, M. V.; Davis, R. C.; Linford, M. R. *Accepted by J. of Nano. Sci. & Nano. Tech.*

(50) Jiang, G.; Niederhauser, T. L.; Davis, S. D.; Lua, Y.-Y.; Cannon, B. R.; Dorff, M. J.; Howell, L. L.; Magleby, S. P.; Linford, M. R. *Coll. Surf. A* **2003**, 226, 9.

(51) Bronikowski, M. J.; Hamers, R. J. *J. Vac. Sci. Technol. A* **1995**, *13*, 777.

(52) Jiang, G.; Niederhauser, T. L.; Fleming, S. A.; Asplund, M. C.; Linford, M. R. *Langmuir* **2004**, *20*(5), 1772.

(53) Owen, J. I.; Niederhauser, T. L.; Wacaser, B. A.; Christenson, M. P.; Davis, R. C.; Linford, M. R. *Lab on a chip* **2004**, *4*, 553.

(54) Zilch, L. W.; Husseini, G. A.; Lua, Y.-Y.; Lee, M. V.; Gertsch, K. R.; Cannon, B. R.; Perry, R. M.; Sevy, E. T.; Asplund, M. C.; Woolley, A. T.; Linford, M. R. *Rev. Sci. Instr.* **2004**, *75*(9), 3065.

(55) Linford, M. R.; Davis, R. C.; Magleby, S. P.; Howell, L. L.; Jiang, G.; Thulin, C. D. *Nanolithography and Pattering Techniques in Microelectronics. Chapter 4.* Woodhead Publishing, 2005.

(56) Brodie, I.; Murray, J.; Muray, J. J. *The Physics of Microfabrication*; Plenum, 1982.

(57) Sheats, J. R.; Smith, B. W. *Microlithography: Science and Technology*; Marcel Dekker: New York, 1998.

(58) Xia, Y.; Whitesides, G. M. *Annu. Rev. Mater. Sci.* **1998**, *28*, 153.

(59) Piner, R. D.; Zhu, J.; Xu, F.; Hong, S.; Mirkin, C. A. *Science* **1999**, *283*, 661.

(60) Linford, Stanford University **1996**.

(61) Sieval, A. B.; Linke, R.; Zuilhof, H.; Sudhölter, E. J. R. *Adv. Mater.* **2000**, *12*, 1457.

(62) Eves, B. J.; Sun, Q.-Y.; Lopinski, G. P.; Zuilhof, H. *J. Am. Chem. Soc.* **2004**, *126*(44), 14318.

(63) Cai, W.; Lin, Z.; Strother, T.; Smith, L. M.; Hamers, R. J. *J. Phys. Chem. B* **2002**, *106*, 2656.

(64) Lee, E. J.; Ha, J. S.; Sailor, M. J. *J. Am. Chem. Soc.* **1995**, *117*, 8295.

(65) Lee, E. J.; Bitner, T. W.; Ha, J. S.; Shane, M. J.; Sailor, M. J. *J. Am. Chem. Soc.* **1996**, *118*, 5375.

(66) Li, Y; Lua, Y.-Y.; Jiang, G.; Tyler, B. J.; Linford, M. R. *Anal. Chem.* **2005**, *77*, 4654.

(67) Smentkowski, V. S.; Keenan, M. R.; Ohlhausen, J. A.; Kotula, P. G. *Anal. Chem.* **2005**, *77*, 1530.

The major sections of the following chapters have been previously published. Permissions to include them in this dissertation have been granted by the corresponding publishers.

Chapter II: Reproduced with permission from STABILITY OF ALKYL MONOLAYERS ON CHEMOMECHANICALLY SCRIBED SILICON TO AIR, WATER, HOT ACID, AND X-RAYS. Jiang, G.; et al. *Colloids and Surfaces A: Physicochem. Eng. Aspects* **2003**, *226*, 9-16. Copyright 2003 Elsevier.

Chapter III: Reproduced with permission from EVIDENCE FOR A RADICAL MECHANISM IN MONOLAYER FORMATION ON SILICON GROUND (OR SCRIBED) IN THE PRESENCE OF ALKYL HALIDES. Jiang, G.; et al. *Langmuir* **2004**, *20*, 1772-1774. Copyright 2004 American Chemical Society.

Chapter IV: Reproduced with permission from NANOLITHOGRAPHY AND PATTERNING TECHNIQUES IN MICROELECTRONICS. CHAPTER 4: CHEMOMECHANICAL SURFACE MODIFICATION OF MATERIALS FOR PATTERINING. Copyright Woodhead Publishing 2005.

– CHAPTER II –

STABILITY OF ALKYL MONOLAYERS ON CHEMOMECHANICALLY SCRIBED SILICON TO AIR, WATER, HOT ACID, AND X-RAYS

II.1 INTRODUCTION

The Linford group recently reported a facile, new method of modifying and patterning silicon, which essentially consists of scribing silicon after it has been wet with a reactive compound (a scribing liquid).[1-8] It is believed that this new technique is an enabling technology for surface modification and patterning that will find wide application. Diamond tips, tungsten carbide balls, or atomic force microscopy (AFM) probes used in this process penetrate through silicon's native oxide layer[1,3,4,6] or layer of hydrogen passivation,[5,7] to chemically activate silicon, which then reacts with 1-alkene,[1,6,7] 1-alkyne,[1,6] 1-haloalkane,[1,4,6] alcohol,[3] and epoxide[2] scribing liquids to produce alkyl monolayers on silicon surfaces. The fact that monolayer formation occurs in the air suggests that scribing liquids react with the surface more quickly than oxygen can diffuse to it.[1,4] With this new technique, hydrophobic corrals on silicon were prepared, *i.e.*, checkerboard patterns of hydrophobic lines on a more hydrophilic background.[1,5] The hydrophobic corrals held droplets of water and liquids of lower surface tensions,[1,4,5] and their interior surfaces were selectively functionalized with polyelectrolyte multilayers and other materials.[1,5] It is anticipated that the hydrophobic corrals will prove useful in optimizing surface reactions and in studying adsorption events in a combinatorial fashion.

The incorporation of a new material into a device requires an understanding of its stability to the conditions it will be exposed to. Earlier reports contained a few preliminary results of the stability of monolayers on scribed silicon. It was found that after the hydrophobic corrals, prepared from 1-hexadecene, were extracted with hot *m*-xylene in a Soxhlet apparatus overnight and then immersed in boiling water for an hour, they still held droplets of water.[1] It was also observed that the C1s/Si2p ratios of X-ray photoelectron spectroscopy (XPS) and the water contact angles of monolayers on scribed silicon prepared from 1-decene remained nearly constant after immersion in boiling 0.1 M H_2SO_4 for 1 h; while under identical conditions monolayers prepared from 1-decanol lost carbon and their water contact angles decreased significantly.[3] It was hypothesized that monolayers derived from 1-alkenes were tethered to the surface through robust Si-C bonds, but that those derived from alcohols were primarily tethered through hydrolysable Si-O bonds.[1,3] An increase in the O1s/Si2p XPS ratios in stability tests for monolayers prepared from 1-decene, 1-decanol, and from mixtures of these two liquids was also observed. This result suggested oxidation of the silicon substrate.

Here initial studies were substantially extended by addressing the important issues of a) the long-term stability of alkyl monolayers, b) the kinetics of silicon (substrate) oxidation and halogen loss in the presence of air and water, c) the kinetics of the decrease in hydrophobic corral water capacity, and d) the stability of alkyl monolayers to boiling, aqueous H_2SO_4, and X-rays. While not every monolayer was subjected to every test, taken together the data form a composite picture of monolayer stability. Alkyl monolayers prepared from 1-alkenes and 1-haloalkanes were extremely stable to all of the conditions studied here, including the hot acid, but monolayers prepared from

alcohols were less so. Following monolayer formation, oxidation of the underlying silicon substrate took place, which appeared to decrease the water capacity of hydrophobic corrals, but generally not to the point that they ceased to be useful devices. Al Kα X-rays from the X-ray photoelectron spectrometer did not noticeably damage alkyl monolayers. Steric hindrance and/or hydrophobic effects appeared to influence the degree of surface oxidation and halogen loss – the iodine XPS signals from silicon scribed under 1-iodoalkanes decreased with time, but even after substantial exposures to the air or water, some iodine remained. A unifying theme throughout this chapter aiding in the comparison of results was the use of the parameter β, which was an XPS approximation of the ratio of the oxide layer thickness to the monolayer thickness. Substrate oxidation of monolayers produced with 1-haloalkanes appeared to proceed more quickly in the air than in water, and substrate oxidation appeared to take place more rapidly for silicon scribed under 1-haloalkanes than 1-alkenes.

As before, all samples were made with a computer-controlled, diamond-tipped apparatus in the air with scribing liquids that had not been degassed or specially treated in any way.[1] Tools used to monitor the monolayer stability were XPS and hydrophobic corral water capacity, which was measured in a semi-automated fashion using a Gilson 215 liquid handler.

II.2 EXPERIMENTAL SECTION

II.2.1 Materials

1-Pentene (99%), 1-octene (98%), 1-decene (98%), 1-hexadecene (92%), 1-chlorooctane (99%), 1-bromopentane (99%), 1,4-dibromobutane (99%), 1-iodopentane

(98%), and 1-iododecane (98%), were obtained from Aldrich. Methyl iodide (99.8%), 1-Butanol (99.9%), and 1-octanol (Certified) were obtained from Fisher. All reagents were used as received. Acetone was reagent grade. Water was obtained from a Millipore Milli-Q water system. Silicon(100) wafers (p-boron, 1-100 Ω cm, test grade) were obtained from TTI Silicon (Sunnyvale, CA).

II.2.2 Sample Preparation and Handling

All sample preparations were done in the air at room temperature with compounds that had not been degassed. The patches of 1-iodoalkane or 1-alkene monolayers were 8 mm × 8 mm. Silicon wafers were cleaned by immersing them in ~50:50 (v/v) H_2O_2 (30%): NH_4OH (conc.) (*Caution: This solution is caustic and should be handled with great care!*) for ~45 min at room temperature, followed by rinsing with copious amounts of water, and then drying with a jet of nitrogen. The dry wafers were then wet with a reactive compound, and scribed with the diamond-tipped computer-controlled scribing apparatus. To make patches on silicon surfaces, the diamond tip was driven back and forth, producing lines 30 μm apart in one direction, and then the identical pattern was repeated in a direction perpendicular to the original scribing direction. After this process no unscribed silicon remained in a patch. Sets of hydrophobic corrals (5 mm × 5 mm) were made by wetting a clean, dry silicon wafer with a reactive compound and scribing 6 parallel lines, 5 mm apart, in one direction followed by 6 parallel lines in the perpendicular direction. After scribing, samples were rinsed with acetone followed by water, cleaned with a soft artist's brush using a 2% sodium dodecyl sulfate solution, then rinsed again with copious amounts of water, and finally dried with a jet of nitrogen. After

every exposure to the air or water, samples were similarly cleaned with a soft artist's brush using a 2% sodium dodecyl sulfate solution and rinsed with copious amounts of water and dried prior to analysis.

II.2.3 Corral Water Capacity Measurements

Corral water capacity measurements were made with a Gilson 215 Liquid Handler controlled by a Visual Basic computer program written in the Linford group. The program allows a user to position the tip of a thin (~0.70 mm) needle from the Gilson Liquid Handler slightly (~1.5 mm) above the level of the surface of silicon at approximately the center of a hydrophobic corral. After allowing needle positioning, the Gilson instrument dispenses 0.5 μL of water per second from the needle into the corral. When water from the drop overruns the boundaries of the corral, the user hits a key on the keyboard to stop the addition of water. The computer then returns the value of the total quantity of water added to the corral. Each corral was a square: 5 mm × 5 mm. For each 5 × 5 pattern of 25 corrals, the water capacities of 5 corrals along one of the diagonals were measured from which a mean datum was calculated for a given exposure time.

II.2.4 Other Instrumentation

X-ray photoelectron spectroscopy (XPS) (SSX-100, Surface Science Instrument) was performed with a monochromatic Al Kα X-ray source. The instrument was regularly calibrated to the Au $4f_{7/2}$ peak at 84.0 eV. The power at the X-ray anode was ~200 W and the nominal spot size of the X-ray during stability tests was 800 μm × 1000 μm, although

the actual spot size was probably larger. Calculations of the number of oxygen or iodine atoms per alkyl chain ignored attenuation of photoelectrons in the alkyl monolayer. XPS peak areas used to calculate ratios were obtained using the XPS instrument software.

II.2.5 Estimation of the Oxide Thickness Using XPS Data

The system was modeled as a monolayer (ML) of alkyl chains of thickness t_{ML} on a layer of oxide (SiO_2, abbreviated ox) of thickness t_{ox} on a flat silicon substrate. The attenuation of photoelectrons was not take into account because the thin film and oxide layer probably have a combined thickness of about 15 Å, which was not large compared to the mean free path of C1s and O1s photoelectrons in a hydrocarbon monolayer.[9] Effects of substrate roughness were also ignored. For a given area, A, on the surface, the volumes occupied by the monolayer and the oxide layer were $V_i = At_i$, where i = ML or ox. The masses of these volumes were $g_i = \rho_i V_i$, where ρ_i is the density of the material. ρ_{ML} was taken as 0.90 g/cm^3, slightly below the density of low-density polyethylene (*ca.* 0.92 g/cm^3), but above that of a hydrocarbon liquid (*ca.* 0.80 g/cm^3). ρ_{ox} was taken as the density of quartz (2.33 g/cm^3).[10] It was then assumed that the monolayer was entirely composed of CH_2 units, *i.e.*, the molecular weight of the monolayer (MW_{ML}) was taken as 14 g/mol. MW_{ox} was taken as the molecular weight of SiO_2 (60.085 g/mol). g_i was divided by MW_i to obtain the number of moles of carbon (mol_C) and oxygen (mol_O) in the monolayer and oxide layer, respectively. Next, mol_C was divided by mol_O to obtain:

$$\frac{mol_C}{mol_O} = \frac{\frac{\rho_{ML} A t_{ML}}{MW_{ML}}}{2\frac{\rho_{ox} A t_{ox}}{MW_{ox}}} \qquad (1)$$

where the factor of 2 appears because there are two oxygen atoms per SiO_2 unit. It was recognized that the ratio of the corrected areas of the XPS narrow scans of C1s and O1s, C_{XPS}/O_{XPS}, was mol_C/mol_O. Thus it was found:

$$t_{ox} = \left(\frac{O_{XPS}\rho_{ML}MW_{ox}}{2\,C_{XPS}\rho_{ox}MW_{ML}} \right) t_{ML} = \beta\, t_{ML} \qquad (2)$$

where $\beta = \frac{O_{XPS}\rho_{ML}MW_{ox}}{2\,C_{XPS}\rho_{ox}MW_{ML}}$. Thus, if assuming a reasonable value for the thickness of the monolayer, t_{ML}, an estimate for the thickness of the silicon oxide layer, $t_{ox,}$ can be obtained. A formula for estimating the thickness of monolayers on hydrogen-terminated silicon has previously been published.[11]

II.2.6 Finite Element Analysis

Finite element analysis was performed as described elsewhere.[1,12] Briefly, all calculations were carried out with the Surface Evolver program using 71.99 mN/m and 0.9970 g/cm^3 for its surface tension and density of water, respectively.[10] The program was written by K. A. Brakke as part of the Geometry Supercomputing Project (now the Geometry Center), sponsored by the National Science Foundation, the Department of Energy, Minnesota Technology, and the University of Minnesota. The source code is written in C and runs on many systems. Surface Evolver and documentation are available free of charge on the Internet at http://www.geom.umn.edu/software/evolver/.

II.2.7 Data Analysis

Data in Figures II.2, II.3 and II.5 were fit to single exponential curves using Origin 6 or 7.

II.3 RESULTS AND DISCUSSION

II.3.1 Monolayer Stability in Air

Figure II.1 shows four X-ray photoelectron survey spectra and accompanying Si2p narrow scans of monolayers prepared by scribing silicon under 1-iododecane and analyzed a) immediately, and after b) 20 h, c) 45 h and d) 70 h of exposure to the air. The spectrum taken immediately after sample preparation (Figure II.1a) contains a strong C1s peak, a weaker O1s peak, prominent iodine peaks (I3d and 4d), and very little chemically shifted Si2p signal at ~103 eV due to silicon oxide[13] (see inset to Figure II.1a). However, after exposure to the air, XPS spectra exhibited notable differences from the original spectrum, including (1) a decrease in the iodine signals, (2) an increase in the O1s peak intensity, and (3) an increase in the amount of oxidized silicon at ~103 eV in the Si2p narrow scan (Figure II.2b, c, d and the right shoulders of the Si2p peaks in the insets). In all spectra the C1s to Si2p area ratios stayed essentially constant. These results can be rationalized in terms of the previously proposed alkyl monolayer formation model for 1-haloalkanes on scribed silicon. That is, a silicon radical on the scribed silicon surface homolytically abstracts a halogen atom from a 1-haloalkane and thus the resulting alkyl radical may diffuse back to the surface to form a silicon-carbon bond with another silicon radical.[4] Si-I bonds formed during scribing should be subject to hydrolysis, which is limited by steric hindrance from the monolayer, and by monolayer hydrophobicity.

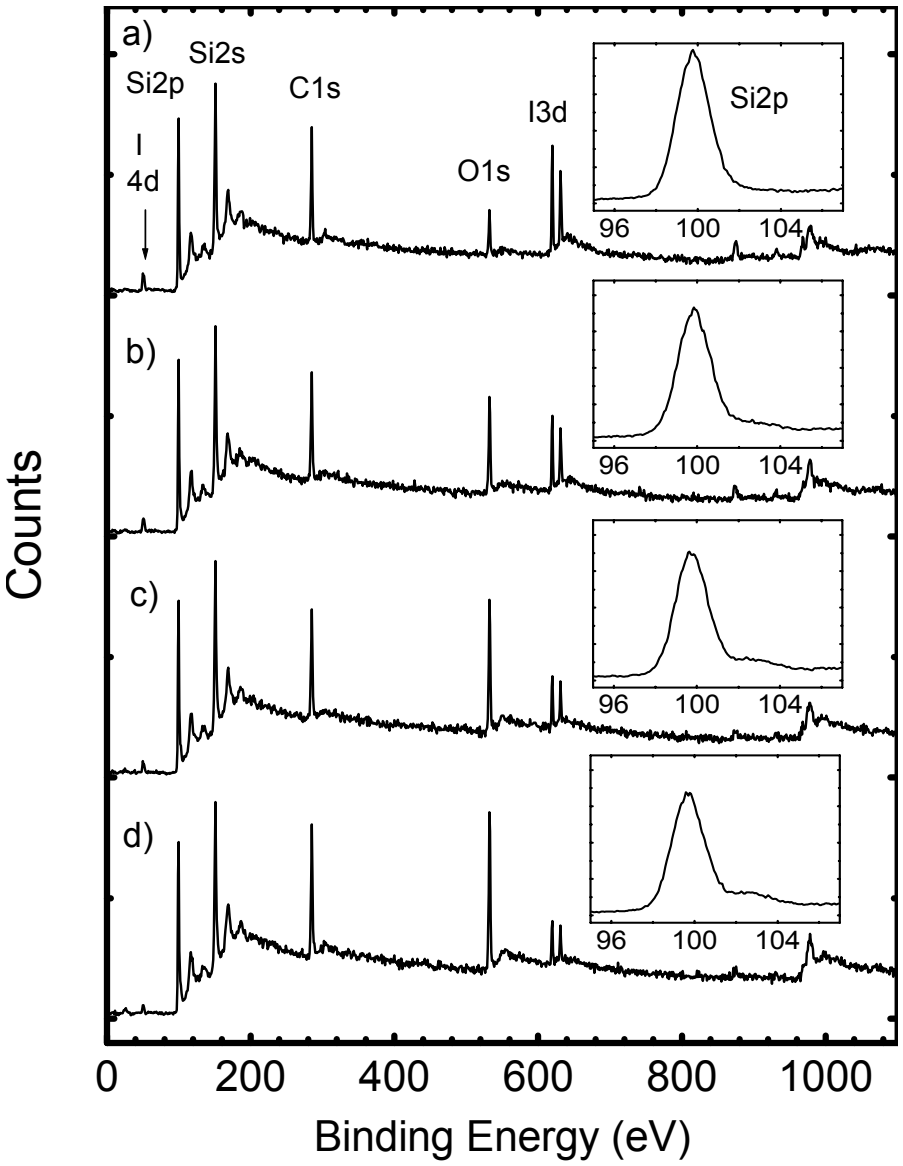

Figure II.1. X-ray photoelectron spectra of silicon scribed in the presence of 1-iododecane and kept in the air for: (a) 0 h, (b) 20 h, (c) 45 h, and (d) 70 h.

However, Si-C bonds are robust and not easily hydrolyzed, so the nearly constant C1s signal is not unexpected.

To better understand the kinetics of oxidation and iodine loss in monolayers of 1-iododecane on scribed silicon, peak areas from XPS narrow scans of oxygen, carbon, and iodine vs. silicon were measured and plotted as a function of exposure time (Figure II.2). As expected, O1s/Si2p ratios increased with time and I3d/Si2p ratios decreased. However, even after extensive exposures to the air, the surface still contained some iodine; initially and after ~200 h, the I3d/Si2p data points in Figure II.2 corresponded to approximately 0.6 and 0.1 iodine atoms/alkyl chain, respectively. XPS also shows approximately 2 oxygen atoms per alkyl chain on the surface initially. After ~200 h there were approximately 7. These data, and the presence of oxide (at ~103 eV) in the Si2p narrow scans in Figure II.1 indicate that surface oxidation was not simply a result of iodine hydrolysis. The fact that some iodine atoms remained even after extended periods of time suggests that there were different environments for chemisorbed surface iodine that had varying degrees of steric hindrance and hydrophobicity. The small increase in the XPS C1s/Si2p ratio was attributed to the surface contamination by adventitious carbon.

II.3.2 Monolayer Stability in Water

Both the hydrolysable nature of the Si-I moiety and the ability of hydrophobic corrals to hold aqueous solutions make them important to study the stability of the scribed monolayer patches and the hydrophobic corrals in water. Figure II.3 shows the O1s/Si2p and I3d/Si2p XPS ratios, the β-values and the hydrophobic corral water

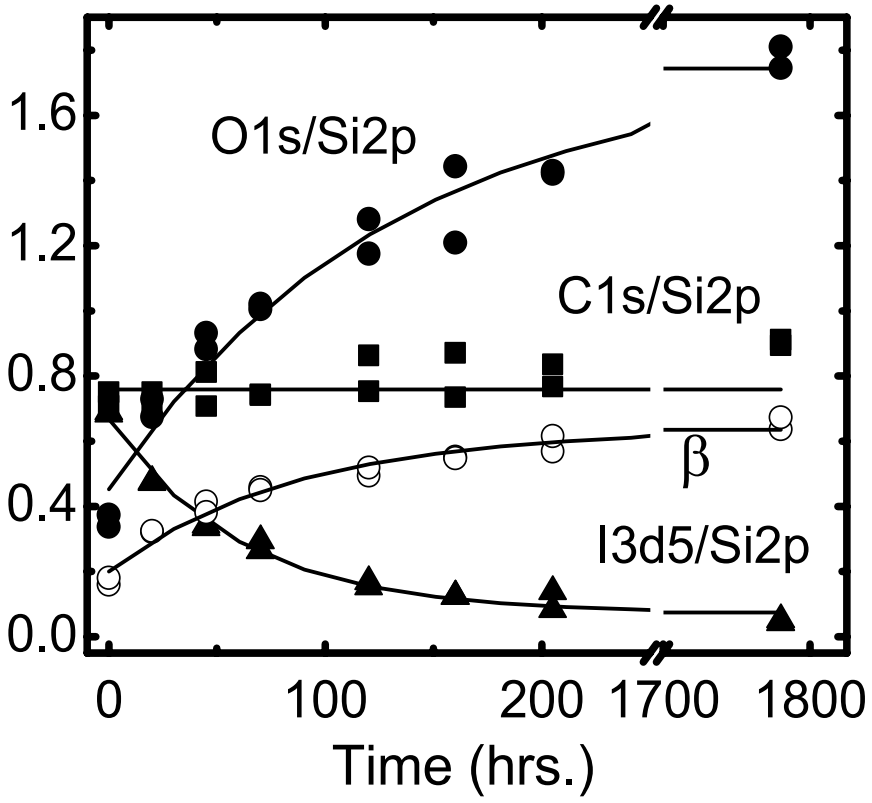

Figure II.2. XPS ratios of the O1s, C1s and I3d peak areas to the Si2p peak area and *β*-values of 1-iododecane monolayers on scribed silicon as a function of exposure time to the air.

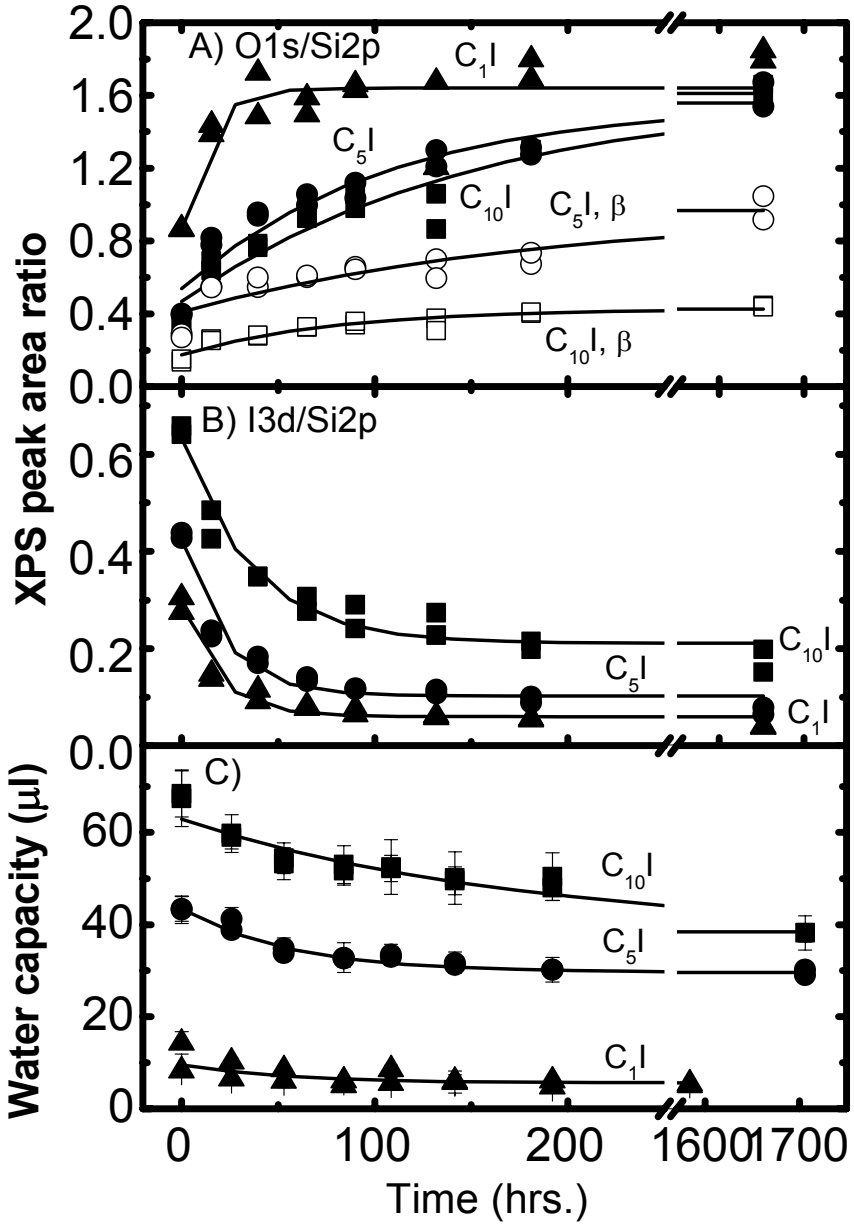

Figure II.3. (A) O1s/Si2p XPS ratios and *β*-values (from patches), (B) I3d/Si2p XPS ratios (from patches), and (C) water capacity measurements (from hydrophobic corrals) of silicon scribed under methyl iodide (C_1I), 1-iodopentane (C_5I) and 1-iododecane ($C_{10}I$) as a function of immersion time in water.

capacities as a function of immersion time in water for silicon scribed under methyl iodide, 1-iodopentane and 1iododecane. The C1s/Si2p ratios (not shown) stayed constant or rose slightly during these tests. The initial O1s/Si2p ratios of silicon surfaces scribed under 1-iodopentane and 1-iododecane were the same to within experimental error (see also Figure II.3), but they were lower than the initial O1s/Si2p ratio from the surface scribed under methyl iodide. These results are consistent with the fact that a methyl monolayer from CH_3I provides less steric hindrance and a less hydrophobic environment than a monolayer made from longer chain adsorbates.[6]

After preparation, the O1s/Si2p ratios of all of these surfaces rose, and after more than 1600 h the O1s/Si2p ratios for silicon scribed under 1-iodopentane and 1-iododecane almost reached the level of silicon scribed with methyl iodide. The β-values show that after more than 1600 h, the oxide layer in the surface prepared using 1-iodopentane was about as thick as the monolayer, and the oxide layer in the surface prepared using 1-iododecane was a little less than half the thickness of the monolayer. A comparison of the O1s/Si2p ratios and the β-values from monolayers made from 1-iododecane and then stored in the air or water indicates that silicon oxidation takes place more rapidly in the air than in water. This result implicates oxygen as the major oxidizing agent in the oxidation of the silicon substrate.

Figure II.3B shows the kinetics of iodine loss from silicon surfaces. It demonstrates that a) iodine was gradually lost from all surfaces after scribing and, b) scribing liquids with longer alkyl chains produced surfaces that had higher initial and final iodine levels. These results are, again, in general agreement with a model of greater steric hindrance and hydrophobicity from longer alkyl chains over shorter ones that more

effectively limit surface reactivity (hydrolysis). Figure II.3C shows that the water capacities of the 5 mm × 5 mm hydrophobic corrals decreased with immersion time in water. As shown before,[1,4] hydrophobic corrals made from scribing liquids with longer alkyl chain length reagents had a greater ability to hold liquids. The decrease in corral capacity parallels the increase in oxygen on these surfaces. Although corrals produced by scribing under 1-iodopentane and 1-iododecane lose ~30% and ~45% of their water capacities after ~1700 h (more than 2 months), respectively, they still retained their utility as devices for isolating and holding significant amounts of aqueous solutions. As a visual aid to the reader, Figure II.4 shows finite element analysis calculations of 20, 40, 60, 80, 100, and 120 μL water droplets in 5 mm × 5 mm hydrophobic corrals.

Figure II.5 shows that the alkyl chain length of 1-alkene scribing liquids plays a significant role in determining both the substrate oxidation and water capacities of hydrophobic corrals as a function of immersion time in water. After 200 h under water the O1s/Si2p ratio and the β-values were the highest for surfaces prepared with 1-pentene, lower for those prepared with 1-decene, and the lowest for those prepared with 1-hexadecene. The C1s/Si2p ratios (not shown) again stayed constant or even increased by a small amount during the stability tests. Similar trends were also observed in water capacities of hydrophobic corrals made from these 1-alkenes (see Figure II.5B). Corrals made with longer chain 1-alkenes held more water than those made from shorter 1-alkenes. Although water corral capacities decreased with the immersion time in water, hydrophobic corrals prepared with 1-decene and 1-hexadecene continued to hold significant amounts of water and can still function as useful devices (see also Figure II.4). A comparison of the O1s/Si2p ratios and the β-values given in Figures II.3 and II.5

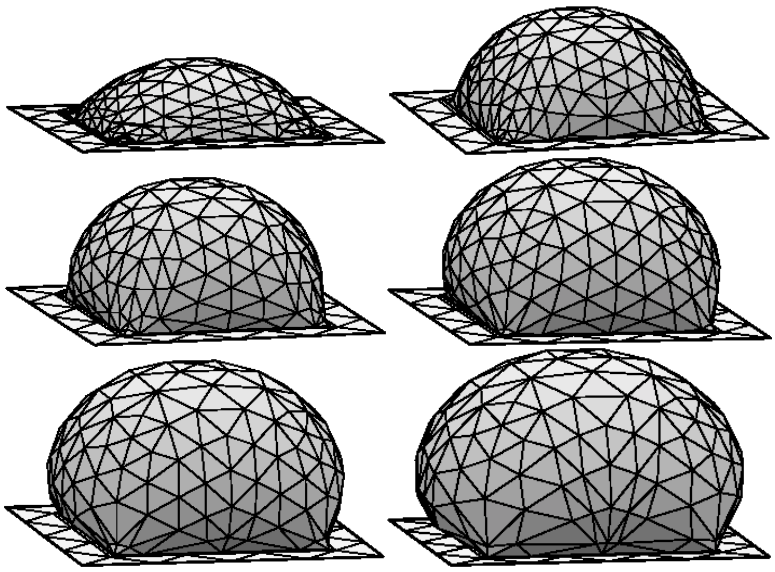

Figure II.4. Finite element analyses of 20, 40, 60, 80, 100, and 120 μL water droplets constrained to the 5 mm × 5 mm hydrophobic corrals. Volumes increase from left to right and from top to bottom in the figure.

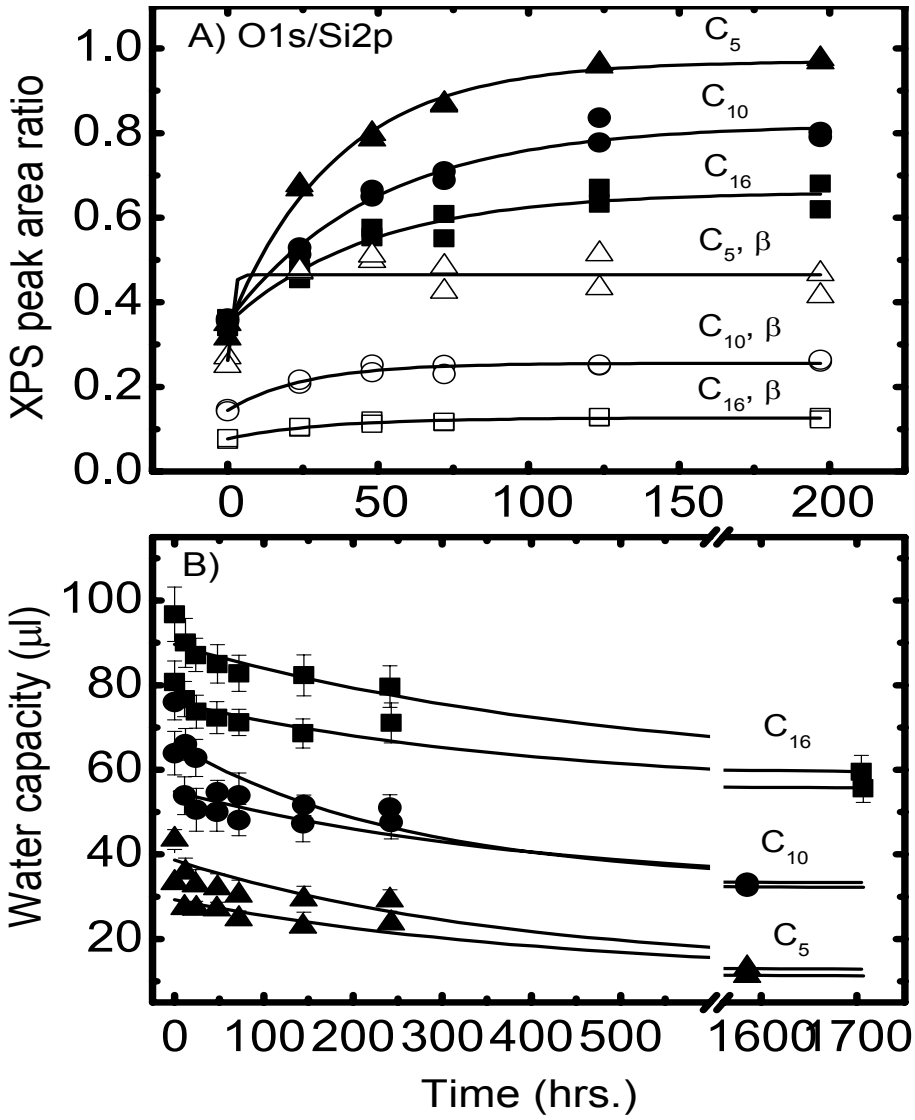

Figure II.5. (A) O1s/Si2p XPS ratios and β-values (from patches), and (B) water capacity measurements (from hydrophobic corrals) of silicon scribed under 1-pentene (C_5), 1-decene (C_{10}), and 1-hexadecene (C_{16}) as a function of immersion time in water.

indicates that silicon oxidizes more quickly when it was scribed with a 1-iodoalkane than with a 1-alkene. The oxide layer formation of 1-haloalkane derived surfaces was probably promoted by hydrolysis of the surface halogen.

XPS results from patches scribed under reactive liquids were very reproducible (see Figures II.3A, B and II.5A). However, there was a fair amount of variation in water capacities of different sets of hydrophobic corrals as shown in Figure II.5B. For example, although two sets of corrals prepared from 1-hexadecene showed similar final values of water capacities, their initial results differed by 15-20%. This was attributed to the variation in the scribing technique, which appears to be a complex function of tip shape and wear, the velocity (feed rate) of the tip across the surface, and the force applied on the tip.[8] Figure II.6 shows diamond tips before (as received) and after a significant amount of use. Scribed features may also be affected by the nature of the scribing liquid.

II.3.3 Monolayer Stability to Boiling 0.1 M H_2SO_4 and to X-rays

The Linford group previously measured C1s/Si2p XPS ratios of alkyl monolayers prepared by scribing silicon under 1-decene or 1-decanol before and after immersion in boiling 0.1 M H_2SO_4 (aq.) for 1 h.[3] Under these rigorous conditions the C1s/Si2p ratio for 1-decene was essentially unchanged, or perhaps rose by a small amount, and the C1s/Si2p ratio for 1-decanol decreased considerably. Here it is found that C1s/Si2p XPS ratios of alkyl monolayers prepared by scribing silicon under 1- octene and 1-chlorooctane did not change, or slightly increase, after two 1-h immersions in boiling 0.1 M H_2SO_4. The small increase in the C1s/Si2p ratio was attributed to the adventitious carbon. C1s/Si2p ratios of alkyl monolayers prepared with 1-octanol, however, decreased

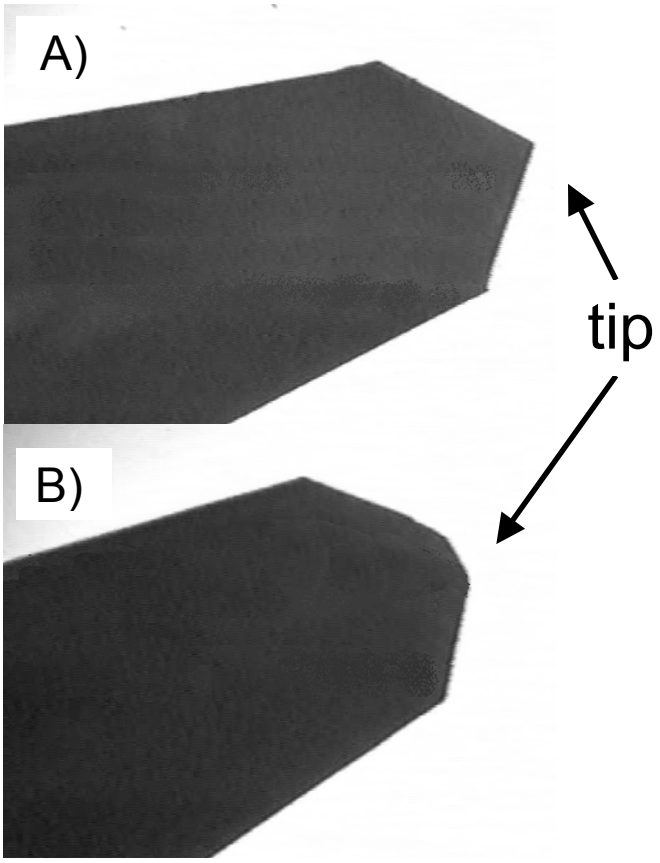

Figure II.6. Optical micrographs of the diamond tips used to scribe silicon: A) before, and B) after a considerable amount of use.

by about 50% after two 1-h immersions in boiling 0.1 M H_2SO_4.

These chemical tests are important because they: i) support the hypothesis that alkyl halides bind to scribed silicon through robust Si-C bonds,[4] ii) show that alkyl monolayers on silicon made from a shorter chain (eight-carbon) 1-alkene than that previously reported[3] also had excellent chemical stability, and iii) provide additional evidence that alcohols bind to silicon through hydrolysable Si-O bonds.[3]

Alkyl monolayers on the scribed silicon were also exposed to monochromatic Al Kα X-rays from our X-ray photoelectron spectrometer[14] for nearly 4 h (a typical XPS analysis takes 30 min or less). During these stability tests the spectrometer continuously acquired C1s, O1s, Si2p, and, where appropriate, Br3d narrow scans. Ratios of C1s, O1s, and Br3d peak areas to the Si2p peak area from the same cycle were then calculated. C1s/Si2p, O1s/Si2p, and Br3d/Si2p ratios stayed constant over the full analysis time for silicon scribed under a) 1-hexadecene, b) 1-butanol, c) 1-bromopentane, and d) 1,4-dibromobutane. Although XPS cannot fully assess X-ray-induced damage to organic materials because it cannot sense hydrogen,[15] it should come as no great surprise that monochromatic X-rays (the monochromator eliminates the high-energy Bremsstrahlung generated during the X-ray production) did not noticeably damage these materials. However, these stability tests are important because they validate previous (and future) XPS analyses of alkyl monolayers on the scribed silicon surface using monochromatic Al Kα X-rays.

II.4 REFERENCES

(1) Niederhauser, T. L.; Jiang, G.; Lua, Y.-Y.; Dorff, M. J.; Woolley, A. T.; Asplund, M. C.; Berges, D. A.; Linford, M. R. *Langmuir* **2001**, *17*, 5889.

(2) Lua, Y.-Y.; Lee, M. V.; Fillmore, W. J. J.; Matheson, R.; Sathyapalan, A.; Asplund, M. C.; Fleming, S. A.; Linford, M. R. *Angew. Chem. Int. Ed.* **2003**, *42*. 4046.

(3) Niederhauser, T. L.; Lua, Y.-Y.; Jiang, G.; Davis, S. D.; Matheson, R.; Hess, D. A.; Mowat, I. A.; Linford, M. R. *Angew. Chem. Int. Ed.* **2002**, *41*(13), 2353.

(4) Niederhauser, T. L.; Lua, Y.-Y.; Sun, Y.; Jiang, G.; Strossman, G. S.; Pianetta, P.; Linford, M. R. *Chem. Mater.* **2002**, *14*, 27.

(5) Lua, Y.-Y.; Niederhauser, T. L.; Wacaser, B. A.; Mowat, I. A.; Woolley, A. T.; Davis, R. C.; Fishman, H. A.; Linford, M. R. *Langmuir* **2003**, *19*(4), 985.

(6) Lua, Y.-Y.; Niederhauser, T. L.; Matheson, R.; Bristol, C.; Mowat, I. A.; Asplund, M. C.; Linford, M. R. *Langmuir* **2002**, *18*, 4840.

(7) Wacaser, B. A.; Maughan, M. J.; Mowat, I. A.; Niederhauser, T. L.; Linford, M. R.; Davis, R. C. *Appl. Phys. Lett.* **2003**, *82*(5), 808.

(8) Cannon, B. R.; Magleby, S. P.; Howell, L. L.; Jiang, G.; Niederhauser, T. L.; Linford, M. R. *Proceedings of the 2002 ASME International Mechanical Engineering Congress and Exposition.*

(9) Bain, C. D. and Whitesides, G. M. *J. Phys. Chem.* **1989**, *93*, 1670.

(10) *Handbook of Chemistry and Physics*; CRC Press: Boca Raton, 2000.

(11) Linford, M. R.; Fenter, P.; Eisenberger, P. M.; Chidsey, C. E. D. *J. Am. Chem. Soc.* **1995**, *117*, 3145.

(12) Abbott, N. L.; Whitesides, G. M.; Racz, L. M.; Szekely, J. *J. Am. Chem. Soc.* **1994,** *116*, 290.

(13) Moulder, J. F.; Stickle, W. F.; Sobol, P. E.; Bomben, K. D. *Handbook of X-ray Photoelectron Spectroscopy*; Physical Electronics, Inc.: Eden Prarie, MN, 1995.

(14) Graham, R. L.; Bain, C. D.; Biebuyck, H. A.; Laibinis, P. E.; Whitesides, G. M. *J. Phys. Chem.* **1993**, *97*, 9456.

(15) Frydman, E.; Cohen, H.; Maoz, R.; Sagiv, J. *Langmuir* **1997**, *13*, 5089.

− CHAPTER III −

EVIDENCE FOR A RADICAL MECHANISM IN MONOLAYER FORMATION ON SILICON GROUND (OR SCRIBED) IN THE PRESENCE OF ALKYL HALIDES

III.1 INTRODUCTION

It was recently shown that silicon surfaces can be simultaneously patterned and functionalized when they are chemomechanically modified (scribed) in the presence of 1-haloalkanes,[1] 1-alkenes,[2,3] 1-alkynes,[2] alcohols,[3] epoxides, [4] and aldehydes.[5] In these reports, it was hypothesized that scribing broke through silicon's passivation layer to expose highly reactive silicon species, such as dangling bonds and silicon-silicon dimers, which readily reacted with reactive molecules in their immediate vicinity to produce monolayers. Using this scribing method, *ca.* 10 μm features were prepared by using a low force on a diamond tip,[6] *ca.* 20 μm features with very sharp edges that were only 1-2 nm deep were produced using a miniature tungsten carbide ball,[7] and *ca.* 30 nm features were patterned using an AFM tip.[8] It was also reported that coated particles were formed when silicon wais ground in the presence of 1-hexadecene.[9]

To explain the formation of alkyl monolayers on scribed silicon from 1-haloalkanes, a two-step mechanism was proposed: (1) halogen abstraction, which is driven by the greater Si-X bond strength compared to the lower C-X bond strength[10,11] (X = Cl, Br, I), followed by (2) diffusion of the resulting alkyl radical back to the surface:[1]

$$Si\cdot + XCH_2(CH_2)_{n-1}H \rightarrow Si\text{-}X + \cdot CH_2(CH_2)_{n-1}H \quad (1)$$

$$Si\cdot + \cdot CH_2(CH_2)_{n-1}H \rightarrow Si\text{-}CH_2(CH_2)_{n-1}H \quad (2)$$

A similar mechanism [eqn. (3)] was previously proposed by Bronikowski and Hamers[12] to explain the reaction of CH_3Cl with Si(100)-2 × 1, including the observed 2-fold excess of -Cl over -CH_3.

$$CH_3Cl(g) + Si{=}Si \rightarrow Si\text{-}Cl(s) + Si(s) + CH_3(g) \quad (3)$$

However, to the knowledge of the author, no direct evidence for the radical intermediates in these proposed reactions has ever been given.

It is reasoned that if mechanism (1)-(2) were operative on the scribed silicon, then (a) not every alkyl radical would return and react with the surface and, (b) these "free" radicals could combine and disproportionate. In other words, from a 1-haloalkane, $X(CH_2)_nH$, one would expect to produce $\cdot CH_2(CH_2)_{n-1}H$ as an intermediate, which would lead to the formation of $H(CH_2)_{2n}H$ by combination and, $CH_2{=}CH_2\text{-}(CH2)_{n-2}H$ and $H(CH_2)_nH$ by disproportionation. Other products might also be possible. It is believed that only very small amounts of 1-haloalkanes are consumed during monolayer formation on planar surfaces. Because of the difficulty anticipated in detecting extremely small quantities of possible combination and/or disproportionation products, it was opted to increase the amount of the surface area by performing an analogous experiment of grinding silicon with 1-haloalkanes. The liquids that remained after grinding were then analyzed by gas chromatography-mass spectrometry (GC-MS). It was found that the liquids consisted mostly of unreacted 1-haloalkanes, but measurable quantities of the expected combination and disproportionation products were also present. The presence of

these species provides evidence for the radical mechanism in alkyl monolayer formation on silicon scribed or ground under 1-chloro-, 1-bromo-, and 1-iodoalkanes.

III.2 EXPERIMENTAL SECTION

III.2.1 Materials

1-Chlorooctane (99%), 1-bromooctane (99%), 1-iodooctane (98%), 1-iodoheptane (98%), 1-octene (98%), octane (99%), 1-heptene (97%), heptane (99%), hexadecane (99+%), pentadecane (99+%), and tetradecane (99+%) were obtained from Aldrich and used as received. Silicon chips were rinsed with acetone before use.

III.2.2 Grinding Silicon in the Presence of 1-Haloalkanes

In each experiment, 5 g of silicon chips and 5 mL of 1-haloalkane were loaded in the bowl (with an O-ring seal) of a grinding apparatus (1A Benchmill with a CH-3 bowl, Rocklabs, Auckland, New Zealand). The bowl was flushed with nitrogen, and the mixture of silicon chips and a 1-haloalkane was ground for 1 h. During this time, the grinding bowl warmed to *ca.* 40 °C.

III.2.3 Gas Chromatograph-Mass Spectrometry (GC-MS) Analysis

After grinding, the remaining liquid was filtered through a 0.2 μm Teflon syringe filter (Millex-FG, Millpore, MA) and then 2.6 μL of it was directly injected (without dilution) onto a GC-MS (ThermoQuest, Austin, TX) column (30 m × 0.25 mm i.d., 0.25 μm film thickness, RTX-5MS column, Restek, Bellefonte, PA), that is, the 1-haloalkanes acted as solvents for the anticipated byproducts in the analysis. The split ratio was 35:1,

and the instrument was operated in the EI positive (MS) mode with a programmed temperature ramp. Control experiments, in which the 1-haloalkanes were only filtered, or ground without silicon, and/or kept in an oven as neat liquids at 50 °C for 60 min and then analyzed by GC-MS, were also performed. Assignments of the free-radical byproducts in the 1-haloalkane liquids were based on comparisons to retention times and mass spectra of pure, purchased compounds.

III.2.4 Other Instrumentation

Scanning electron microscopy (SEM) was performed with a JEOL JSM840a microscope. X-ray photoelectron spectroscopy (XPS) was performed with a Surface Science SSX-100 spectrometer. The error reported for the C1s/Si2p ratios of the ground silicon samples is one-half the difference between two measurements from two different samples.

III.3 RESULTS AND DISCUSSION

A broad range of particle sizes is found after silicon was ground in the 1-haloalkanes. The SEM image shows the range of the particle sizes (up to 5 μm, down to nanometer dimensions; see Figure III.1). The XPS of these particles (see Figure III.2) suggests that alkyl and partial halogen monolayers formed on these silicon particle surfaces. The uncorrected C1s/Si2p XPS ratios for these particles (1-chlorooctane, 0.93 ± 0.10; 1-bromooctane, 0.79 ±0.02; 1-iodooctane, 0.93 ± 0.07) are higher than those previously reported for monolayers made on planar silicon in the air.[1] Higher C1s/Si2p XPS ratios were similarly found if the scribing was performed in a glove box

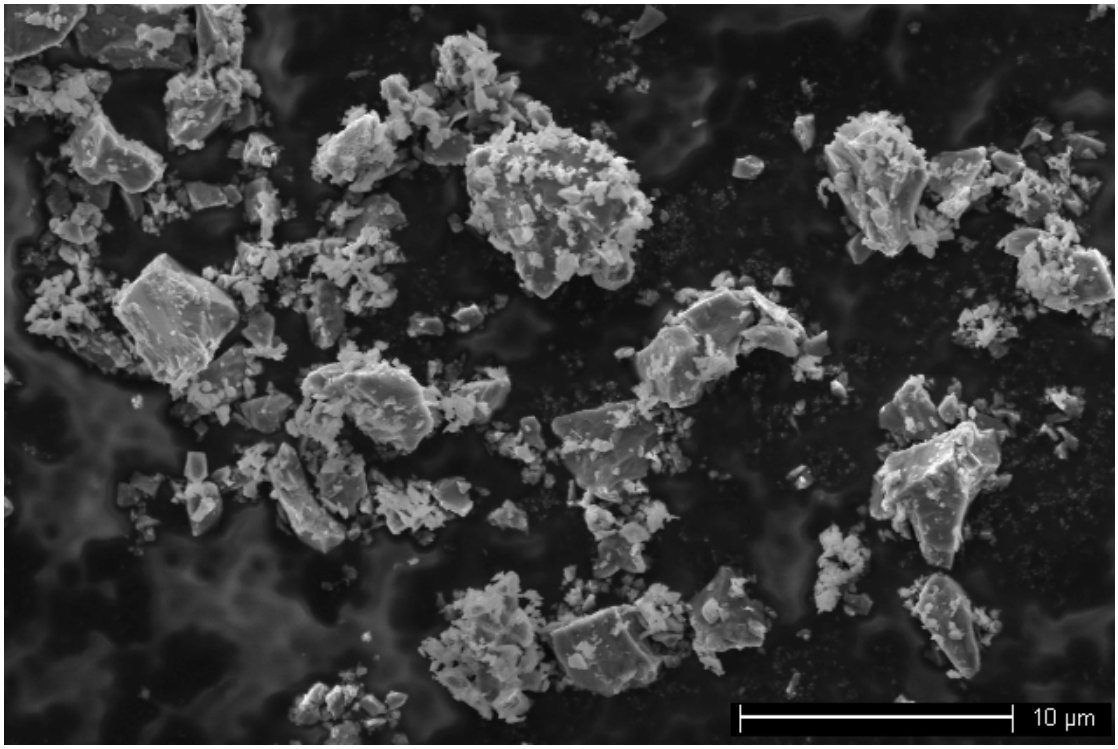

Figure III.1. SEM image of the particles obtained by grinding silicon chips with 1-chlorooctane.

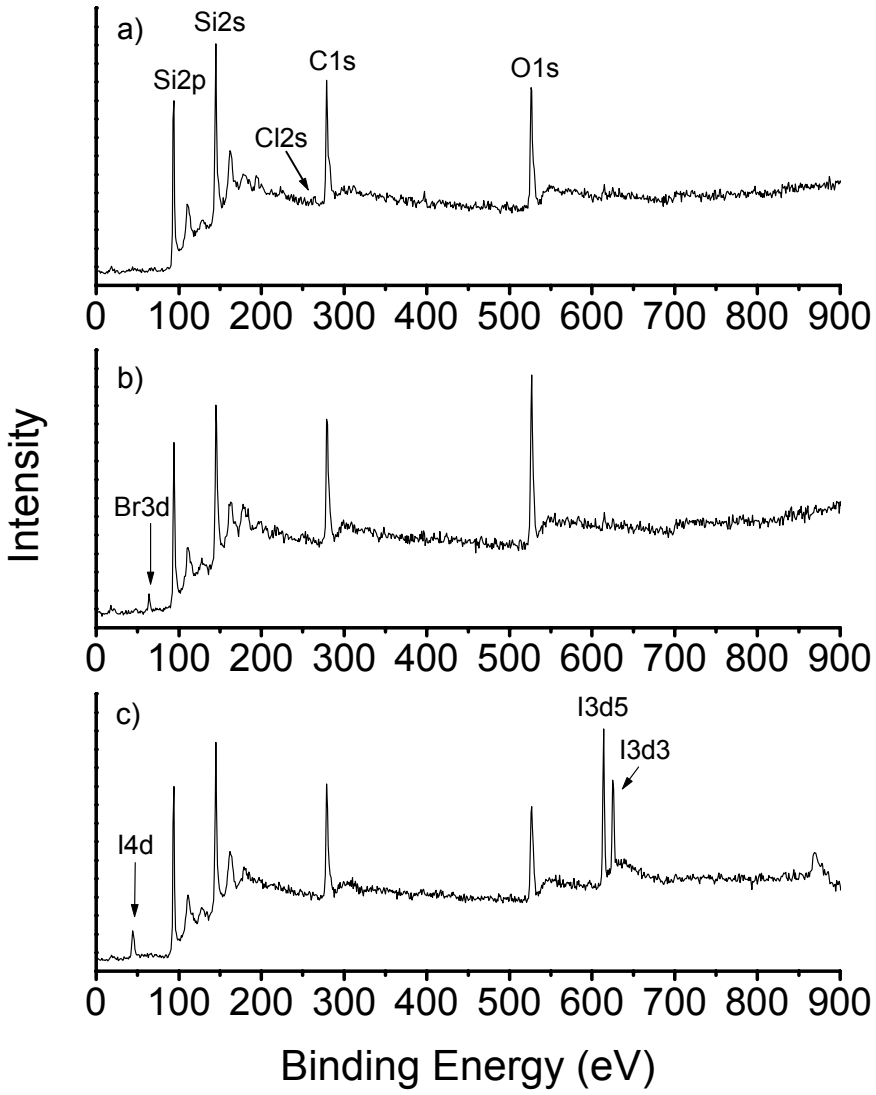

Figure III.2. XPS spectra of powders prepared by grinding silicon with: a) 1-chlorooctane, b) 1-bromooctane, and c) 1-iodooctane.

with degassed compounds.[1] The higher C1s/Si2p ratios observed during grinding are also attributed to the much lower concentration of oxygen in the grinding bowl, compared to the open air, although the change in geometry of the material (from rough planar surface to particles) may also play a role in this effect.

Figure III.3 shows regions of the GC-MS chromatograms of $X(CH_2)_7CH_3$ (X = Cl, Br, or I) before (control) and after silicon grinding. In all cases, some 1-octene (t_R = 6.54-6.56 min) and *n*-octane (t_R = 6.41-6.44 min) are present as impurities in the starting materials (Figure III.3a, c, e). However, after grinding, substantially more *n*-octane is found in all of the 1-halooctanes. For 1-octene, another anticipated product of disproportionation, the story is more complex. When silicon is ground in 1-chlorooctane, which has the largest amount of 1-octene impurity (see Figure III.3a), the concentration of 1-octene decreases. This result can be rationalized by noting that both ground[9] and scribed[2,3] silicon were shown to react with 1-alkenes. The concentrations of 1-octene in 1-bromooctane and 1-iodooctane, which are initially low, increase slightly and substantially, respectively.

Hexadecane, the expected combination product of two eight carbon linear radicals, has a retention time of nearly 15.2 min, and measurable quantities of this compound are not observed in any of the three 1-haloalkanes prior to grinding (see Figure III.3). After grinding, hexadecane is seen in all of the 1-haloalkanes, with the largest concentration in 1-iodooctane and the smallest in 1-chlorooctane. Figure III.3 shows that the ratio of combination to disproportionation products increases going from 1-chloro- to 1-bromo- to 1-iodooctane. This increase is attributed to the steric hindrance in the solvation of radicals produced during grinding by the different 1-haloalkanes. A

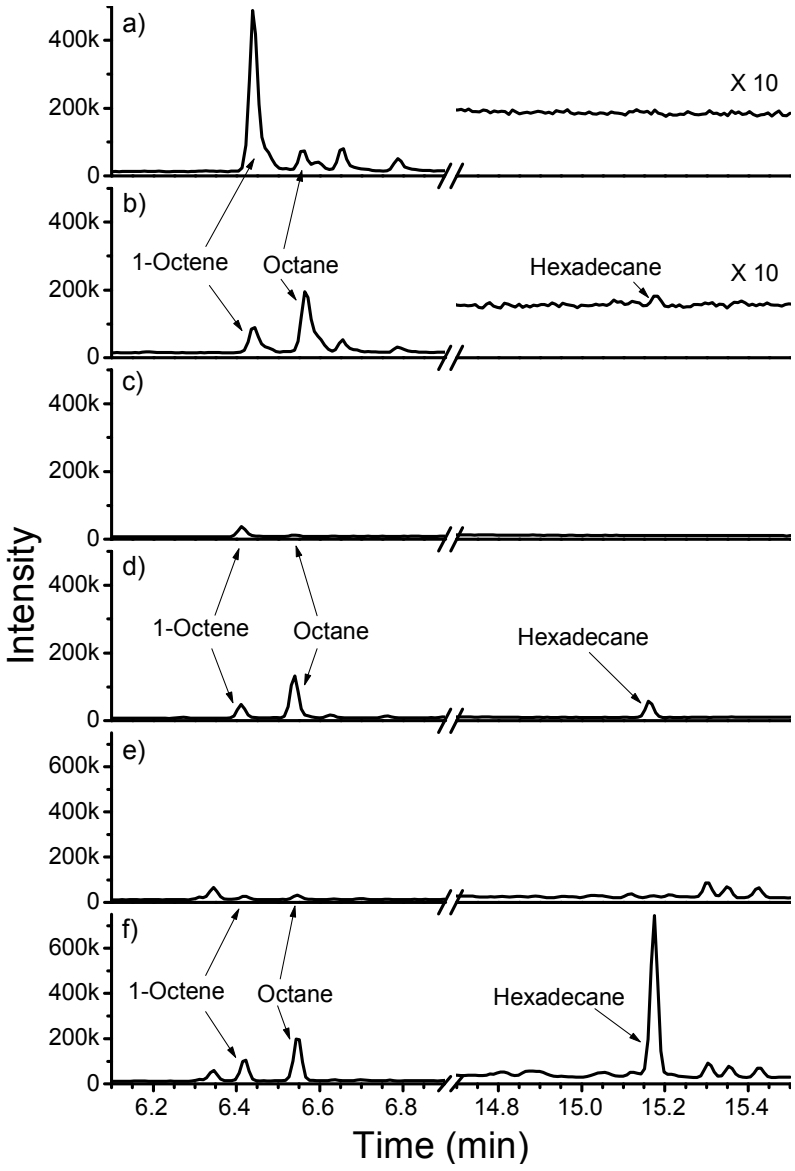

Figure III.3. GC-MS chromatograms of controls: a) 1-chlorooctane (as received), c) 1-bromooctane (ground without silicon for 60 min), and e) 1-iodooctane (kept in an oven at 50 °C for 60 min), and liquids remaining after silicon was ground with: b) 1-chlorooctane, d) 1-bromooctane, and f) 1-iodooctane.

radical is an electron deficient species, and so it should be most stabilized by a concentrated negative charge and less by a diffuse one. The competition between disproportionation and combination of alkyl radicals (both processes are very exothermic) was studied a number of years ago.[13] It was found that primary radicals tend to combine, but as the radical becomes more sterically hindered, disproportionation is increasingly favored. Because electro-negativities of halogens decrease as one moves down the periodic table, 1-chloroalkanes should show the greatest ability to solvate radicals, where a favorable interaction between the chlorine atom in the 1-chloroalkane and the alkyl radical should effectively increase the steric hindrance about the radical. In contrast, 1-iodoalkanes are expected to show the lowest solvation of radicals and thus radicals would be more free, that is, radicals are expected to combine readily with each other (and disproportionate less). Solvation effects are known to strongly influence reaction rates of many radical reactions.[14,15]

If the proposed mechanism for the reaction of silicon with 1-haloalkanes is correct, and if some radicals are unable to return to the surface so that they can combine and disproportionate, then if silicon is ground in the presence of two different 1-haloalkanes, combination products of both alkyl radicals would be expected. This is found to be the case. Figure III.4 shows the GC-MS chromatograms of a 1:1 mixture of 1-iodoheptane and 1-iodooctane before and after silicon was ground in its presence. The expected products of disproportionation (1-heptene, heptane, 1-octene, and octane) are all present (Figure III.4a, b). Significantly, the expected products of combination (tetradecane, pentadecane, and hexadecane) are also produced (Figure III.4c, d) in approximately the ratio that is expected, 1:2:1.

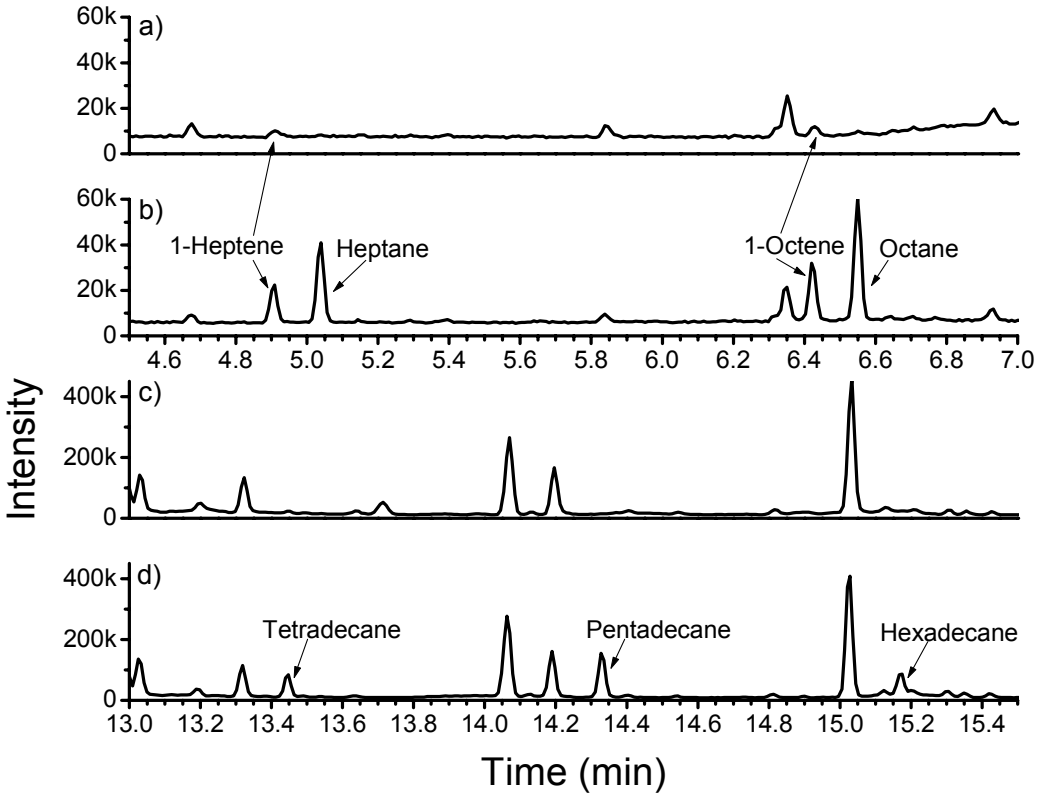

Figure III.4. GC-MS chromatograms of 1-iodoheptane and 1-iodooctane (1:1 mixture): (a, c) a control (kept in an oven at 50 °C for 60 min) and (b, d) the liquid remaining after silicon was ground in the presence of the mixture. The peak areas of tetradecane, pentadecane, and hexadecane in panel d are 100,321, 201,504, and 104,927, respectively. In a separate, replicate experiment, the peak areas were 99,918, 168,101, and 92,269, respectively.

In conclusion, this study provides experimental evidence for a free-radical mechanism in alkyl monolayer formation on silicon ground/scribed with alkyl halides.

III.4 REFERENCES

(1) Niederhauser, T. L.; Lua, Y.-Y.; Sun, Y.; Jiang, G.; Strossman, G. S.; Pianetta, P.; Linford, M. R. *Chem. Mater.* **2002**, *14*, 27.

(2) Niederhauser, T. L.; Jiang, G.; Lua, Y.-Y.; Dorff, M. J.; Woolley, A. T.; Asplund, M. C.; Berges, D. A.; Linford, M. R. *Langmuir* **2001**, *17*, 5889.

(3) Niederhauser, T. L.; Lua, Y.-Y.; Jiang, G.; Davis, S. D.; Matheson, R.; Hess, D. A.; Mowat, I. A.; Linford, M. R. *Angew. Chem., Int. Ed.* **2002**, *13*, 2353.

(4) Lua, Y.-Y.; Lee, M. V.; Fillmore, W. J. J.; Matheson, R.; Sathyapalan, A.; Asplund, M. C.; Fleming, S. A.; Linford, M. R. *Angew. Chem., Int. Ed.* **2003**, *42*, 4046.

(5) Lua, Y.-Y.; Fillmore, W. J. J.; Linford, M. R. *Appl. Surf. Sci.* **2004**, *231-232*, 323.

(6) Cannon, B. R.; Magleby, S. P.; Howell, L. L.; Jiang, G.; Niederhauser, T. L.; Linford, M. R. 2002 ASME International Mechanical Engineering Congress and Exposition, November 17-22, 2002, New Orleans, LA.

(7) Lua, Y.-Y.; Niederhauser, T. L.; Wacaser, B. A.; Mowat, I. A.; Woolley, A. T.; Davis, R. C.; Fishman, H. A.; Linford, M. R. *Langmuir* **2003**, *19*, 985.

(8) Wacaser, B. A.; Maughan, M. J.; Mowat, I. A.; Niederhauser, T. L.; Linford, M. R.; Davis, R. C. *Appl. Phys. Lett.* **2003**, *82*, 808.

(9) Linford, M. R. U.S. Patent 6,132,801, 2000.

(10) *Handbook of Chemistry and Physics*; CRC Press: Boca Raton, FL, 2000.

(11) Dean, J. A. *Lange's Handbook of Chemistry*; McGraw-Hill: New York, 1999.

(12) Bronikowski, M. J.; Hamers, R. J. *J. Vac. Sci. Technol., A* **1995**, *13*, 777.

(13) Gibian, M. J.; Corley, R. C. *Chem. Rev.* **1973**, *73*, 441.

(14) Mayo, F. R. *J. Am. Chem. Soc.* **1967**, *89*, 2654.

(15) Dneprovskii, A. S.; Kuznetsov, D. V.; Eliseenkov, E. V.; Fletcher, B.; Tanko, J. M. *J. Org. Chem.* **1998**, *63*, 8860.

− CHAPTER IV −

PREPARATION OF SURFACES FOR MATRIX-ASSISTED LASER DESORPTION/IONIZATION MASS SPECTROMETRY

IV.1 INTRODUCTION

The matrix-assisted laser desorption/ionization (MALDI) technique was developed in 1987 for the ionization of relatively large polypeptides and proteins.[1] Koichi Tanaka of Shimadzu Corporation shared half of the 2002 Nobel Prize in Chemistry for developing MALDI coupled with mass spectrometry (usually using a time-of-flight (TOF) analyzer) for analysis of biological macromolecules[2], culminating in development of instrumentation that has significantly advanced drug development and proteomics. To date, MALDI TOF mass spectrometry has been successfully used for the analysis of a wide range of different analyte molecules including peptides, proteins, oligosaccharides, oligonucleotides, lipids, complex carbohydrates, complexes of metal ions with biomolecules,[3-9] synthetic polymers,[10-16] *etc*. A great advantage of MALDI-MS is that the process of soft-ionization causes little or no fragmentation of analytes,[17] allowing the molecular ions of analytes to be identified, even within mixtures. Furthermore, if relatively pure material is available, unequivocal identification of that material can be achieved by a process known as mass-mapping.[18-20]

The mechanism of MALDI is not fully understood yet.[21] It is believed that the laser-light absorbing matrix molecules are excited by high intensity, short duration laser pulses. The absorbed energy is then transferred to the analyte molecules, causing them to

be desorbed and ionized. Since the analyte does not directly absorb the energy of the laser, it generally does not undergo fragmentation, which is important for determining the mass of intact molecular ions of the analyte. Intact analyte masses facilitate their identification.

The key aspect of MALDI-MS is to mix the analyte with a large excess of highly absorbing small organic molecules (the matrix), such as α-cyano-4-hydroxycinnamic acid (α-CHCA), sinapinic acid (SA), or 2,5-dihydroxybenzoic acid (DHB), and to then allow the mixture droplet to dry on a MALDI sample support into a crystalline deposit.[21]

Typically, a conventional MALDI-MS sample plate is made of stainless steel, on which 10 × 10 sample supports (2 mm diameter circles) are etched[22]. Usually, 0.5-2.0 μL of 0.1-10 pmol/μL peptide or protein solution and the same volume of a 10 g/L matrix solution are applied on each sample support. As soon as the analyte-matrix co-crystallization mixture is loaded into the mass spectrometer, a spectrum can be generated within seconds.

Since its unique advantage in identifying molecular ions of analytes, MALDI-MS has become one of the most important tools for the analysis of the proteome, *i.e.*, proteomics.[23] In addition, it is the major tool for the analysis of the products of peptide synthesis.[24-27] However, because the crystallization of the analyte-matrix mixture on a sample support is heterogeneous, and as mentioned above, the typical size of a sample support is over 100 times that of the cross-section of the ionization laser beam (diameter *ca.* 200 μm), the laser beam only hits a small part of a sample support, and the signal intensity varies significantly and data reproducibility between supports is usually poor. Thus one needs to search for "hot spots," which are regions in an analyte-matrix spot that give significant signals. These problems also limit the analytical sensitivity, which is a

critical issue for the analysis of many biomolecules. Accordingly, if the cross-section of the ionization laser beam could be increased to the size of the sample supports, or, on the other hand, if the size of the sample supports could be decreased down to that of the cross-section of the laser beam, both reproducibility and sensitivity of MALDI-MS analysis might be improved significantly.

It was previously shown that the idea of downsizing MALDI-MS sample supports did work.[28-33] One such approach was to directly etch *ca.* 200 μm diameter nanovials on a single crystal silicon wafer or other materials by using micromachining methods, which usually consisted of multi-step photolithography.[28-30,32] This approach was usually coupled with using a microdispenser for handling analyte-matrix mixture solutions because of the nanoliter scale capacities of these nanovials. The other approach was to exploit the hydrophobic-hydrophilic interactions to make analyte-matrix droplets focus onto the hydrophilic anchors of *ca.* 200 μm diameter, which were usually created on a hydrophobic polymeric layer that was coated on a conventional sample plate,[31] or on a gold coated silicon wafer with alkyl monolayers grown on it as hydrophobic substrates.[33] In the case of gold-coated substrates, sophisticated micromachining techniques were needed to make a mask or a stamp, which then transferred anchor patterns to substrates, as well as the sputtering equipment for gold coating. It is seen that, those designs of miniaturized MALDI-MS sample supports have not been used in routine MALDI-MS analysis because of the cost and time required to make them. So, obviously, a more direct approach to make miniaturized MALDI-MS sample supports at low cost would be very valuable for MALDI-MS analysis.

Here the application of chemomechanical surface modification in improving signal reproducibility and intensity of MALDI-MS analysis is reported. Briefly, miniaturized MALDI-MS sample supports are made on a silicon surface by directly scribing a sample support pattern onto a water-wet, hydrophobic silicon wafer. Before scribing, the silicon wafers were treated with a neat silane[34] to produce extremely hydrophobic surfaces. Water is believed to react with silicon radicals during the scribing and create HO-terminated hydrophilic sample supports on the hydrophobic silicon surface. Either the silane treating (silanizing) or the scribing of silicon can be completed in a few minutes. Then these miniaturized MALDI-MS sample supports are immediately ready for use once cleaned and dried. When tiny droplets of an analyte-matrix water solution are dispensed onto these sample supports, these droplets gradually dry in the air and are finally focused on top of hydrophilic sample supports by hydrophobic-hydrophilic interactions, and then crystallize as usual. As expected, with these miniaturized MALDI-MS sample supports, the signal intensity and reproducibility for a test peptide are both improved. Meanwhile, it is found that the shape of a scribed sample support has an effect in the MALDI-MS signal.

In addition, miniaturized MALDI-MS sample supports are also successfully scribed on glass, which, as is well known, has similar chemical composition and properties of a silicon surface. However, the mass spectrum of the test peptide acquired from a sample support scribed on glass is slightly different from that acquired from a sample support scribed on silicon.

IV.2 EXPERIMENTAL SECTION

IV.2.1 Materials

Trichloro-(1H,1H,2H,2H-perfluorooctyl)silane (97%), α-cyano-4-hydroxycinnamic acid (α-CHCA, 99%) and 2,5-dihydroxybenzoic acid (DHB, 98%) were obtained from Aldrich. Glu-Fibrinopeptide B was obtained from Sigma. All reagents were used as received. Deionized water was obtained from a Millipore Milli-Q water system. Silicon(100) wafers (p-boron, 2-6 Ω cm, test grade) were obtained from Montco Silicon Technologies. Microscope glass slides (plain, pre-cleaned) were obtained from Premiere.

IV.2.2 Silanization of Silicon and Glass Surfaces

Silicon chips or glass slides were first cleaned and dried,[35,36] then silanized[34] with neat trichloro(1H,1H,2H,2H-perfluorooctyl)silane in a common laboratory oven at 90 ºC for 15 min. The silanized silicon chips or glass slides were washed with isopropanol to remove the excess silane, and then cleaned and dried as before. After this treatment, silicon or glass surfaces were extremely hydrophobic (average advancing water contact angle of silicon or glass surfaces was measured to be 120º or higher, see Figure IV.1).

IV.2.3 Scribing Miniaturized MALDI-MS Sample Supports

To scribe miniaturized MALDI-MS sample supports, a clean hydrophobic silicon chip or glass slide was first laid on the sample stage of the scribing apparatus, wet with deionized water. A pattern of hydrophilic sample supports (*ca.* 200 μm diameter round patches, single circles and single crosses) was then scribed with a diamond tip that was

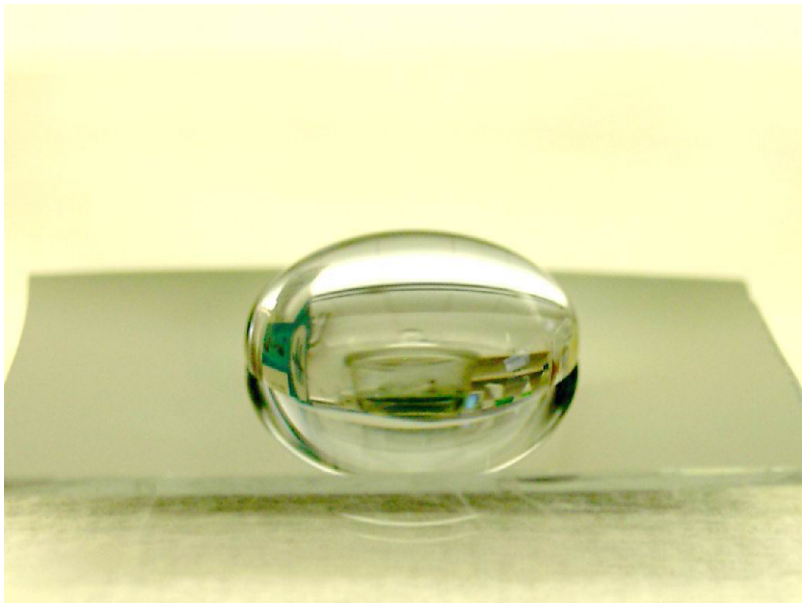

Figure IV.1. A water drop stays on a silanized, hydrophobic silicon surface. Advancing water contact angle of the surface was measured to be > 120º.

mounted on a device called end-effector[37] and driven by the scribing apparatus (see Figure IV.2 and Figure I.2). With this specially designed end-effector, very gentle forces can be applied on the diamond tip and fine features can be scribed on silicon or glass.

IV.2.4 Sample Handling

Specific sample handling equipment, *e.g.*, a microdispenser, was required for handling very small volumes of solutions on miniaturized MALDI-MS sample supports.[38,39] Here, however, because much more solution could be dispensed onto each sample support, a manual micro-syringe is sufficient for the sample handling. The sample handling procedure is very similar to that used in conventional MALDI-MS, except that analyte and matrix solutions were mixed at a 50:50 (v/v) ratio before sample dispensing. It was found that only a limited amount of analyte-matrix mixture was focused and crystallized on each miniaturized sample support. On the other hand, 0.3 μL is the minimum volume that a manual micro-syringe (1 μL) can handle for hydrophobic surfaces. Thus, only a 0.3 μL of analyte-matrix mixture solution was dispensed onto a sample support. A watch glass covering the whole sample plate (the silicon wafer or glass slide with sample supports scribed) was used to slow down the drying of droplets for better focusing effects. When sample droplets were focused, dried and crystallized on sample supports in the air, the silicon or glass sample plate was then attached to a home-built MALDI sample plate that is similar to a commercially available PAGE gel MALDI plate with a recessed area in its center.[22] The attachment was made with single-sided tape over the edge of the silicon or glass sample plate. MALDI-MS analysis was then performed as usual, except there was no searching for the "hot spots."

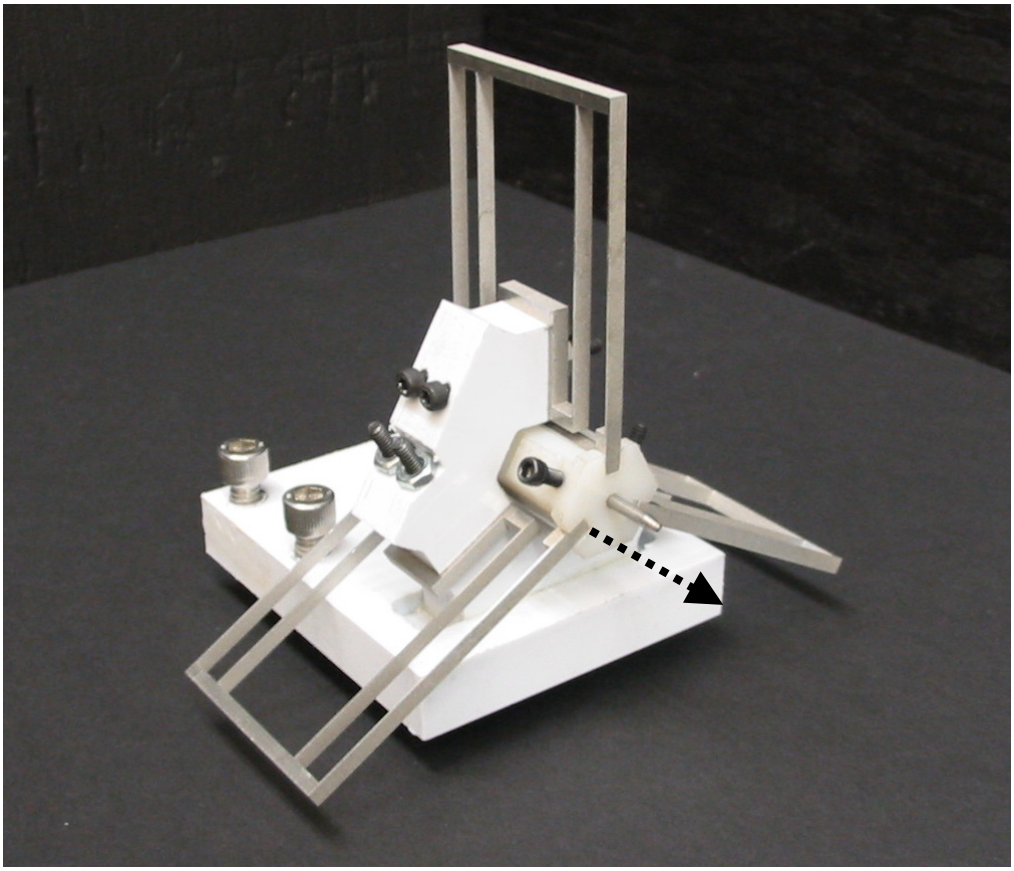

Figure IV.2. The compliant end-effector for scribing. Three folded beam segments were combined 120° apart to provide high lateral stiffness and low axial stiffness. The dashed arrow indicates the axial movement of the end-effector.[37]

IV.2.5 Instrumentation

MALDI-MS analysis was performed with an API QSTAR Pulsar LC/MS/MS System equipped with an orthogonal MALDI (oMALDI) source using 337 nm pulsed nitrogen laser and a TOF analyzer (Applied Biosystems/MDS-SCIEX, Framingham, MA). A 25% laser power level (equal to 28.2 μJ) was chosen for all analyses. The laser beam was adjusted to focus and cover a whole sample spot. For each sample spot, an accumulated spectrum was acquired until counts stopped growing. Because the laser energy desorbs the analyte from a support, sometimes it is necessary to move around the sample stage during data acquisition to avoid analyte loss.

IV.3 RESULTS AND DISCUSSION

SEM and optical microscope pictures of circular miniaturized MALDI-MS sample supports scribed on a hydrophobic silicon wafer (see Figure IV.3) show that circular sample supports have the focusing capability as expected. However, subsequent MALDI-MS analyses for the samples focused inside these circles in Figure IV.3 did not capture any signal. This is attributed to the fact that the analyte-matrix (α-CHCA) mixture did not crystallize at all (see the dried sample in Figure IV.3). It is known that though α-CHCA is commonly used as a matrix in MALDI-MS, it is not water soluble at room temperature. On the other hand, water has the highest surface tension, which makes sample droplets on the hydrophobic substrate gradually focus on hydrophilic anchors (the sample supports). In the experiment of Figure IV.3, α-CHCA was dissolved in boiling water. Thus, when this solution and the analyte solution were then dispensed on the silicon sample plate in the air, it can be imagined that water insoluble α-CHCA quickly

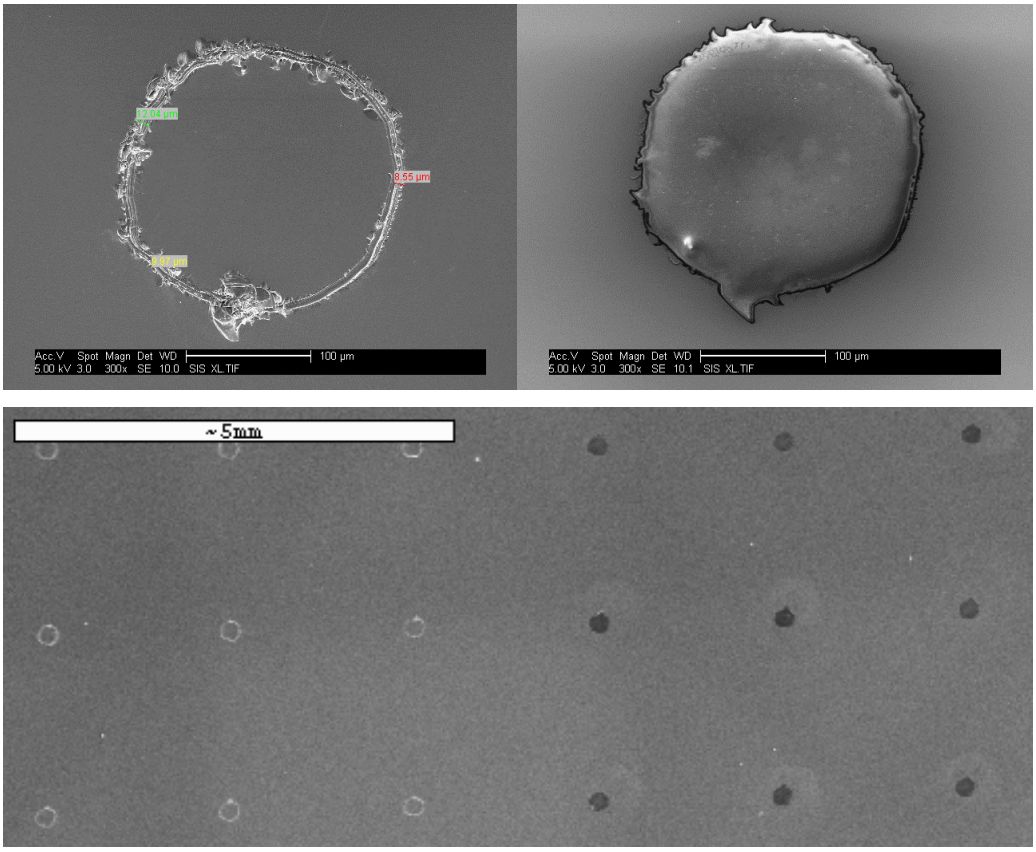

Figure IV.3. SEM pictures of a bare circular sample support (upper left) and a circular sample support loaded with 0.3 μL 1.0 pmol/μL Glu-Fibrinopeptide B and 0.3 μL 1mg/mL α-CHCA (upper right, focused and dried in air), and an optical microscope picture of a 3 × 6 pattern of the circular sample supports (right half loaded with the same sample solution).

precipitated from the surface of a sample mixture droplet and formed a shell on the surface, which then prevented the sample mixture from drying and crystallizing. However, crystallization of a sample mixture is a prerequisite for MALDI-MS analysis. That means, only can water soluble matrices be used here. So DHB water solution was then used as the matrix for the following experiments. It is found for the 1.0 pmol/μL Glu-Fibrinopeptide B test solution, 20 mM DHB solution gives stronger signals than 50 mM, 10 mM and 5 mM DHB, and so it is used. To avoid photo degradation of DHB, a fresh 20 mM DHB water solution is prepared every week and stored in a brown plastic vial that is kept in a refrigerator when not in use.

Meanwhile, it is imagined that the geometry of sample supports might influence the MALDI signal intensity. Thus, a pattern of miniaturized MALDI-MS sample supports of different shapes (single cross, single circle and round patch, 10 each) (see Figure IV.4) was scribed on a hydrophobic silicon chip to investigate the influence of the geometry on the MALDI signal intensity. Figure IV.5 shows the same silicon wafer in Figure IV.4 with 0.3 μL sample droplets of the Glu-Fibrinopeptide B-DHB solution loaded and subsequently focused and crystallized sample spots. The MALDI-MS spectrum acquired from a sample spot on a cross shape sample support shows a strong molecular ion peak of Glu-Fibrinopeptide B and several fragmentation peaks, as well as low noise level (Figure IV.6). Sincer only 0.15 pmole Glu-Fibrinopeptide B is loaded on each miniaturized sample support, compared to the amount usually loaded on a conventional MALDI sample support (1.0 pmole Glu-Fibrinopeptide B used for MALDI-MS instrument calibration generates a spectrum of similar signal intensity, with α-CHCA as the matrix), however, this spectrum shows a 6-7 times improvement in signal intensity. Interestingly,

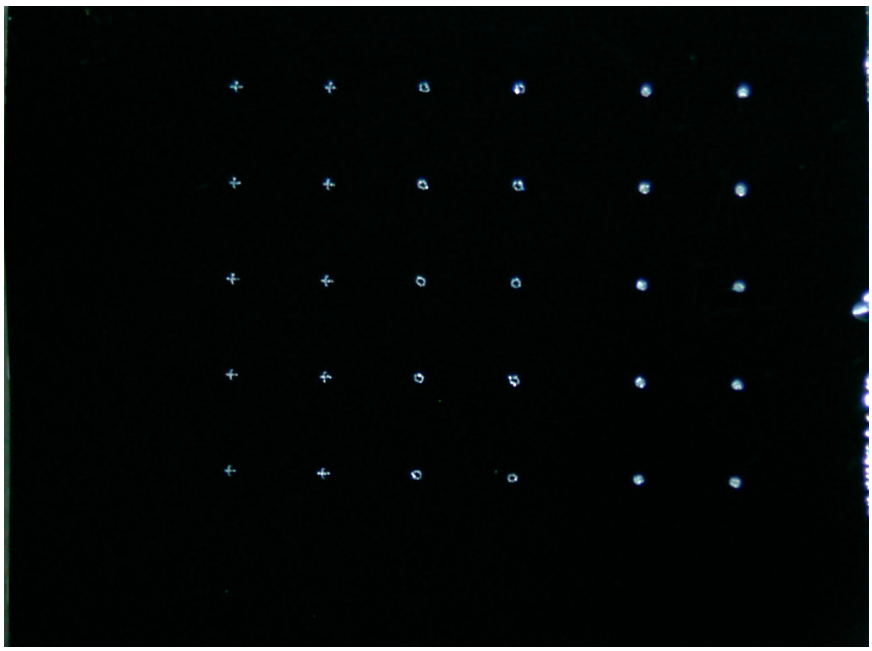

Figure IV.4. A pattern of 10 single cross (left), 10 single circular (middle) and 10 round patch (right) sample supports scribed on a hydrophobic silicon chip.

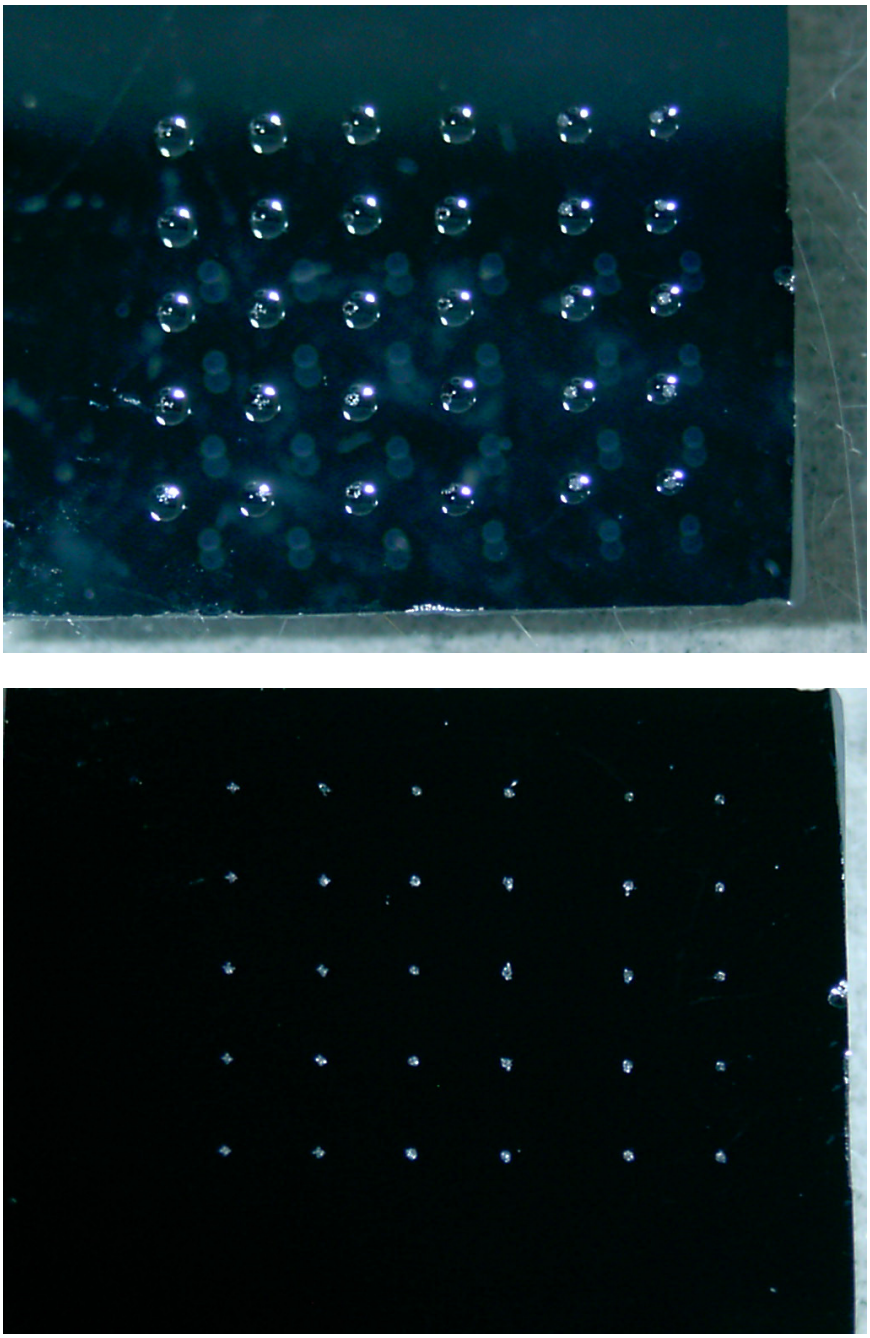

Figure IV.5. The same sample support pattern 0.3 μL Glu-Fibrinopeptide B and DHB mixture solution droplets loaded (upper) and the subsequently focused and crystallized sample spots.

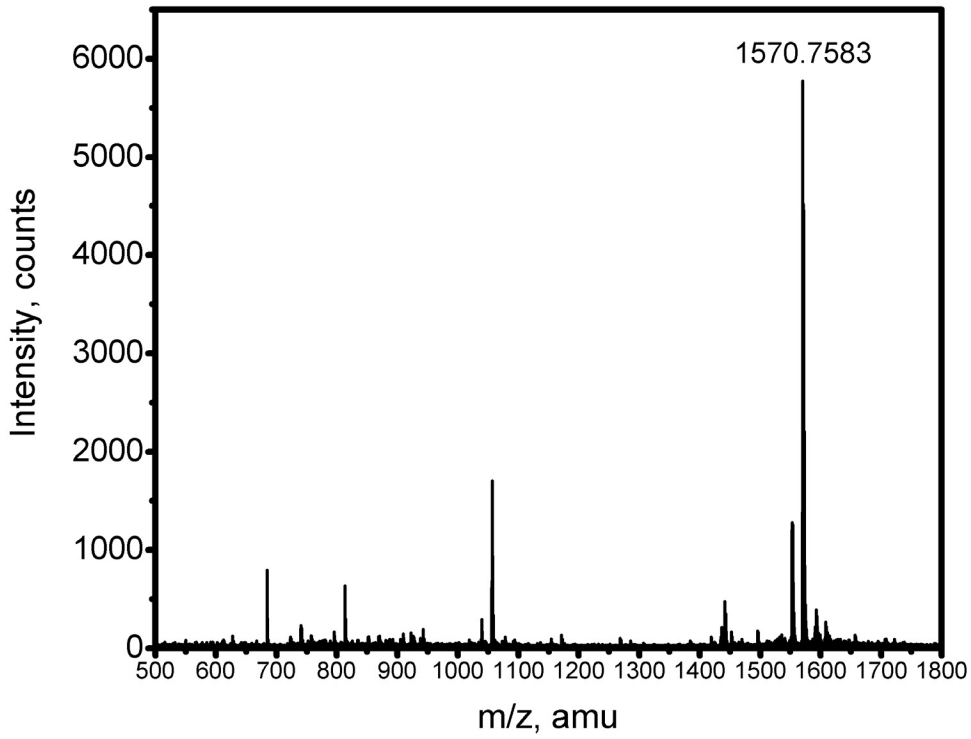

Figure IV.6. A MALDI-MS spectrum of a 50:50 mixture (v/v) of 0.3 μL 1.0 pmol/μL Glu-Fibrinopeptide B solution and 20 mM DHB solution crystallized on a cross-shaped miniaturized MALDI-MS sample support scribed on silicon.

the most intense signals were obtained from the crosses, followed by the circles, which were followed by the round patches (see Figure IV.7). It is also of interest that the standard deviation of the measurements (the error bars) increases with increasing signal intensity, although in all cases the results are far more reproducible than those typically obtained with conventional MALDI sample supports, which give no signal at some points and strong signals elsewhere on the same spot because of much larger inhomogeneous sample spots. The average S/N ratios and standard deviations for the crosses, circles, and round patches are 194.6 ± 102.1, 113.2 ± 48.2, and 89.4 ± 23.3, respectively. A possible explanation for these results is that the smooth, hydrophobic surface released the analyte and matrix more readily than the hydrophilic scribed regions. Indeed, it is observed that dried particles of the sample spots on anchor regions with little hydrophilic area (crosses) under them are fairly easily knocked free by the laser beam.

While silicon is found to be an ideal substrate for making miniaturized MALDI-MS sample supports, silicon wafers are not cheap. It is known that chemical composition and properties of glass are very similar to that of the silicon surface (SiO_2), and glass slides are much cheaper and more readily available than silicon wafers. Most importantly, silane chemistry works equally well on glass slides as on the silicon's native oxide layer,[40] so miniaturized MALDI-MS sample supports can also be scribed on glass slides the same way (cleaning, silanizing and followed by scribing under water) as on silicon chips. Figure IV.8 shows a MALDI-MS spectrum obtained from a circular sample support scribed on a glass slide with a strong molecular ion peak of the test peptide (again, Glu-Fibrinopeptide B), as expected. As mentioned above, MALDI-MS spectra acquired from silicon surfaces (see Figure IV.6) are very similar to that acquired from a

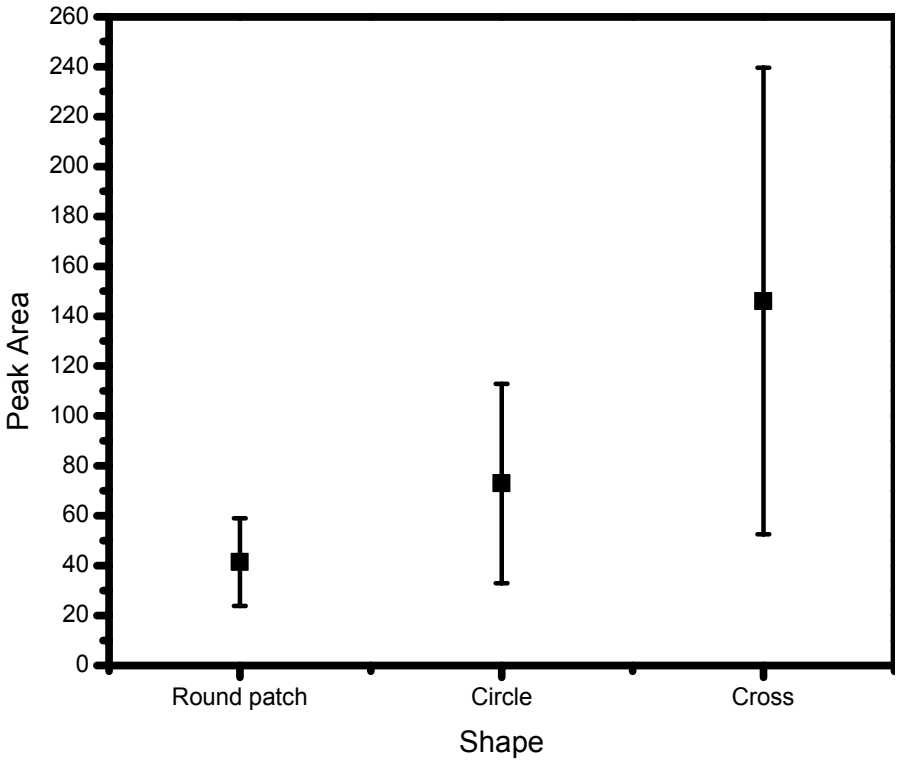

Figure IV.7. Sensitivity and reproducibility of the Glu-Fibrinopeptide B data collected with the miniaturized MALDI-MS sample supports on silicon.

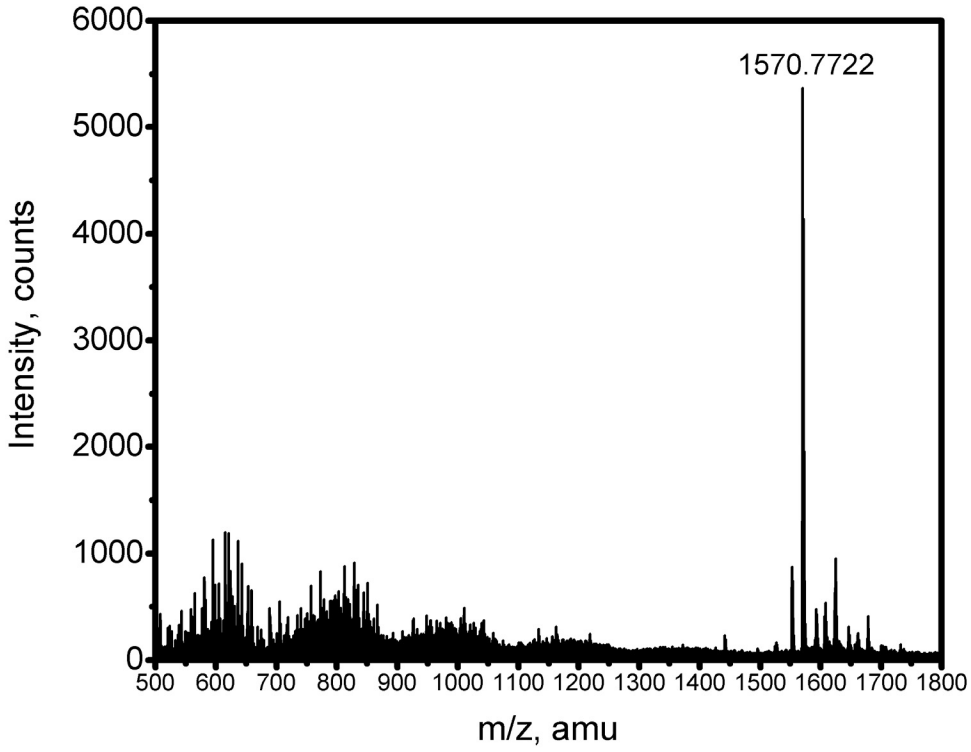

Figure IV.8. A MALDI-MS spectrum of a 50:50 mixture (v/v) of 0.3 μL 1.0 pmol/μL Glu-Fibrinopeptide B solution and 20 mM DHB solution crystallized on a circular miniaturized MALDI-MS sample support scribed on glass.

conventional (metal) MALDI sample plate. However, it can be seen that the spectrum of the test peptide acquired from the glass sample support is slightly different from that acquired from a silicon one. Besides the strong molecular ion peak, higher noise level and more fragmentation are found in the peptide's spectrum from the glass sample support. This difference could be attributed to the glass's insulating nature. It is known that silicon is both electrically and thermally conductive. On the other hand, glass is neither electrically nor thermally conductive. Thus, the laser beam energy would accumulate on a sample spot and cause more fragmentation of the analyte on glass surfaces.

In summary, this work shows that miniaturized MALDI-MS sample supports can be made on hydrophobic silicon and glass surfaces by directly scribing. MALDI-MS spectra acquired with these miniaturized sample supports show better signal intensity and reproducibility than that with conventional MALDI-MS sample supports. These results point the way to a simple, readily fabricated sample support pattern for MALDI-MS.

IV.4 REFERENCES

(1) Karas, M.; Bachmann, D.; Bahr, U.; Hillenkamp, F. *Int. J. Mass Spectrom. Ion Process.* **1987**, *78*, 53.

(2) Tanaka, K.; Waki, H.; Ido, Y.; Akita, S.; Yoshida, Y.; Yoshida, T. *Rapid Commun. Mass Spectrom.* **1988**, *2*, 151.

(3) Linnemayr, K.; Rizzi, A.; Allmaier, G. *J. Chromatography A.* **1997**, *791*, 299.

(4) Overberg, A.; Karas, M.; Bahr, U.; Kaufmann, R.; Hillenkamp, F. *Rapid Commun. Mass Spectrom.* **1990**, *4*, 293.

(5) Overberg, A.; Karas, M.; Hillenkamp, F. *Rapid Commun. Mass Spectrom.* **1991**, *5*, 128.

(6) Spengler, B.; Pan, Y.; Cotter, R. J.; Kan, L.-S. *Rapid Commun. Mass Spectrom.* **1990**, *4*, 99.

(7) Yamagaki, T.; Maeda, M.; Kanazawa, K.; Ishizuka, Y.; Nakanishi, H. *Biosci. Biotechnol. Biochem.* **1996**, *60*, 1222.

(8) Kaltashov, I. A.; Doroshenko, V.; Cotter, R. J.; Takayama, K.; Qureshi, N. *Anal. Chem.* **1997**, *69*, 2317.

(9) Okamoto, M.; Takahashi, K.; Doi, T.; Takimoto, Y. *Anal. Chem.* **1997**, *69*, 2919.

(10) Lloyd, P. M.; Scrivener, E.; Maloney, D. R.; Haddleton, D. M.; Derrick, P. J. *Polym. Prepr.* **1996**, *37*, 847.

(11) Kassis, C. M.; Belu, A. M.; DeSimone, J. M.; Linton, R. W.; Lange, G. W.; Friedman, R. M. *Polym. Prepr.* **1996**, *37*, 833.

(12) Mandal, H.; Hay, A. S. *Polym. Prepr.* **1997**, *38*, 193.

(13) Kassis, C. M.; DeSimone, J. M.; Linton, R. W.; Remsen, E. E.; Lange, G. W.; Friedman, R. M. *Rapid Commun. Mass Spectrom.* **1997**, *11*, 1134.

(14) Kassis, C. M.; DeSimone, J. M.; Linton, R. W.; Lange, G. W.; Friedman, R. M. *Rapid Commun. Mass Spectrom.* **1997**, *11*, 1462.

(15) Yoshida, S.; Yamamoto, S.; Takamatsu, T. *Rapid Commun. Mass Spectrom.* **1998**, *12*, 535.

(16) Mandal, H.; Hay, A. S. *J. Polym. Sci.* **1998**, *36*, 2429.

(17) Spengler, B.; Kaufmann, R. *Analusis* **1992**, *20*, 91.

(18) Zhang, W.; Czernik, A. J.; Yungwirth, T.; Aebersold, R.; Chait, B. T. *Protein Sci.* **1994**, *3*, 677.

(19) Zhang, W.; Chait, B. T. *Anal Chem.* **2000**, *72*, 2482.

(20) Jensen, O. N.; Podtelejnikov, A. V.; Mann, M. *Anal Chem.* **1997**, *69*, 4741.

(21) Zenobi, R.; Knochenmuss, R. *Mass Spectrom. Rev.* **1998**, *17*, 337.

(22) Ledman, D. W.; Danis, P. O. *Enabling Sample Plates for Voyager MALDI ToF Mass Spectrometers*; Applied Biosystems, Inc.

(23) Lewis, J. K.; Wei, J.; Siuzdak, G. *Matrix-Assisted Laser Desorption/Ionization Mass Spectrometry in Peptide and Protein Analysis*; John Wiley & Sons Ltd: Chichester, 2000.

(24) Moren, A.; Hellman, U.; Inada, Y.; Imamura, T.; Heldin, C.-H.; Moustakas, A. *J. Biol Chem.* **2003***, 278*, 33571.

(25) Hellman, U.; Bhikhabhai, R. *Rapid Commun. Mass Spectrom.* **2002***, 16*, 1851.

(26) Persson, C.; Engström, U.; Mowbray, S. L.; Östman, A. *FEBS Lett.* **2002***, 517*, 27.

(27) Grönroos, E.; Hellman, U.; Heldin, C.-H.; Ericsson, J. *Mol. Cell.* **2002***, 10*, 483.

(28) Little, D. P.; Cornish, T. J.; O'Donnell, M. J.; Braun, A.; Cotter, R. J.; Köster, H. *Anal. Chem.* **1997***, 69*, 4540.

(29) Ekström, S.; Ericsson, D.; Önnerfjord, P.; Bengtsson, M.; Nilsson, J.; Marko-Varga, G.; Laurell, T. *Anal. Chem.* **2001***, 73*, 214.

(30) Ekström, S.; Önnerfjord, P.; Bengtsson, M.; Nilsson, J.; Laurell, T.; Marko-Varga, G. *Anal. Chem.* **2000***, 72*, 286.

(31) Schuerenberg, M.; Luebbert, C.; Eickhoff, H.; Kalkum, M.; Lehrach, H.; Nordhoff, E. *Anal. Chem.* **2000***, 72*, 3436.

(32) Marko-Varga, G.; Ekström, S.; Helldin, G.; Nilsson, J.; Laurell, T. *Electrophoresis* **2001***, 22*, 3978.

(33) Xu, Y.; Watson, J. T.; Bruening, M. L. *Anal. Chem.* **2003***, 75*, 185.

(34) Husseini, G.; Peacock, J. G.; Sathyapalan, A.; Zilch, L. W.; Asplund, M. C.; Sevy, E. T.; Linford, M. R. *Langmuir* **2003***, 19*, 5169.

(35) Niederhauser, T. L.; Jiang, G.; Lua, Y.-Y.; Dorff, M. J.; Woolley, A. T.; Asplund, M. C.; Berges, D. A.; Linford, M. R. *Langmuir* **2001***, 17*, 5889.

(36) Jiang, G.; Niederhauser, T. L.; Davis, S. D.; Lua, Y.-Y.; Cannon, B. R.; Dorff, M. J.; Howell, L. L.; Magleby, S. P.; Linford, M. R. *Coll. Surf. A* **2003***, 226*, 9.

(37) Cannon, B. R.; Lillian, T. D.; Howell, L. L.; Magleby, S. P.; Niederhauser, T. L.; Linford, M. R. *In Press Precision Engineering* **2003**.

(38) Ekström, S.; Önnerfjord, P.; Bengtsson, M.; Nilsson, J.; Laurell, T.; Marko-Varga, G. *Anal. Chem.* **2000**, *72*, 286.

(39) Ekström, S.; Ericsson, D.; Önnerfjord, P.; Bengtsson, M.; Nilsson, J.; Marko-Varga, G.; Laurell, T. *Anal. Chem.* **2001,** *73*, 214.

(40) Plueddemann, E. P. *Silane Coupling Agents*; Plenum Press: New York, 1991.

− CHAPTER V −

LASER-ACTIVATION MODIFICATION OF SURFACES (LAMS)

V.1 INTRODUCTION

Surface modification and surface patterning continue to be topics of much interest in the literature and in industry. Thus a wide variety of methods have been recently developed and studied. These include photolithography,[1] e-beam lithography,[2] microcontact printing,[3] dip pen nanolithography,[4] and chemomechanical surface modification.[5, 6] Light plays the central role in photolithography. Light has also been used to induce monolayer formation on and/or pattern hydrogen-terminated,[7-12] iodine-terminated,[13] and porous silicon.[14, 15] In these latter reports, the exposure time to light ranged from a few minutes up to a few hours, where 30 min was typical.

It is well known that the high power of modern lasers can cause surface ablation. For example, laser ablation of solids is an important method for laser-induced breakdown spectroscopy (LIBS),[16,17] direct solid sampling for inductively coupled plasma mass spectrometry (ICP-MS)[18] and for micromachining a variety of different materials.[19] Nanosecond laser pulses cause both ablation and melting of the surface, while femtosecond pulses cause ablation with minimal surface heating.[20] Feature size is limited by the focusing optics, and by the wavelength of light, with features less than 10 μm being recently reported.[21]

Here a new and extremely rapid technique for surface modification is reported, which is termed as laser activation-modification of surfaces, or LAMS. This method

consists of wetting a surface, *e.g.*, silicon or germanium, with a compound and then firing an intense, nanosecond pulse of laser light through the liquid onto the surface. It is believed that the high energy of these pulses ablates a thin layer (oxide layer) from the surface, exposes a highly reactive surface (pure silicon or germanium with radicals generated by the laser energy) that appears to react essentially instantaneously with the liquid it is in contact with. These initial studies represent a compromise between two extremes that should be easily attainable with this method: extreme ablation with the formation of deep features, and little or no damage to the surface.

V.2 EXPERIMENTAL SECTION

V.2.1 Materials

Water was obtained from a Millipore Milli-Q water system. Silicon(100) wafers (p-boron, 2-6 Ω cm, test grade) were obtained from Montco Silicon Technologies. Germanium(100) wafers (n-type) were obtained from Universal wafer. Octane (99+%), 1-dodecene (95%), 1,7-octadiene (98%), 1-chlorooctane (99%), 1-bromooctane (99%), 1-iodooctane (98%), 1,2-epoxyoctane (96%), 1,2,7,8-diepoxyoctane (97%), perfluorodecalin (95%) were obtained from Aldrich. 1-Hexene (97%) and 1-octene (97%) were obtained from Acros. 1-Tetradecene (97%) and 1-hexadecene (99%) were obtained from Fluka. 1-Decene (96%) was obtained from Lancaster and 1-octanol (certified) was obtained from Fisher Scientific. All reagents were used as received except silicon(100) and germanium(100) were cleaned as described in the literature[24] before use.

V.2.2 Laser Setting and Sample Preparation

All LAMS experiments were carried out with pulses from a Nd:YAG (Coherent Infinity) laser (see Figure V.1) in an open laboratory with compounds that were not degassed or specially treated in any way. To prepare a LAMS sample, first, a clean silicon or germanium chip is loaded on a manually controlled two-dimensional translation stage and wet with a reagent; the laser energy is then focused by a short focus lens (50 mm) onto the reagent-wet silicon or germanium wafer. Obviously the size and/or depth of laser-burned sample spots are determined by many factors, such as laser wavelength, laser energy and the distance of the wafer to the focal plane of the lens. Here LAMS samples are prepared by using 1 mJ of a 532 nm laser light with a pulse length of 4 ns (a 532 nm laser is ideal for this purpose because most liquid reagents, but not silicon or germanium, are transparent to it). A 335 nm laser is also used in preparing laser-burned miniaturized MALDI-MS sample supports. The lasers are run at 1 Hz to guarantee that only one laser pulse is incident on each spot on the sample.

V.2.3 XPS and ToF-SIMS Analyses

XPS with a monochromatic Al Kα source and a hemispherical analyzer was performed with either an SSX-100 spectrometer (Figures V.2 and V.8) or a PHI Quantum 2000 instrument (Figure V.3). The PHI instrument employed a small spot size (50, 100, or 200 μm) that fitted inside the spots it analyzed. For the SSX-100 instrument, a larger area of the surface was functionalized and analyzed. Time-of-flight secondary ion mass spectrometry (ToF-SIMS) analysis was performed with an ION-TOF TOF-SIMS IV instrument with monoisotopic 25 KeV $^{69}Ga^{+}$ primary ions run in bunched mode.

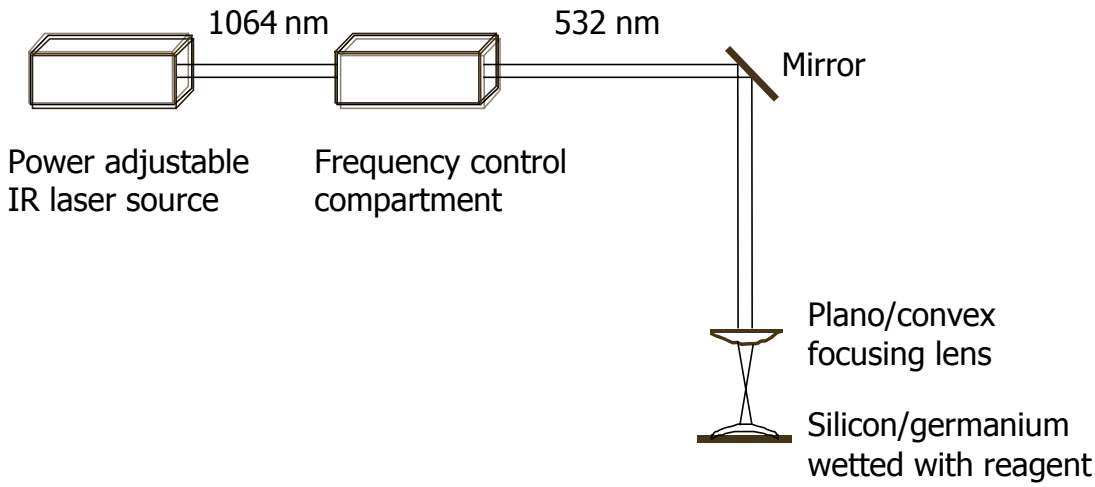

Figure V.1. Schematic of laser settings for LAMS.

V.3 RESULTS AND DISCUSSION

As an initial demonstration of LAMS, Figure V.2 shows XPS survey spectra of silicon after laser irradiation in the presence of the air and four liquids. The dominant features of spectrum (a) (the air) are strong O1s and appreciable Si signals. Small N1s and C1s signals are also present. In contrast, LAMS on silicon under a liquid (b-e) shows much less oxygen, along with notable C1s signals that are comparable to Si2s and Si2p peak intensities. These carbon signals are consistent with monolayer quantities of carbon.[22, 23] The surface prepared under 1-iodooctane (d) shows a very small amount of iodine (the atomic sensitivity factor for iodion is large), and the surface prepared with perfluorodecalin (e) shows a strong F1s signal, as well as a strong C1s signal. A C1s narrow scan (not shown) of the spot created under perfluorodecalin indicates carbon is chemically shifted by fluorine. Thus, the high energy of laser pulses appears to allow surface functionalization with compounds (like perfluorodecalin) that do not contain reactive functional groups. This possibility will be explored further below.

To better understand the surface chemistry of LAMS, high resolution small-spot XPS was used to probe inside regions functionalized with four different hydrocarbons: 1-octene, 1-dodecene, 1-hexadecene, and 1-iodooctane. The unfunctionalized control regions near the functionalized areas were also studied. All of the functionalized (or unfunctionalized) features were similar, and representative spectra are shown in Figure V.3 (also see the supporting figures). For example, Figure V.3a shows the high-resolution C1s peak from a spot functionalized with 1-hexadecene. This spectrum contains two prominent features attributable to silicon carbide (SiC) and hydrocarbon, *i.e.*, unoxidized carbon (C-C/C-H), and small amounts of oxidized carbon. In contrast, the spectra from

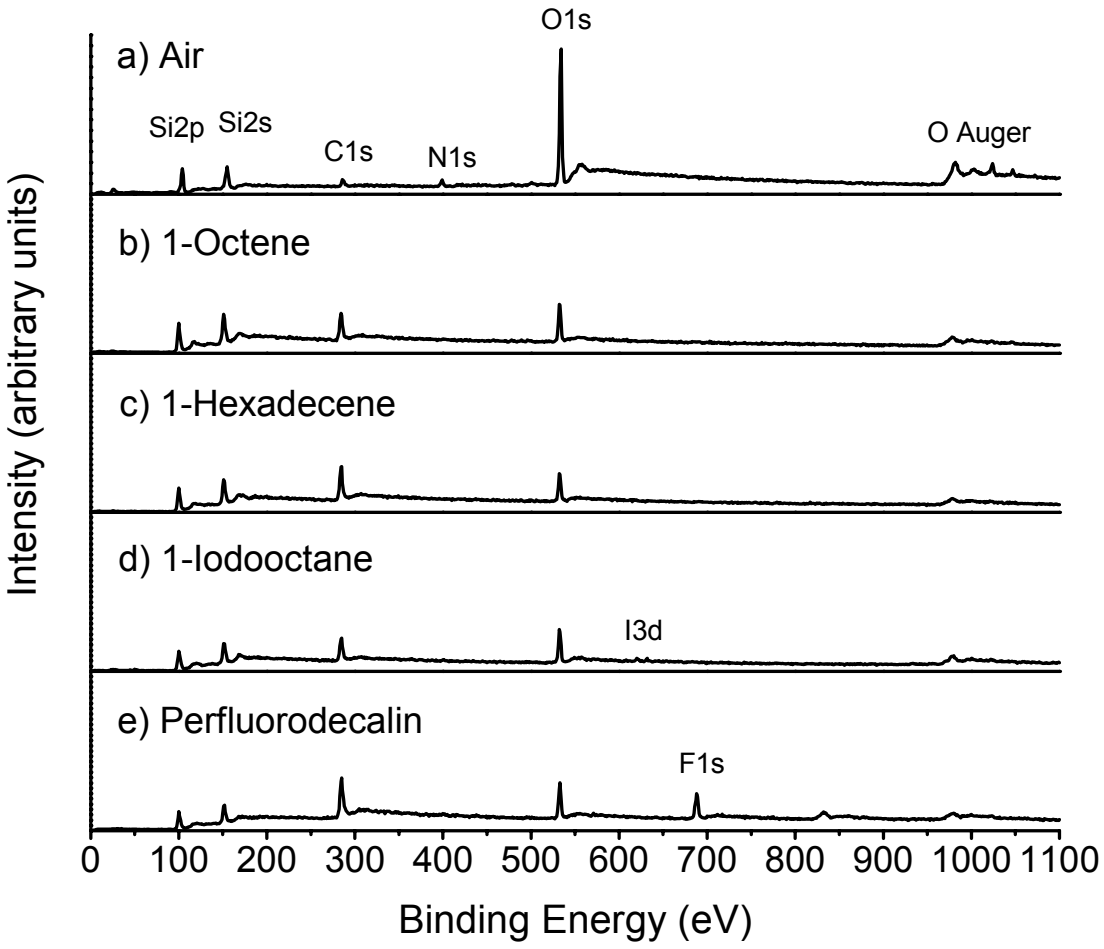

Figure V.2. XPS survey spectra of LAMS of silicon irradiated under a) the air, b) 1-octene, c) 1-hexadecene, d) 1-iodooctane, and e) perfluorodecalin.

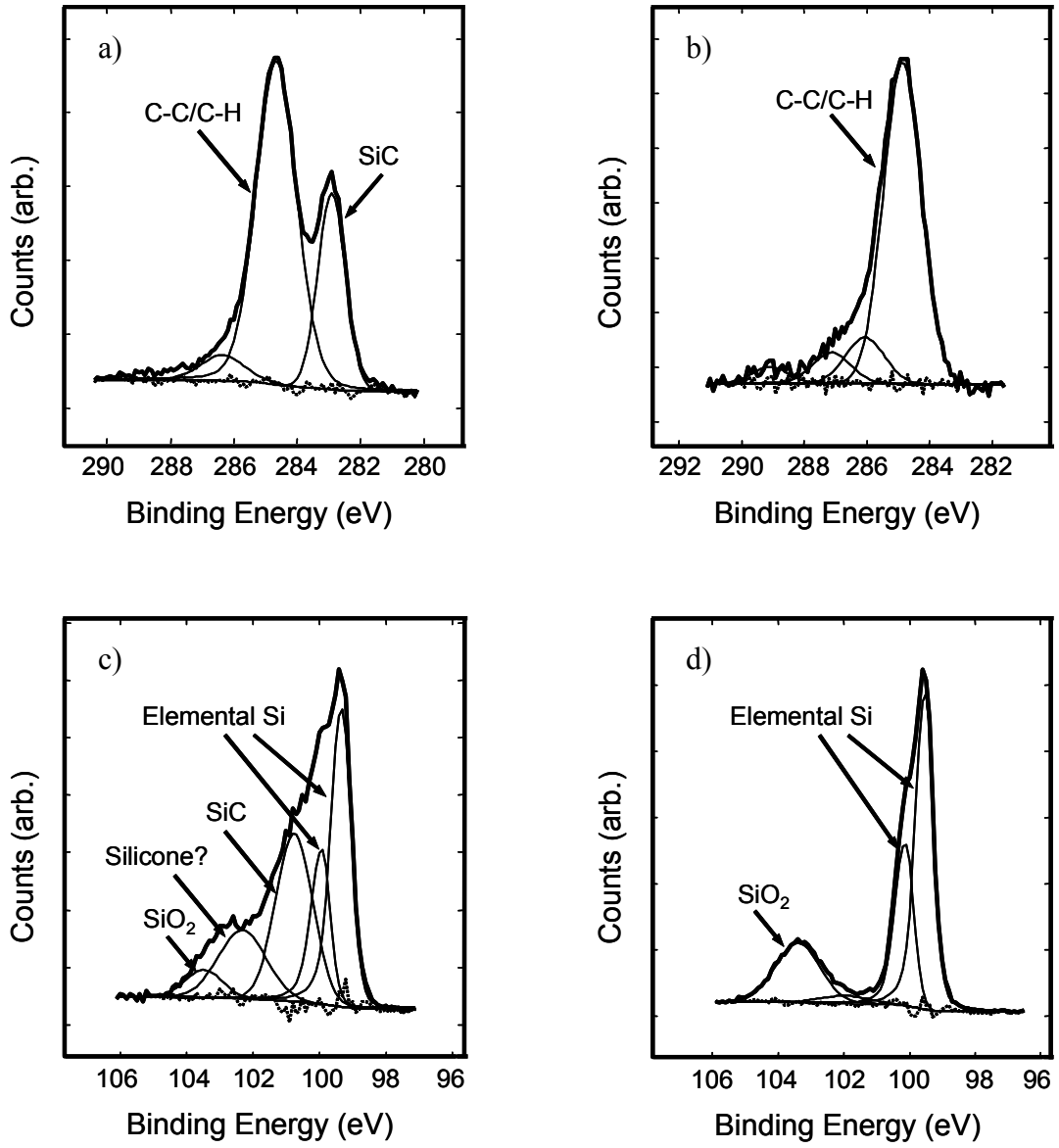

Figure V.3. LAMS of silicon using 1-hexadecene: a) C1s and c) Si2p narrow XPS scans, and control regions (not irradiated) that were wet with 1-iodooctane: b) C1s and d) Si2p narrow XPS scans. (Data taken by Greg Strossman at Charles Evans & Associates.)

surrounding control areas that were not irradiated, and which presumably contain only adventitious carbon, show hydrocarbon and small amounts of oxidized carbon, but no carbide (see Figure V.3b). The spectra that are similar to Figure V.3a and Figure V.3b were obtained from other functionalized and unfunctionalized regions, respectively (see the supporting figures). The lability of C-I bond no doubt contributes to the somewhat lower carbon (and iodine) content of the surface ablated under 1-iodooctane (the iodine content in three scans was 0.13 ± 0.06 atom percent). C1s/Si2p XPS ratios obtained for LAMS with 1-alkenes are generally about 1.5 - 2 times higher than C1s/Si2p ratios for silicon scribed in the presence of the same reagents.[24,25]

High-resolution Si2p XPS scans were similarly taken of silicon modified (and unmodified) by LAMS. Figure V.3c shows a representative Si2p region from silicon modified by LAMS with 1-hexadecene. Peaks attributable to elemental silicon, SiC, SiO_2, and to what appears to be a silicone-like species that contains both oxygen and carbon bonds are present. In contrast, Figure V.3d shows the Si2p narrow scan from a control region of the silicon that was not irradiated. It consists mostly of bulk silicon and SiO_2. XPS Spectra that are similar to Figure V.3c for LAMS and similar to Figure V.3d for regions that were not irradiated were obtained from other functionalized and unfunctionalized regions, respectively (see the supporting figures).

With little effort it is possible to create functionalized spots by LAMS with diameters between 100 and 500 μm. Figure V.4 shows the ToF-SIMS negative-ion images of a small spot (*ca.* 100 μm) and a rather large spot (*ca.* 450 μm) of silicon functionalized with octane and 1-bromooctane, respectively. These images clearly show more H^-, C^-, CH^-, C_2^-, C_2H^-, $^{79}Br^-$, and $^{81}Br^-$, and less O^-, OH^- and SiO_2^- from

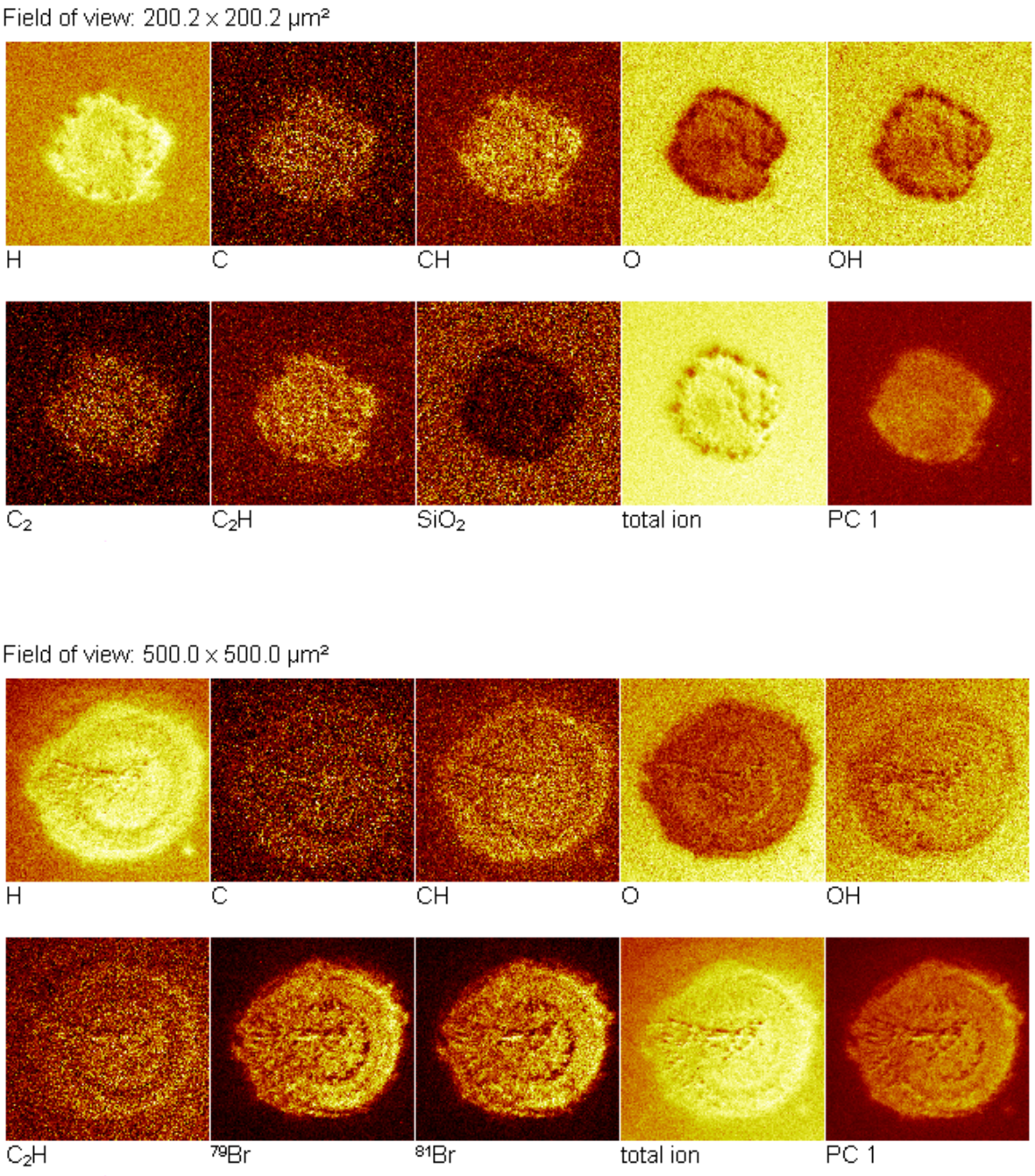

Figure V.4. ToF-SIMS negative-ion images of LAMS spots on silicon (higher image brightness indicates stronger signal intensity). Upper panel: silicon wet with octane. Lower panel: silicon wet with 1-bromooctane.

functionalized regions. Total ion images of functionalized and unfunctionalized regions suggest some chemical variation between LAMS spots and backgrounds; the first principal components (PC1s) from a principal components analysis (PCA) show a clear chemical difference between these regions. In general, the best chemical contrast in ToF-SIMS imaging is obtained for anions based on heteroatoms in negative-ion images. While some fragments in positive-ion spectra do show the expected chemical contrast, these spectra tend to be dominated by hydrocarbon fragments, which are also formed from the adventitious hydrocarbon contamination in background regions. However, PC1s of essentially all positive- or negative-ion image analyses show functionalized and background areas to be chemically homogeneous to themselves and distinct from each other (see the supporting figures). Little chemical variation appears to be present between the spot and the background on silicon ablated in the air (Figure V.5).

To show the generality of LAMS, ToF-SIMS images were obtained for spots made by LAMS on silicon for a variety of liquids and conditions, including a homologous series of 1-alkenes (1-hexene, 1-octene, 1-decene, 1-dodecene, 1-tetradecene, and 1-hexadecene), two other alkyl halides (1-chlorooctane and 1-iodooctane), the air (as a control), 1,2-epoxyoctane, and 1-octanol (their ToF-SIMS images are shown in the supporting information). All liquids showed strong reactivity with the surface. Both XPS and ToF-SIMS data (Figure V.6) show that C/Si ratios of LAMS samples prepared with different chain length 1-alkenes slightly increase with carbon numbers in 1-alkenes, while O/Si ratios (XPS) slightly decrease. These trends provide further support to the surface functionalization by LAMS.

Because of huge energy densities that can be created with focused laser pulses,

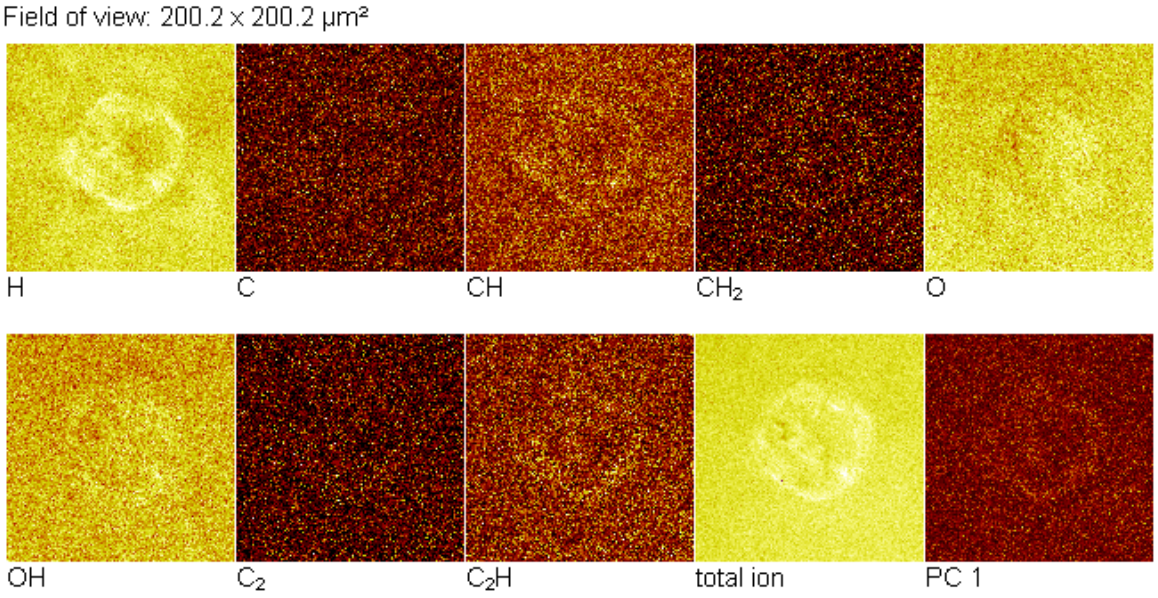

Figure V.5. ToF-SIMS negative-ion images of a spot on silicon made by LAMS in the air.

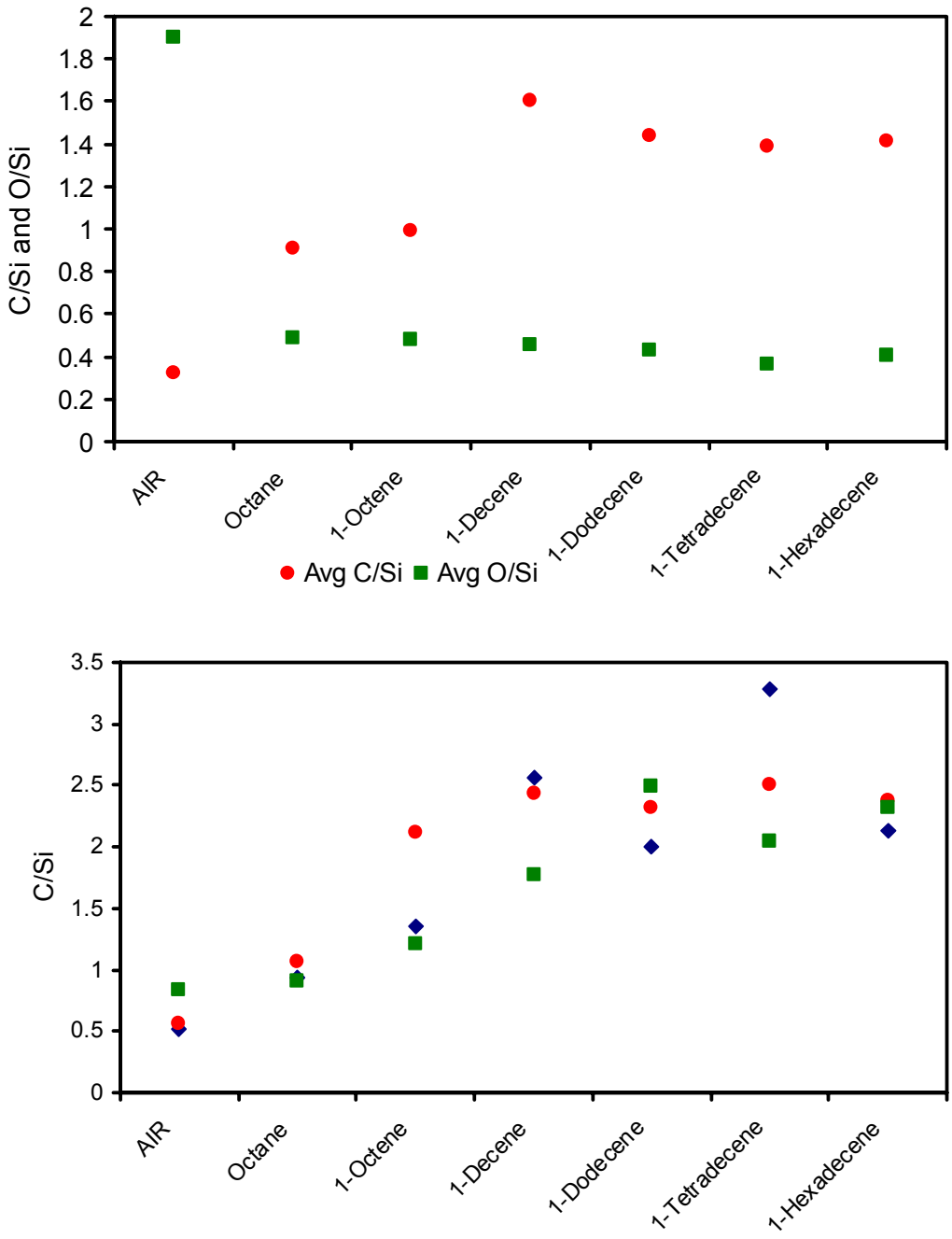

Figure V.6. Carbon and/or oxygen to silicon ratios of XPS (upper panel) and ToF-SIMS (lower panel, positive data: carbon = $\sum C_xH_y^+$, silicon = $\sum Si_xO_y^+$) of the functionalized spots by LAMS.

the possibility of modifying surfaces with LAMS under a liquid without obvious functionality was further investigated. ToF-SIMS negative-ion images and positive-ion spectral data, as well as XPS data (Figure V.4, V.6 and V.2) of LAMS of silicon wet with octane suggest the silicon surface functionalization with non-reactive reagents. It is noteworthy that total ion yields from octane's functionalized and unfunctionalized regions are similar, but PC1 shows them to be chemically distinct (see Figure V.4). Based on the fact that the silicon surface functionalization by LAMS with non-reactive reagents (octane and perfluorodecalin) and both XPS and ToF-SIMS C/Si ratios only slightly increase with carbon numbers in 1-alkenes, different from what were seen in the silicon surface functionalization by scribing, where no reaction was observed under octane and C/Si ratios almost linearly increased with carbon numbers in 1-alkenes,[26] here a somewhat different reaction mechanism is suggested for LAMS from that suggested for scribing silicon. That is, unlike scribing, the laser energy in LAMS not only removes the surface oxide layer and breaks Si-Si bonds (of course silicon radicals on the surface can initiate reactions with reactive reagents), but also cracks the hydrocarbon molecules in the immediate vicinity of the spots to form small fragment radicals, which then react with the activated silicon surface. The cracking of reagent molecules was not through direct absorption of the laser beam energy (the laser beam travels through a liquid and hits the silicon surface), but by the high temperature in the near vicinity caused by the laser beam energy, which damages the silicon surface and causes liquids to erupt as seen in the LAMS experiments. This is also supported by the SEM image of a laser-burned spot on silicon (see Figure V.7), where the raised features on the spot most probably indicate silicon condensing after being melted by the laser energy (very high temperature at the

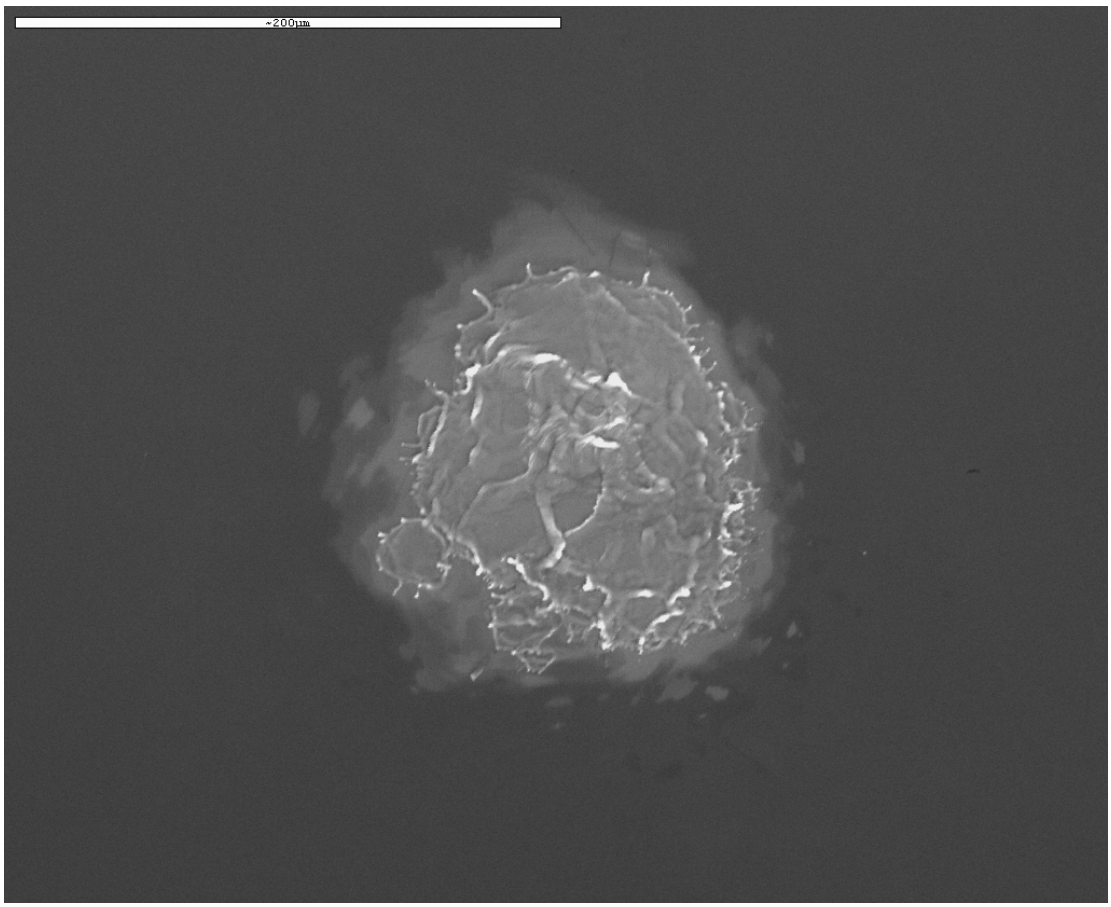

Figure V.7. SEM of a laser burned spot on a silanized hydrophobic silicon chip.

spot), while the big circular shadow around the spot probably indicates a partially damaged surrounding area caused by heat dissipation from the center.

The general approach for preparation of reactive monolayers is to use bifunctional compounds, where one of the functional groups has a special affinity for the substrate and the other imparts desired functionality to the monolayer surface.[22] High energy densities in nanosecond laser pulses of the LAMS change this paradigm. LAMS samples were made on silicon that was wet with the air, octane, 1-octene, and 1,7-octadiene, and then exposed to HCl vapor for 6 days (HCl adds readily across carbon-carbon double bonds). Cl/Si ratios of their ToF-SIMS spectra were then calculated[27] and found to be 0.23 ± 0.04, 6.4 ± 1.8, 5.8 ± 2.3, and 14.7 ± 1.4 for LAMS of silicon in the air, octane, 1-octene, and 1,7-octadiene, respectively (three measurements each). Thus, the high energy imparted to the surface in LAMS appears to create surface functionality from unfunctionalized starting materials. This can also be explained with the reaction mechanism suggested above.

A more detailed view of the feature depth and morphology was obtained with AFM (see the supporting information). For example, section analyses of *ca.* 100 μm spots created by LAMS are shown to be craters that are *ca.* 1.0 – 1.5 μm deep, with a ridge of silicon that is also *ca.* 1.0 - 1.5 μm higher than the surrounding substrate.[28] Typically, a few protruding features are also present within the functionalized region. By using different laser conditions, it should be possible to control the depth and morphology of these features.

It is believed that LAMS has the potential to become a general method for surface modification and patterning of a wide variety of substrates and reagents, where

requirements are some degree of activation of substrates by the laser pulse and at least some level of transparency of reagents, which might even be a gas. A first step towards generality is to demonstrate that a second substrate can be functionalized by LAMS. Figure V.8 shows the XPS survey spectra of germanium that underwent LAMS in the presence of a) the air, and b) 1-hexadecene. Notable differences between the spectra are that the surface irradiated in the air shows weak C1s and strong O1s signals, while the surface prepared in 1-hexadecene shows much stronger C1s and weaker O1s signals. ToF-SIMS images similar to those shown in Figure V.4 for silicon were also obtained for germanium ablated in the presence of 1-hexadecene and 1-iodooctane (see the supporting information).

While this investigation only shows functionalization/patterning with two substrate materials, there probably exists a wide variety of reagents and materials (organic/polymeric, ceramic, and metallic) that would react in this manner. It is believed that LAMS will become an important technique for modifying and patterning surfaces at dimensions that range from the diffraction limit of light up to hundreds of microns or larger because the lasers and optics required for it are readily accessible to many in the technical community. The fact that microcontact printing[3] is so widely practiced is an evidence for the need for effective methods to functionalize surfaces at micron dimensions. Also, with optics and/or masks that are readily available, entire surfaces could be rapidly functionalized with LAMS in a parallel fashion, as is currently done in photolithography. It follows that LAMS could be easily automated for production of large numbers of precisely patterned substrates. Similar to scribing miniaturized MALDI-MS sample supports on a hydrophobic silicon surface,[29] LAMS is also successfully

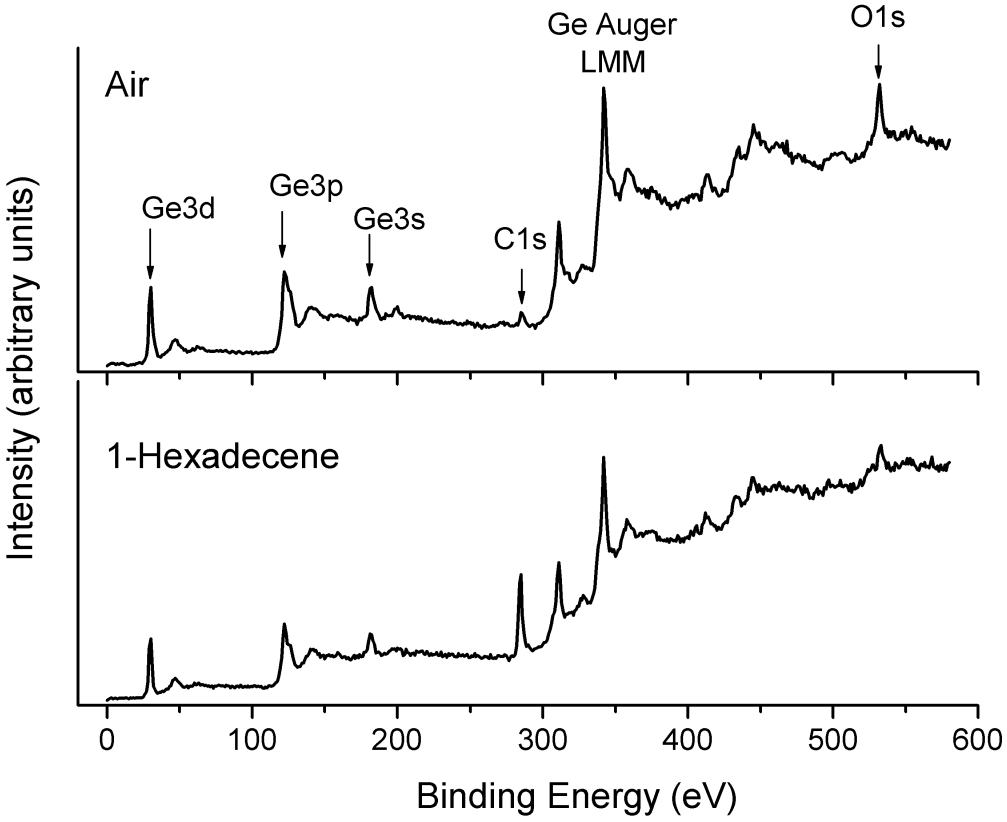

Figure V.8. XPS survey spectra of germanium by LAMS under the air and 1-hexadecene.

applied in making miniaturized MALDI-MS sample supports on hydrophobic silicon (see Figure V.9). Its process is even faster and more precisely controlled than that of scribing. Of course, lasers are more widely available compared to the scribing apparatus. It can be seen that test analyte-matrix water solution droplets focused and crystallized on the tiny sample supports (*ca.* 200 μm diameter). Again, the large shadow surrounding each sample support indicates a partially damaged area by the heat dissipation from the laser-burned sample support. Expected MALDI-MS spectra for a test peptide were also acquired from miniaturized sample supports made by LAMS (not shown).

In summary, this work shows the development of a new and general technique, LAMS, for extremely rapid, simultaneous functionalization and patterning of materials. Examples of functionalization using an alkane, a perfluoroalkane, 1-alkenes, and alkyl halides were given. Two different substrates were patterned. Functionalization by LAMS is carried out with inexpensive precursor materials and straightforward surface preparations. Surface modification is also demonstrated with reagents that are quite inert. Laser intensities and wavelengths used in LAMS functionalization mean that this technique can be extended to inexpensive pulsed lasers. Also, high energies available with pulsed lasers open up new possibilities in surface modification by driving chemistry that cannot be performed at room temperature, as was suggested in the formation of silicon nitride (Figure V.2a) and silicon carbide (Figure V.3). Its possible reaction mechanism was discussed and an application of it in MALDI-MS was investigated.

Supporting information is available, including high resolution XPS C1s and Si2p scans, ToF-SIMS and AFM images of LAMS of silicon, tables containing peak fitting results from XPS C1s and Si2p narrow scans of LAMS of silicon with different reagents.

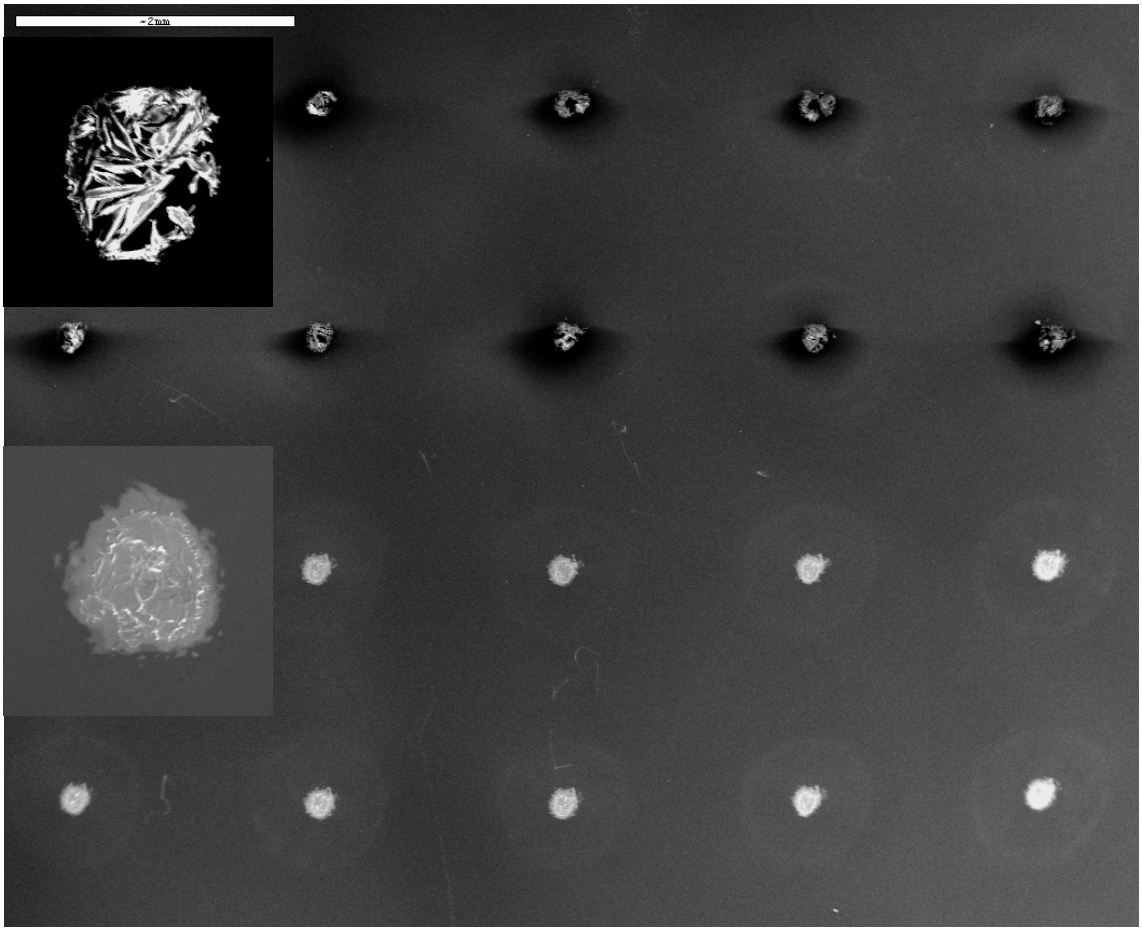

Figure V.9. SEM of a pattern of the miniaturized MALDI-MS sample supports on the hydrophobic silicon by LAMS (*ca.* 200 μm diameter; scale bar = 2 mm). Upper part: the sample supports loaded with the dried and crystallized test samples (also see the upper left inset); lower part: the bare sample supports (also see the lower left inset).

V.4 REFERENCES

(1) Brodie, I.; Murray, J.; Muray, J. J. *The Physics of Microfabrication*; Plenum, 1982.

(2) Sheats, J. R.; Smith, B. W. *Microlithography: Science and Technology*; Marcel Dekker: New York, 1998.

(3) Xia, Y.; Whitesides, G. M. *Annu. Rev. Mater. Sci.* **1998**, *28*, 153.

(4) Piner, R. D.; Zhu, J.; Xu, F.; Hong, S.; Mirkin, C. A. *Science* **1999**, *283*, 661.

(5) Niederhauser, T. L.; Lua, Y.-Y.; Jiang, G.; Davis, S. D.; Matheson, R.; Hess, D. A.; Mowat, I. A.; Linford, M. R. *Angew. Chem., Int. Ed.* **2002**, *41*, 2353.

(6) Lua, Y.-Y.; Lee, M. V.; Fillmore, W. J. J.; Matheson, R.; Sathyapalan, A.; Asplund, M.C.; Fleming, S. A.; Linford, M. R. *Angew. Chem. Int. Ed.* **2003**, *42*, 4046.

(7) Linford, Stanford University (Thesis), 1996.

(8) Cicero, R. L.; Linford, M. R.; Chidsey, C. E. D. *Langmuir* **2000**, *16*, 5688.

(9) Effenberger, F.; Götz, G.; Bidlingmaier, B.; Wezstein, M. *Angew. Chem., Int. Ed.* **1998**, *37*, 2462.

(10) Wojtyk, J. T. C.; Tomietto, M.; Boukherroub, R.; Wayner, D. D. M. *J. Am. Chem. Soc.* **2001**, *123*, 1535.

(11) Sieval, A. B.; Linke, R.; Zuilhof, H.; Sudhölter, E. J. R. *Adv. Mater.* **2000**, *12*, 1457.

(12) Eves, B. J.; Sun, Q.-Y.; Lopinski, G. P.; Zuilhof, H. *J. Am. Chem. Soc.* **2004**, *126*(44), 14318.

(13) Cai, W.; Lin, Z.; Strother, T.; Smith, L. M.; Hamers, R. J. *J. Phys. Chem. B* **2002**, *106*, 2656.

(14) Lee, E. J.; Ha, J. S.; Sailor, M. J. *J. Am. Chem. Soc.* **1995**, *117*, 8295.

(15) Lee, E. J.; Bitner, T. W.; Ha, J. S.; Shane, M. J.; Sailor, M. J. *J. Am. Chem. Soc.* **1996**, *118*, 5375.

(16) Loree, T. R.; Radziemski, L. J. *Proceedings of the Technical Program - Electro-Optics/Laser Conference & Exposition* **1981**, 28.

(17) Radziemski, L. J.; Loree, T. R.; Cremers, D. A. *Springer Series in Optical Sciences* **1983**, *39*, 303.

(18) Russo, R. E.; Mao, X.; Liu, H.; Gonzalez, J.; Mao, S. S. *Talanta* **2002**, *57*, 425.

(19) Salle, B.; Gobert, O.; Meynadier, P.; Perdrix, M.; Petite, G.; Semerok, A. *Appl. Phys. A* **1999**, *69*, S381.

(20) Chichkov, B. N.; Momma, C.; Nolte, S.; von Alvensleben, F.; Tunnermann, A. *Appl. Phys. A* **1996**, *63*, 109.

(21) Korte, F.; Serbin, J.; Koch, J.; Egbert, A.; Fallnich, C.; Ostendorf, A.; Chichkov, B. N. *Appl. Phys. A* **2003**, *77*, 229.

(22) Ulman, A. *An Introduction to Ultrathin Organic Films: from Langmuir-Blodgett to Self-Assembly*; Academic Press: Boston, 1991.

(23) Linford, M. R.; Fenter, P.; Eisenberger, P. M.; Chidsey, C. E. D. *J. Am. Chem. Soc.* **1995**, *117*, 3145.

(24) Niederhauser, T. L.; Jiang, G.; Lua, Y.-Y.; Dorff, M. J.; Woolley, A. T.; Asplund, M. C.; Berges, D. A.; Linford, M. R. *Langmuir* **2001**, *17*, 5889.

(25) Niederhauser, T. L.; Lua, Y.-Y.; Sun, Y.; Jiang, G.; Strossman, G. S.; Pianetta, P. Linford, M. R. *Chem. Mater.* **2002**, *14*, 27.

(26) Niederhauser, T. L.; Lua, Y.-Y.; Jiang, G.; Davis, S. D.; Matheson, R.; Hess, D. A.; Mowat, I. A.; Linford, M. R. *Angew. Chem. Int. Ed.* **2002**, *41*(13), 2353.

(27) The Cl/Si ratio was obtained by integrating and performing the following calculation on peaks from negative ion spectra: (35Cl + 37Cl)/(SiO2 + SiHO2 + SiO3 + SiHO3 + SiHO + Si + SiH).

(28) Yoo, H. J.; Jeong, S. H.; Greif, R.; Russo, R. E. *J. Appl. Phys.* **2000**, *88*, 1638.

(29) Linford, M. R.; Davis, R. C.; Magleby, S. P.; Howell, L. L.; Jiang, G.; Thulin, C. D. Woodhead Publishing, 2005.

− CHAPTER VI −

MUTIVARIATE ANALYSIS OF TOF-SIMS IMAGES OF LASER-ACTIVATION MODIFICATION OF SURFACES OF SILICON WITH 1-ALKENES.

VI.1 INTRODUCTION

Time-of-flight secondary ion mass spectrometry (ToF-SIMS) is a powerful tool for surface analysis. Secondary ion spectra, secondary ion images or depth profiles can be easily acquired with ToF-SIMS. With typical, conventional data analysis methods, an analysis would be focused only on a few characteristic peaks according to the pre-knowledge to the samples, and these peaks would be compared from sample to sample. This approach usually works well for known samples. However the risk of missing important information for unknown samples is real since the majority of sample data is wasted with this approach. In contrast, in multivariate data analysis methods, for example, principal component analysis (PCA), which is often used in spectral data analysis, the majority of spectral data is used to avoid the risk of missing important information in a data set.[1] The automated expert spectral image analysis (AXSIA) method, which has been used in ToF-SIMS image data analysis, also extracts information from the ToF-SIMS total ion image of a sample instead of some selected individual ion images.[2]

PCA takes into account the majority of a sample data set to extract essential factors, or principal components (PCs) that capture major variations of a data set and cause differences among samples. In other words, PCA can usually simplify a complex data set into several PCs that account for major differences among samples of concern.

Each PC is associated with scores, or projections of samples in the data set on that PC, which essentially separate samples into subgroups by similarities, and loadings, which describe contributions of original variables or peaks to the PC. So, a PCA analysis for a ToF-SIMS data set reveals major factors that cause variations among samples, and compositions of these major factors. This is very useful for handling overwhelming data sets acquired by modern instruments like ToF-SIMS.

AXSIA was originally developed by Sandia National Laboratories and broadly used for analysis of data sets collected with many different instruments. AXSIA uses a multivariate curve resolution (MCR) methodology to interpret a ToF-SIMS total ion image by a limited number of major component images.[3-7] Each component image is determined by a same scale spectrum with characteristic spectral signatures. Compared to individual ToF-SIMS ion images, these components are more representative in describing the chemical information of sample surfaces.

Here AXSIA analysis of ToF-SIMS images of laser-activation modification of surfaces (LAMS) of silicon with a homologous series of 1-alkenes followed by PCA analysis of AXSIA component spectra is reported. The AXSIA analysis of ToF-SIMS images of LAMS of silicon with 1-alkenes generates essentially two types of AXSIA components for each sample, the background or unmodified part and the functionalized region. A PCA analysis of component spectra generated by AXSIA shows that all component spectra comprising the background form a cluster based on similarity showing significant inorganic spectral characteristics; while, in contrast, all component spectra from functionalized regions form a separate cluster showing significant organic spectral characteristics, all as expected. These results provide additional characterization

for the surface modification by LAMS of silicon wet with 1-alkenes. This type of analysis should be useful for other ToF-SIMS imaging as well.

VI.2 EXPERIMENTAL SECTION

VI.2.1 Materials

Silicon(100) wafers (p-boron, 2-6 Ω cm, test grade) were obtained from Montco Silicon Technologies (Spring-City, PA). 1-Hexene (97%) and1-octene (97%) were obtained from Acros. 1-Decene (96%) was obtained from Lancaster. 1-Dodecene (95%) was obtained from Aldrich. 1-Tetradecene (97%) and 1-hexadecene (99%) were obtained from Fluka. All chemicals were used as received. Water was obtained from a Millipore Milli-Q water system, and acetone was reagent grade.

VI.2.2 Sample Preparation

All LAMS experiments were carried out with pulses from a Nd:YAG (Coherent Infinity) laser in an open laboratory with compounds that were not degassed or specially treated in any way, as described in Chapter V. Briefly, to prepare a LAMS sample, a clean silicon wafer is loaded on a manually controlled two-dimensional translation stage and then wet with a reagent. A laser beam is then focused onto the reagent-wetted silicon chip. Here LAMS samples are usually prepared by using 1 mJ of a 532 nm laser light with a pulse length of 4 ns. The laser is run at 1 Hz to guarantee that only one laser pulse is incident on each spot on the sample. Samples are then cleaned again with a standard procedure described before and stored in a vacuum chamber before ToF-SIMS analysis.

VI.2.3 ToF-SIMS Imaging

ToF-SIMS was performed with an ION-TOF TOF-SIMS IV instrument with a monoisotopic 25 KeV $^{69}Ga^{+}$ primary ion beam run in bunched mode. 1-Alkene-modified LAMS spots on silicon are around 100 μm in diameter. ToF-SIMS images were then taken over an imaging area of 201 μm × 201 μm, with a LAMS spot in each imaging area. Imaging resolution of 128 × 128 pixels, 5 shots per pixel and 30 scans per image were used. A bunch of single ions and total ions for each sample were selected for real-time imaging and these images were then saved for subsequent comparison. Raw data files were saved for AXSIA analysis.

VI.2.4 AXSIA Analysis of ToF-SIMS Imaging

AXSIA was running in a PC Microsoft Windows 2000 operation system. To do AXSIA analysis, ToF-SIMS raw data files were first converted into a format that could be read by AXSIA. To reduce file size, the mass range of 0-400 was binned every 0.5 amu (e.g., 0.25-0.75 amu is 0.5 amu, 0.75-1.25 amu is 1.0 amu, etc.). The AXSIA analysis generated component images that were visualized in different colors to express chemical variations among a ToF-SIMS imaging area, and corresponding spectra of the components for a given ToF-SIMS raw data file. The data file before AXSIA analysis was visualized as a so-called mean image, similar to its ToF-SIMS total ion image.

VI.2.5 PCA Analysis of AXSIA Components

PCA analysis of AXSIA component spectra helps to interpret chemical variations shown on the component images. To do PCA, a data matrix was created with all major

positive or negative component spectra of all samples. In other words, a component spectrum became a row and every binned 0.5 amu unit became a column of the matrix. After normalization of each row, the matrix was then loaded and analyzed using a PLS_Toolbox 3.0 PCA program (Eigenvector Research Inc.) that runs on a PC Matlab platform, where a mean centering data preprocessing and a CL of 95% were used. The first principal component (PC1) generated by PCA that captured the majority of the variation in the data matrix and its loadings plot were chosen for further consideration.

VI.3 RESULTS AND DISCUSSION

Figure VI.1 shows the comparison of AXSIA images and original ToF-SIMS images of silicon modified with 1-decene and 1-tetradecene by LAMS. As expected, AXSIA analysis on negative ToF-SIMS image data files shows that there are essentially two major distinct regions on each sample, the unmodified region or background represented by AXSIA component 1 or C1 (in red), and the modified spot represented by C2 (in green) and C3 (in blue). Different colors of component images serve as a visual aid, and the dark area on any image means low signal intensity. The composite image shows contributions of C1, C2 and C3 in each sample. It is obvious that AXSIA's component images (C1, C2, C3) and the composite image reveal that the background and 1-alkene modified regions are significantly different in chemical characteristics, while the mean image prior the AXSIA analysis and the ToF-SIMS total ion image do not show much variation over the imaging areas. Though the same general variation is also shown by the individual ToF-SIMS images (O-, H^-, C_2H^-, Si^-, etc.), AXSIA results that consider a much larger fraction of ToF-SIMS data have better contrast. The reason why C2 and C3

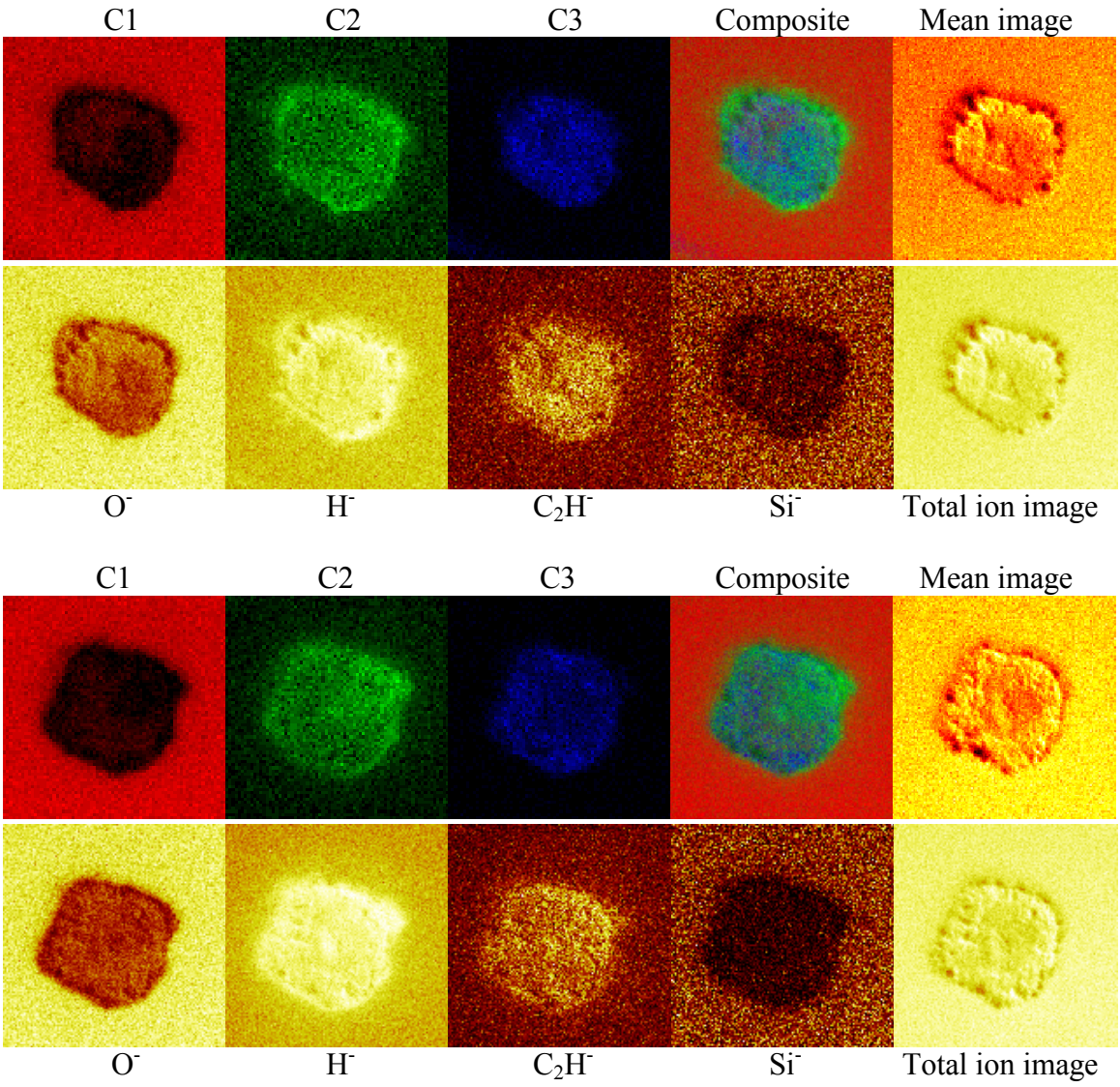

Figure VI.1. AXSIA images and selected ToF-SIMS images of the negative-ion imaging of LAMS of silicon with 1-decene (upper panel), and 1-tetradecene (lower panel) (Data analysis by Vincent S. Smentkowski at GE).

both come out from modified regions is most probably because of the roughness of modified regions burned by the laser energy and/or chemical heterogeneity in modified regions. This reason may also explain the darker rings that surround the modified regions on the mean and total ion images.

Consistent results were again obtained from the AXSIA analysis of positive ToF-SIMS images of 1-alkene modified silicon surfaces by LAMS, which again basically have two chemically distinct regions, the background and the modified area (see Figure VI.2). Here each row includes a sample's AXSIA component images, the composite image and its original Si^+ image by ToF-SIMS for comparison. Again C1 indicates the background and C2 and/or C3 indicate 1-alkene modified regions. It is seen that samples modified with 1-decene and 1-tetradecene (the 3rd and 5th rows in Figure VI.2) contain only two major components C1 and C2; and the C2 of the sample modified with 1-dodecene (4th row) is closer to C1, instead of C3.

Component spectra of AXSIA components give spectral sources for chemical variations over the imaging area or among components of each sample. Figure VI.3 shows negative-ion AXSIA component spectra (mass range 0-100) of silicon surfaces modified with 1-hexene and 1-hexadecene. It is obvious that component spectra of two C1s of these two samples are similar but are significantly different from C2s and C3s, which are similar to each other and from sample to sample. These are consistent with component image results. These spectra clearly show variations among components. For example, SiO_2^- and SiO_3^- peaks are seen in C1 spectra from unmodified silicon, while $Si_2C_2^-$ peaks are seen in C3 spectra, which provide additional evidence for alkyl surface modification by LAMS. In contrast, a typical univariate analysis would easily miss this information.

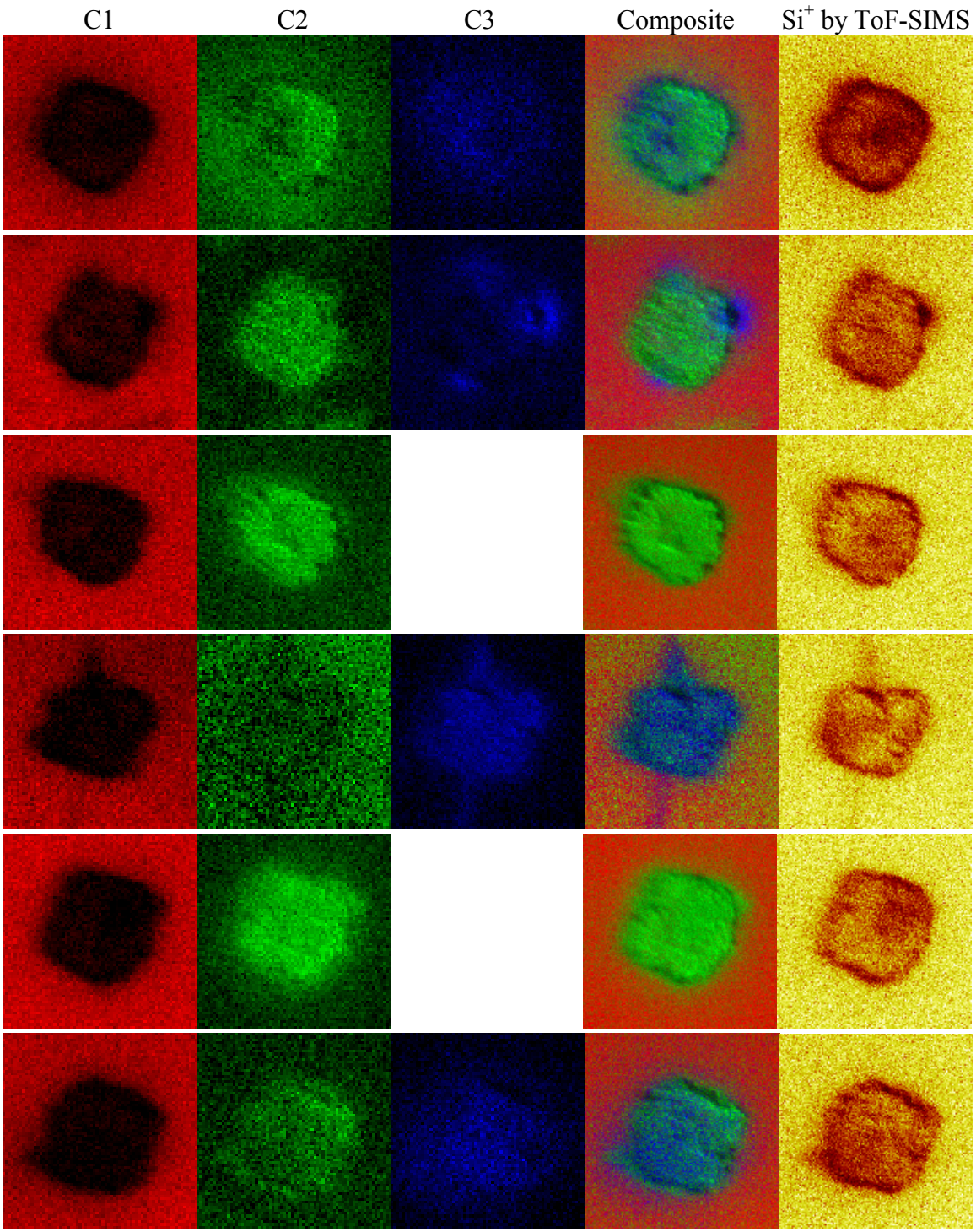

Figure VI.2. AXSIA and Si^+ images of ToF-SIMS positive-ion imaging of LAMS of silicon with 6, 8, 10, 12, 14, and 16 carbon 1-alkenes, respectively (from top to bottom). (Data analysis by Vincent S. Smentkowski at GE).

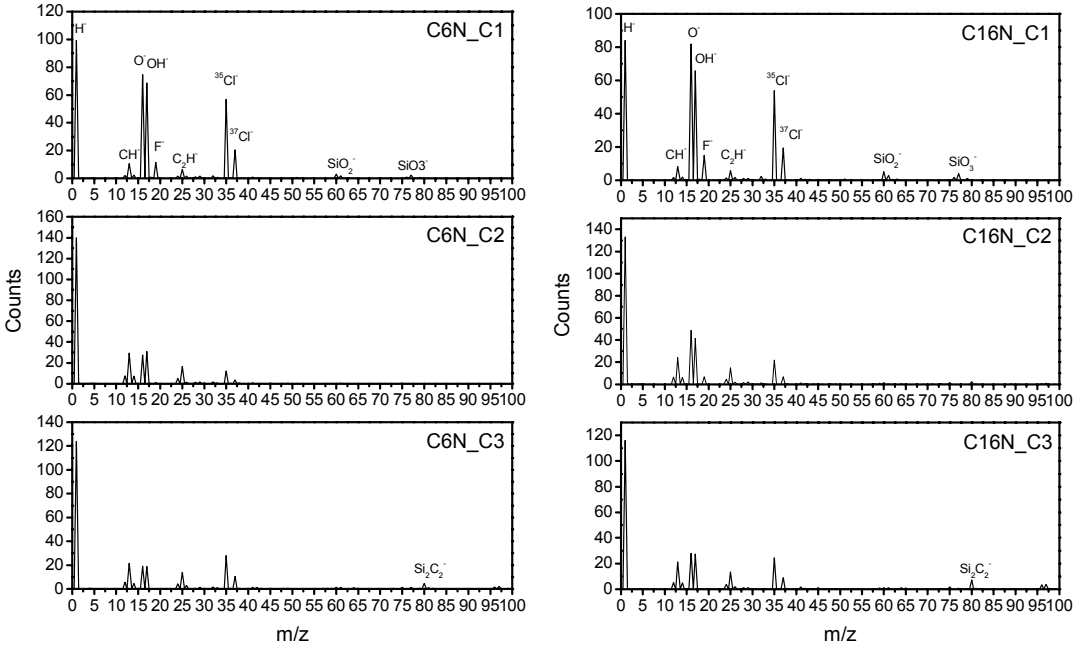

Figure VI.3. Negative-ion AXSIA component spectra of the ToF-SIMS imaging of LAMS of silicon with 1-hexene (left) and 1-hexadecene (right).

Similarly, Figure VI.4 shows positive component spectra (mass range 0-100) of silicon surfaces modified with 1-octene and 1-hexadecene. Compared to negative spectra, these positive spectra look more complicated and similar to each other, except their intensities. Thus obvious differences are not as easily discerned. This makes it even more difficult to do the conventional spectral comparison by univariate analysis.

To more fully understand the chemistry of LAMS of silicon surfaces modified with 1-alkenes, PCA analyses were conducted separately for negative and positive peak data matrices of AXSIA component spectra from all different samples. Figure VI.5 and 6 show scores plots (left panel) and loadings plots (right panel) of PC1s of the PCA analyses of negative- and positive-ion AXSIA component spectra, respectively. Note that here the negative PC1 captures over 82% of the total variation of the whole negative data matrix and the positive PC1 captures over 70% of the total variation of the positive ion data matrix. Thus it is reasonable to focus following discussions on PC1s of both PCA analyses.

In Figure VI.5, it is seen that all negative-ion C1s and 1-dodecene's C4 have negative scores and form a cluster, while, in contrast, all negative-ion C2s and C3s, as well as 1-octene's C4 have positive scores and form another cluster on the PC1. This result is again consistent to above results from the component images (see Figure VI.1) and spectra (see Figure VI.3). Though C4s of 1-dodecene and 1-octene are not shown either in images or spectra, based on the clusters they fall in to, it is obvious that 1-dodecene's C4 is closer to its C1, or shows mostly the chemical characteristics of the unmodified region; while 1-octene's C4 is closer to its C2 and C3, or shows mostly the chemical characteristics of the 1-octene modified region. Second, the corresponding

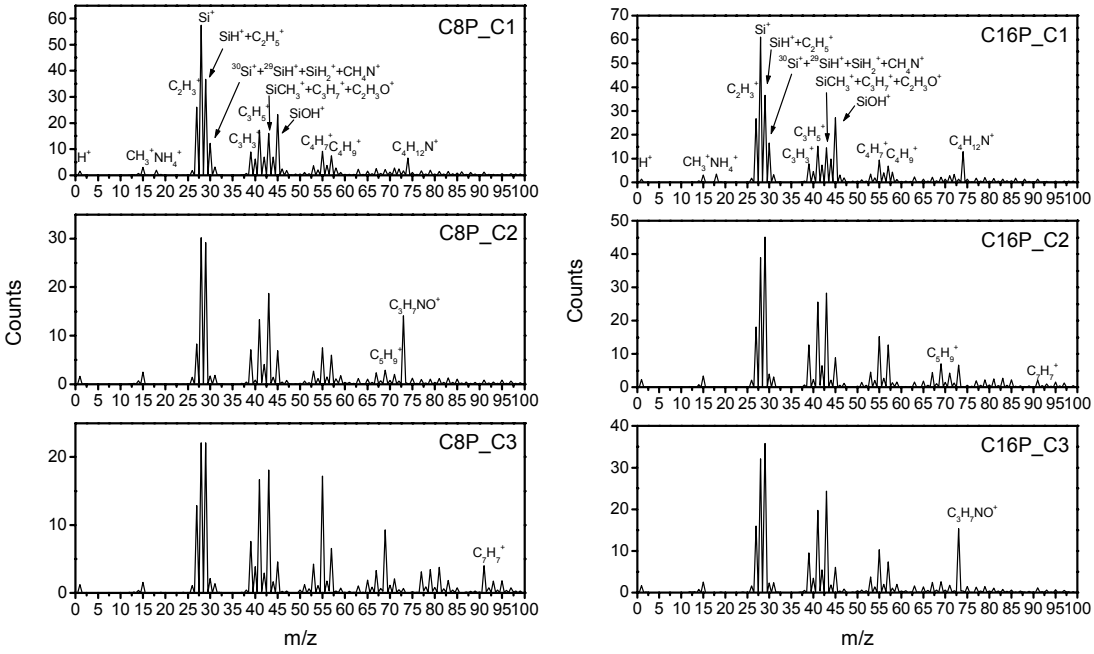

Figure VI.4. Positive-ion AXSIA component spectra of the ToF-SIMS imaging of LAMS of silicon with 1-octene (left) and 1-hexadecene (right).

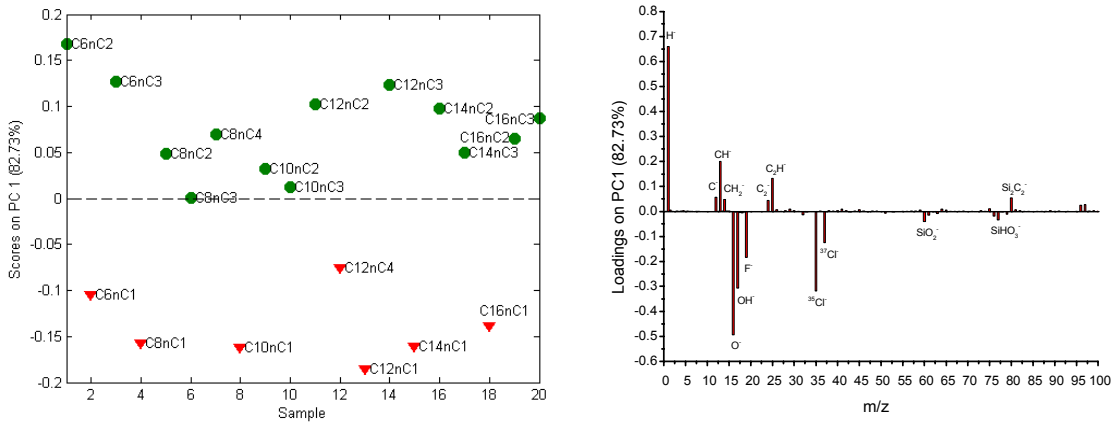

Figure VI.5. PCA analysis on the negative-ion AXSIA component spectra of the ToF-SIMS imaging of LAMS of silicon with 6, 8, 10, 12, 14 and 16 carbon 1-alkenes.

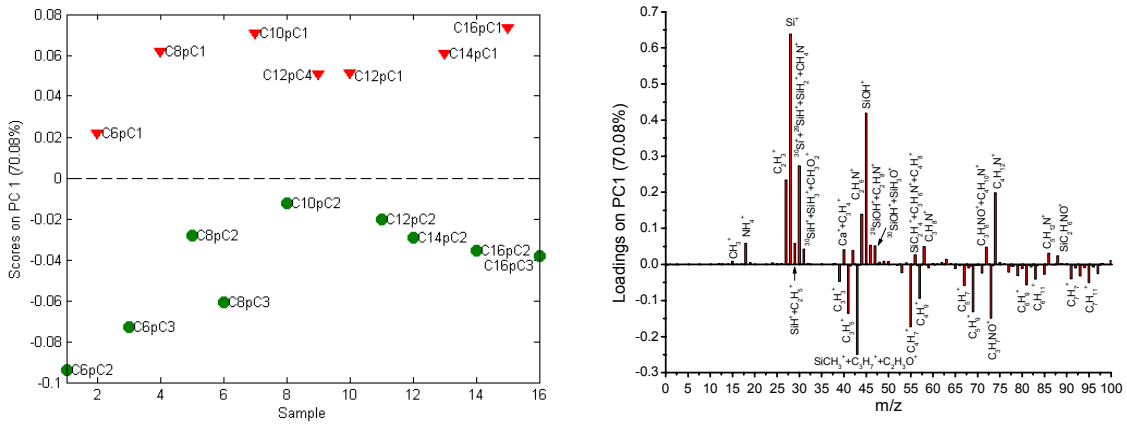

Figure VI.6. PCA analysis on positive-ion AXSIA component spectra of the ToF-SIMS imaging of LAMS of silicon with 6, 8, 10, 12, 14 and 16 carbon 1-alkenes.

PC1's loading plot shows that, in general, positive loadings on the PC1 come from organic peaks (H^-, C^-, CH^-, CH_2^-, C_2^-, C_2H^-, $Si_2C_2^-$, etc.) and negative loadings come from inorganic peaks (O^-, OH^-, F^-, Cl^-, SiO_2^-, SiO_3^-, etc.) of ToF-SIMS spectra of silicon surfaces. It is usually the case that in PCA all positive loadings of a PC are more or less anti-correlated to all negative loadings of the same PC, while either positive or negative loadings are more or less correlated to themselves. We see these trends in the more organic species and the less inorganic species in an AXSIA analysis. Furthermore, loadings and scores of a PC are also correlated in a positive-positive and negative-negative mode. Thus, based on Figure VI.5 and these relationships among PCA values, it can be deduced that all C1s or the unmodified regions contain more inorganic species and all C2s and C3s or the 1-alkene modified regions contain more organic species.

Figure VI.6 shows basically the same consistent results as that of Figure VI.5 from the positive component data set, however, in a reverse mode that, in general, organic species and all C2s and C3s have negative values while inorganic species and all C1s have positive values. As is known that, in PCA, the variable/peak that captures the most amount of variation in a data matrix always takes positive value, as well as its correlated variables/peaks, and correspondingly, all anti-correlated variables/peaks take negative values.

VI.4 CONCLUSIONS

AXSIA analyses of the ToF-SIMS imaging of silicon surfaces modified with 1-alkenes by LAMS followed by PCA analyses of AXSIA component spectra, effectively reveal chemical variations and their origins of each sample. These results provide

additional evidence for the silicon surface modification by LAMS, as well as a successful example of combining AXSIA and PCA multivariate analysis methods in interpreting ToF-SIMS imaging data. However, neither AXSIA nor PCA results show significant trend corresponding to the change of carbon numbers in 1-alkenes. Repeat sets of data show good reproducibility of ToF-SIMS (see Figure V.6) without multivariate analysis.

VI.5 REFERENCES

(1) Li, Y; Lua, Y.-Y.; Jiang, G.; Tyler, B. J.; Linford, M. R. *Anal. Chem.* **2005**, *77*, 4654.

(2) Smentkowski, V. S.; Keenan, M. R.; Ohlhausen, J. A.; Kotula, P. G. *Anal. Chem.* **2005**, *77*, 1530.

(3) Keenan, M. R.; Kotula, P. G. U.S. Patent 6,584,413, June 24, 2003. Keenan, M. R.; Kotula, P. G. U.S. Patent 6,675,106, Jan 6, 2004.

(4) Ohlhausen, J. A.; Keenan, M. R.; Pebbles, D. E.; Kotula, P. G.; American Vacuum Society 48th International Symposium, October 29, 2001; Abstr. As_MoM3.

(5) Ohlhausen, J. A.; Kotula, P. G.; Keenan, M. R.; Peebles, D. E. 15th Annual Workshop on Secondary Ion Mass Spectrometry, May 1, 2002.

(6) Ohlhausen, J. A.; Keenan, M. R.; Kotula, P. G.; Peebles, D. E. *Appl. Surf. Sci.* **2004**, *231-232*, 230-234.

(7) Smentkowski, V. S.; Ohlhausen, J. A.; Kotula, P. G.; Keenan, M. R. *Appl. Surf. Sci.* **2004**, *231-232*, 245-249.

− CHAPTER VII −

CONCLUSIONS AND FUTURE WORK

VII.1 CONCLUSIONS

Systematic investigations were performed on stability, mechanism of formation and applications of alkyl monolayers that were chemomechanically prepared on silicon surfaces. A new method of surface modification, laser-activation modification of surfaces (LAMS), and multivariate analyses on ToF-SIMS images of LAMS spots were also reported.

XPS and other data show that alkyl monolayers prepared by scribing silicon under reactive compounds, including 1-iodoalkanes and 1-alkenes, were stable over extended periods of time to air, water, a boiling acid and Al Kα X-rays. The stability was attributed to direct Si-C bonding in the monolayers. The observation that the oxygen signal gradually increased and the iodine signal gradually decreased, with both reaching plateaus eventually, is attributed to the oxidation of exposed silicon by scribing, and the hydrolysis of Si-I bonds, respectively. In alkyl monolayers prepared with 1-alcohols, however, the carbon signals decreased about 50% after two 1-h immersions in a boiling acid, suggesting unstable Si-O bonding.

In the analogous experiment of grinding silicon with alkyl halides, the expected free-radical combination and disproportionation byproducts were observed with gas chromatography mass spectrometry (GC-MS). This observation provides evidence for the

free-radical mechanism previously proposed for alkyl monolayer formation on silicon by chemomechanically scribing.

With the chemomechanical scribing technique, miniaturized sample supports for MALDI-MS were made on hydrophobic silicon or glass surfaces at low cost and in short time. With these sample supports, significantly improved MALDI-MS signal intensities and reproducibilities were achieved for a test peptide, as expected.

Similar to chemomechanical modification, a new and promising technique of surface modification, LAMS, was developed. XPS and ToF-SIMS data show that both silicon and germanium were effectively modified by LAMS with even unreactive compounds. This technique was also successfully applied in making miniaturized MALDI-MS sample supports. Compared to scribing, LAMS is faster and can be more precisely controlled.

Multivariate analyses, AXSIA and PCA were successfully used in interpreting ToF-SIMS images of LAMS spots on silicon. Both analyses show that modified and unmodified areas on silicon are chemically different.

VII.2 FUTURE WORK

This work systematically investigated the stability, reaction mechanism and applications of chemomechanically prepared alkyl monolayers on silicon and/or other material surfaces. Combining previous work completed by Linford and coworkers, significant progress has been achieved in chemomechanical surface modification. Though some details, such as factors that affect surface coverage, monolayer orientation, and protection of alkyl monolayers to substrates, are still left unknown and are valuable for

further investigation, as well as to scribe other substrates and/or with other compounds. In the future, it is important to focus on exploring possible applications of this technique in areas like the immobilization of proteins, peptides and DNAs, bioassays, cell cultivations, and some other areas, which would drive the further development of this technique.

While LAMS is a new promising technique in surface modification, there are still many unknowns to be explored. Investigations need to be done in clarifying the mechanism of modification with more solid evidence, influence of laser parameters (wavelength, energy, beam size and pulse duration) on the LAMS surface modification, and the stability and homogeneity of formed monolayers. Since laser equipment is widely available and it is expected to keep improving, application areas of LAMS can be broader than that of chemomechanical scribing if further progress in understanding LAMS is achieved. Also, it might be valuable to investigate inducing surface modification and/or making patterns like miniaturized MALDI-MS sample supports on hydrophobic surfaces with other surface treatment techniques, such as electron beam and plasma.

− APPENDIX −

SUPPORTNG INFORMATION

I. FOR FINITE ELEMENT ANALYSES: DATA FOR SURFACE AREA AND ENERGY OF WATER DROPS OF VARIOUS VOLUMES USING SURFACE EVOLVER

Note: surface area (the surface area at the liquid-air interface) = area – 0.49 (the base area).

1) Results for Volume = 20 μL. Summary: surface area = 0.32389 ± 0.00001, energy = 24.317 ± 0.001. Details (after 7 refinements): Vertices: 197122 Edges: 590336 Facets: 393216 Facet edges: 1179648 Memory: 155824496.

   Last 5 iterations:

   5. area: 0.813897428809947 energy: 24.3173722522362 scale: 0.000469926

   4. area: 0.813897395379322 energy: 24.3173697821892 scale: 0.000819120

   3. area: 0.813897369062029 energy: 24.3173678519052 scale: 0.000469541

   2. area: 0.813897348560813 energy: 24.3173663133566 scale: 0.000817199

   1. area: 0.813897331634152 energy: 24.3173650592901 scale: 0.000469357

2) Results for Volume = 40 μL. Summary: surface area = 0.46161 ± 0.00001, energy = 36.774 ± 0.001. Details (after 7 refinements): Vertices: 197122 Edges: 590336 Facets: 393216 Facet edges: 1179648 Memory: 155824496.

   Last 5 iterations:

   5. area: 0.951618728344227 energy: 36.7746009469853 scale: 0.000334824

   4. area: 0.951618671304419 energy: 36.7745959725226 scale: 0.000542815

3. area: 0.951618620825049 energy: 36.7745917959062 scale: 0.000339572

2. area: 0.951618585036603 energy: 36.7745883664555 scale: 0.000536948

1. area: 0.951618551830462 energy: 36.7745854313419 scale: 0.000342863

3) Results for Volume = 60 μL. Summary: surface area = 0.60617 ± 0.00001, energy = 50.633 ± 0.001. Details (after 7 refinements): Vertices: 197122 Edges: 590336 Facets: 393216 Facet edges: 1179648 Memory: 155824496.

Last 5 iterations:

5. area: 1.09617524446562 energy: 50.6329328505371 scale: 0.000475052

4. area: 1.09617517988721 energy: 50.6329269766974 scale: 0.000602318

3. area: 1.09617512828768 energy: 50.6329222771545 scale: 0.000485459

2. area: 1.09617509229076 energy: 50.6329184861605 scale: 0.000594499

1. area: 1.09617506268794 energy: 50.6329153650943 scale: 0.000491422

4) Results for Volume = 80 μL. Summary: surface area = 0.74772 ± 0.00001, energy = 64.827 ± 0.001. Details (after 7 refinements): Vertices: 197122 Edges: 590336 Facets: 393216 Facet edges: 1179648 Memory: 155824496.

Last 5 iterations:

5. area: 1.23772833024781 energy: 64.8276565279546 scale: 0.000917061

4. area: 1.23772830467924 energy: 64.8276516830126 scale: 0.000848779

3. area: 1.23772829729486 energy: 64.8276478966155 scale: 0.000927707

2. area: 1.23772829612270 energy: 64.8276448016906 scale: 0.000867516

1. area: 1.23772830479607 energy: 64.8276421935107 scale: 0.000938826

5) Results for Volume = 100 μL. Summary: surface area = 0.88550 ± 0.00001, energy = 79.074 ± 0.001. Details (after 7 refinements): Vertices: 197122 Edges: 590336 Facets: 393216 Facet edges: 1179648 Memory: 155824496.

Last 5 iterations:

5. area: 1.37550263992752 energy: 79.0739664075947 scale: 0.00165034

4. area: 1.37550269993565 energy: 79.0739632254390 scale: 0.00177063

3. area: 1.37550276488385 energy: 79.0739608643678 scale: 0.00168342

2. area: 1.37550284188095 energy: 79.0739589798044 scale: 0.00180932

1. area: 1.37550291632369 energy: 79.0739573941969 scale: 0.00171231

6) Results for Volume = 120 μL. Summary: surface area = 1.01988 ± 0.00001, energy = 93.270 ± 0.001. Details (after 7 refinements): Vertices: 197122 Edges: 590336 Facets: 393216 Facet edges: 1179648 Memory: 155824496.

Last 5 iterations:

5. area: 1.50988695002836 energy: 93.2703078607105 scale: 0.00168865

4. area: 1.50988697189052 energy: 93.2703027076679 scale: 0.00166880

3. area: 1.50988701597344 energy: 93.2702991886119 scale: 0.00164974

2. area: 1.50988707206697 energy: 93.2702966223684 scale: 0.00166427

1. area: 1.50988713644003 energy: 93.2702946524017 scale: 0.00165907

II. FOR LASER-ACTIVATION MODIFICATION OF SURFACES (LAMS)

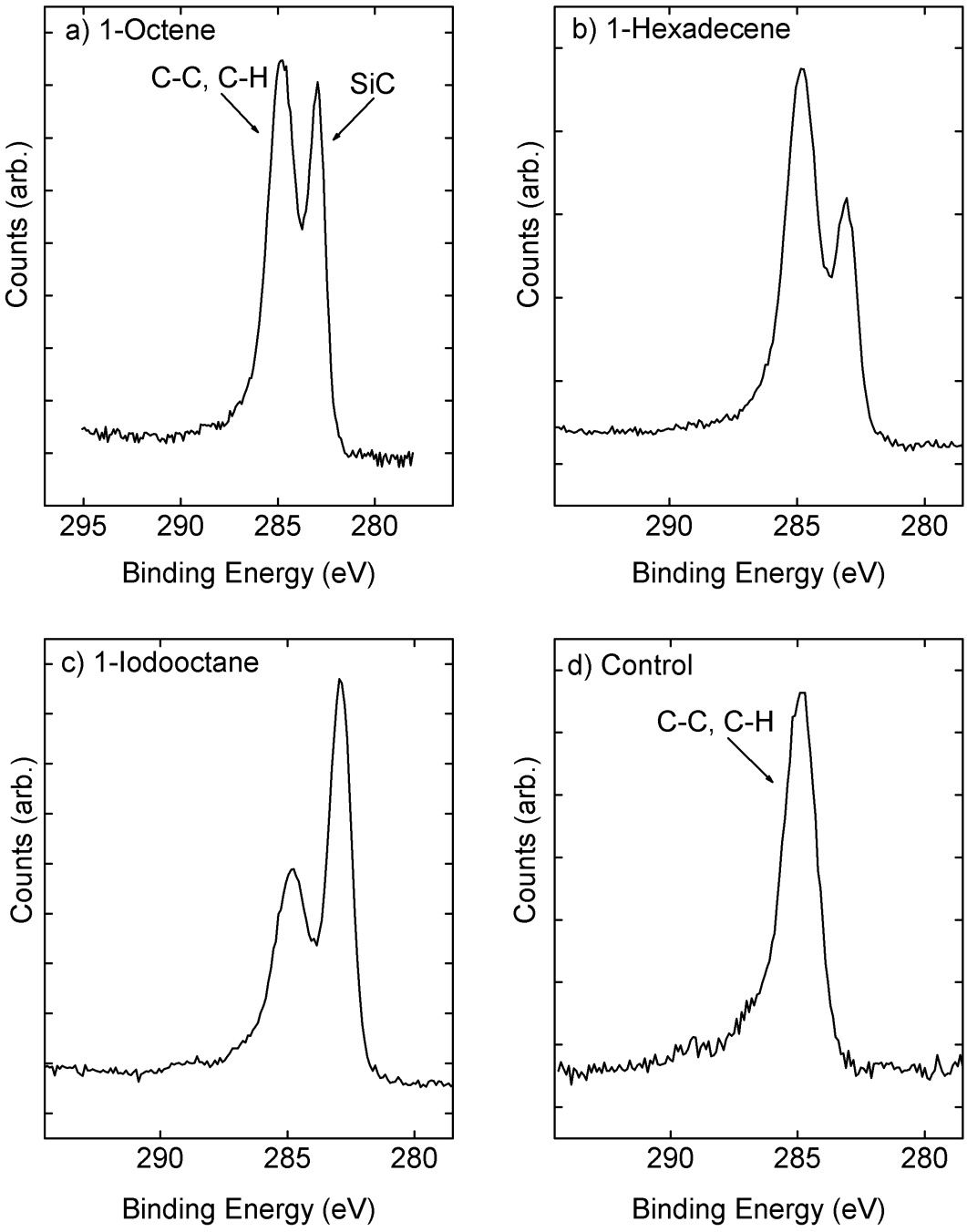

Figure 1. High-resolution C1s XPS spectra of LAMS of silicon with a) 1-octene, b) 1-hexadecene, c) 1-iodooctane, and d) a control surface that had been wet with 1-iodooctane but not irradiated (Taken by Greg Strossman at Charles Evans & Associates).

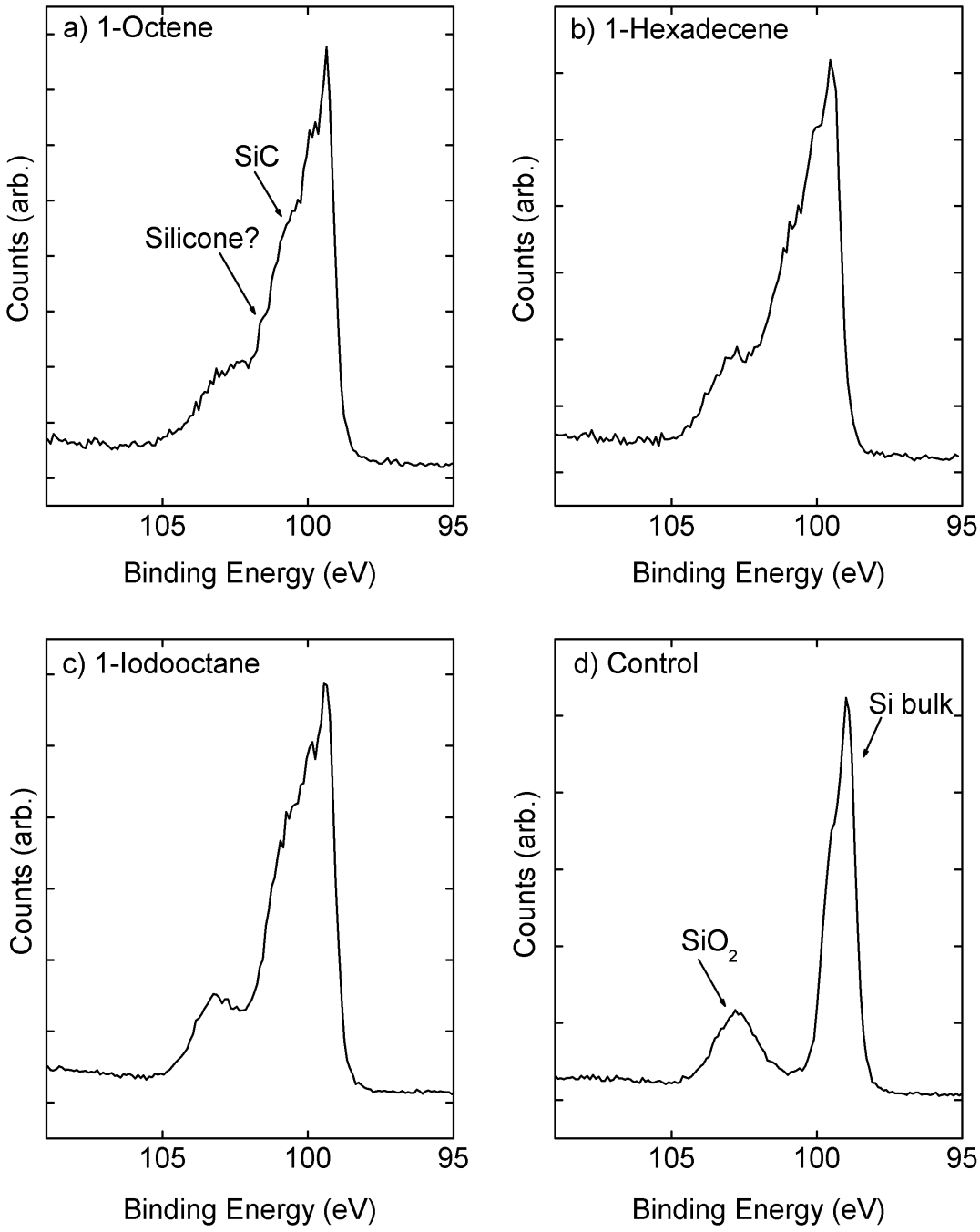

Figure 2. High-resolution Si2p XPS spectra of LAMS of silicon with a) 1-octene, b) 1-hexadecene, c) 1-iodooctane, and d) a control surface that had been wet with 1-iodooctane but not irradiated (Taken by Greg Strossman at Charles Evans & Associates).

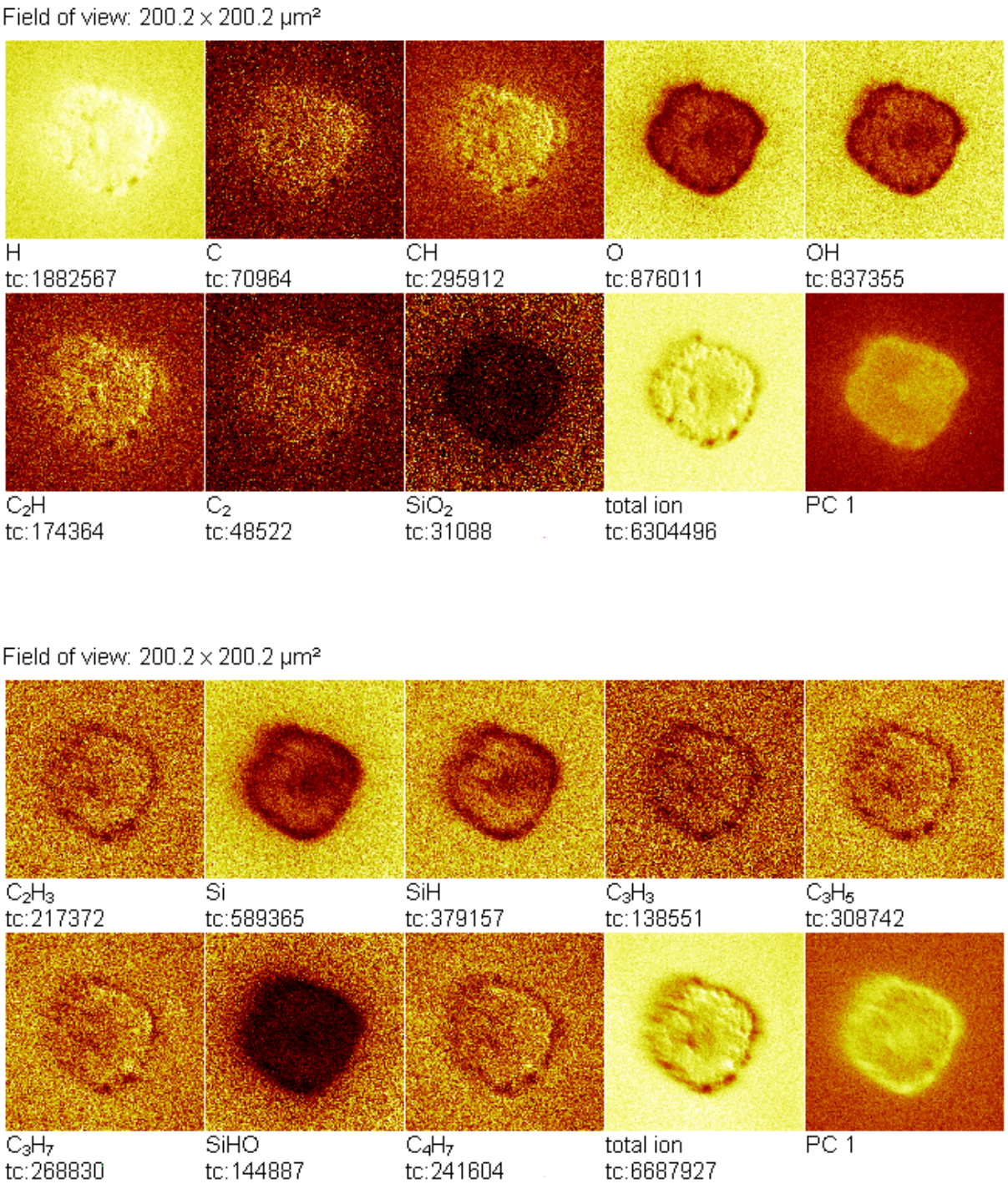

Figure 3. Negative- (upper) and positive- (lower) ion ToF-SIMS images of LAMS of silicon wet with 1-hexene.

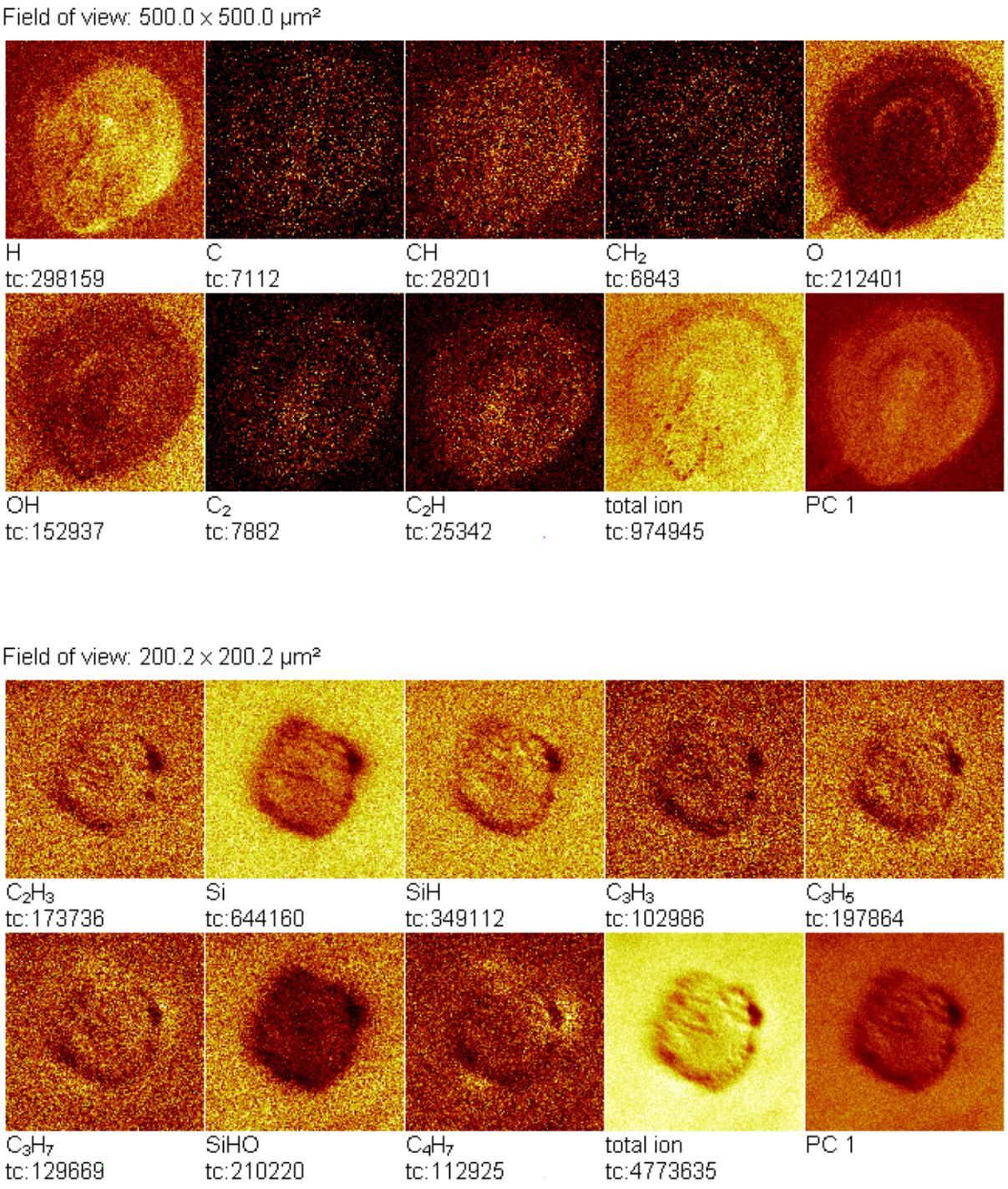

Figure 4. Negative- (upper) and positive- (lower) ion ToF-SIMS images of LAMS of silicon wet with 1-octene.

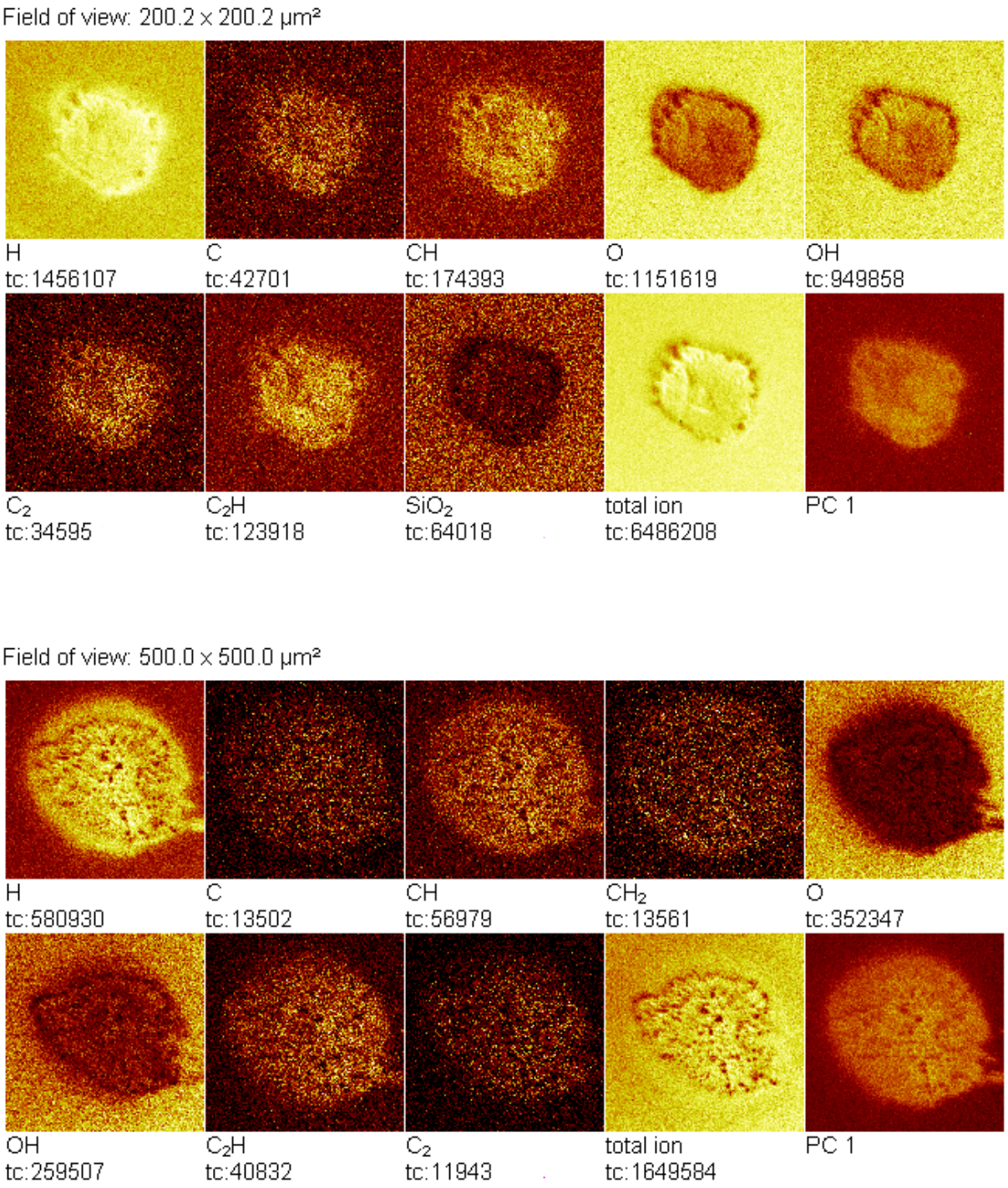

Figure 5. Negative-ion ToF-SIMS images of LAMS of silicon wet with 1-decene (upper) and 1-dodecene (lower).

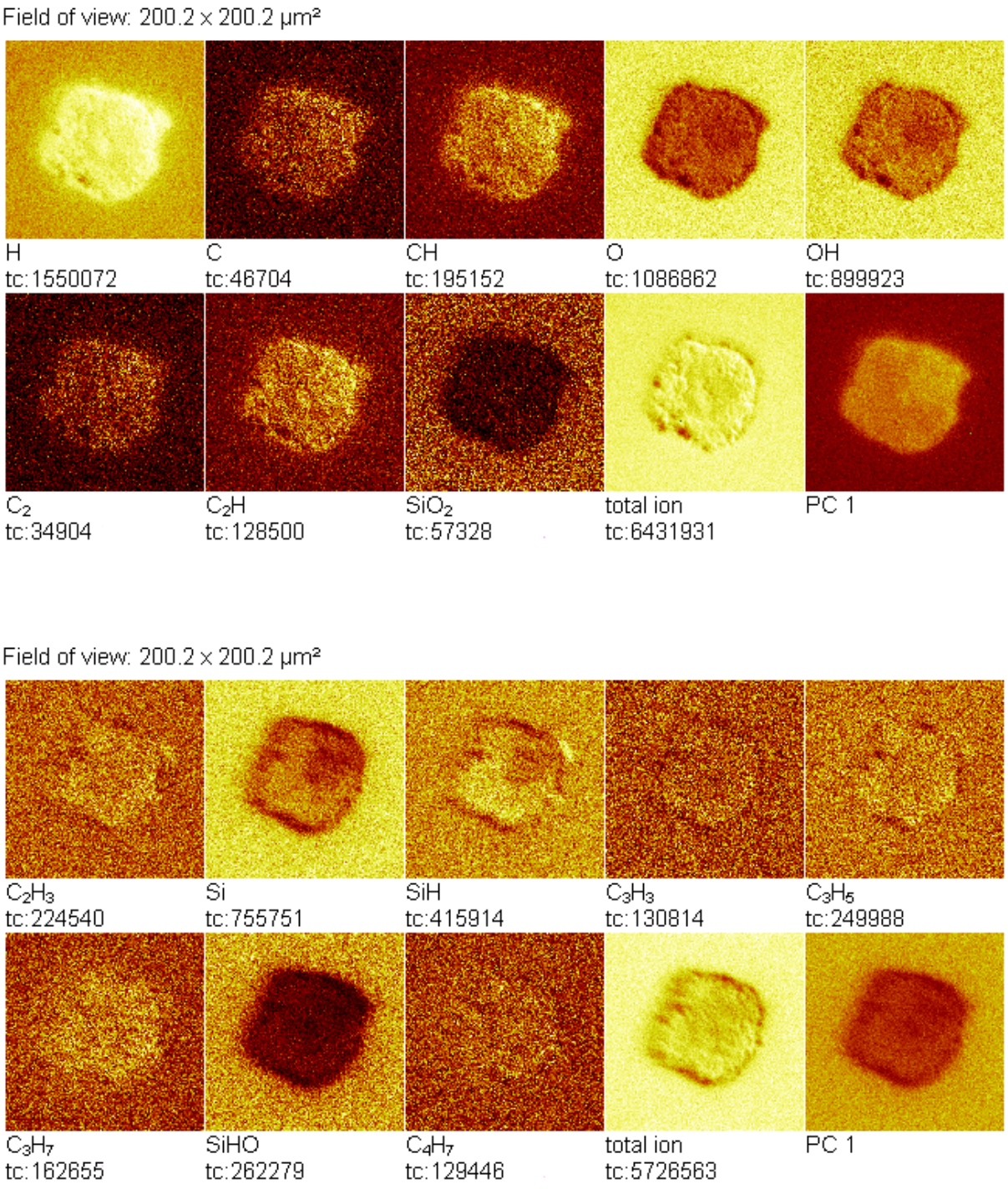

Figure 6. Negative- (upper) and positive- (lower) ion ToF-SIMS images of LAMS of silicon wet with 1-tetradecene.

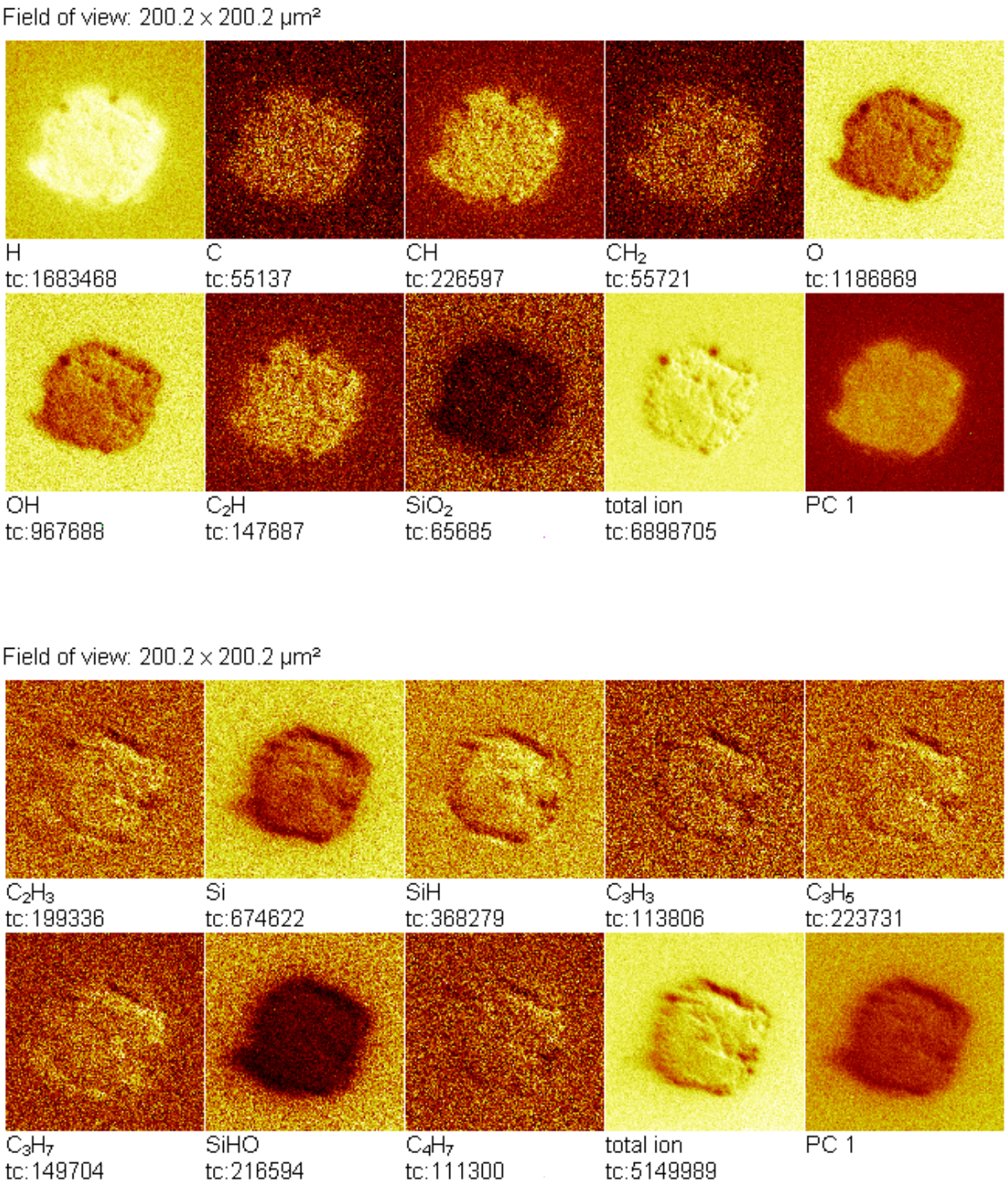

Figure 7. Negative- (upper) and positive- (lower) ion ToF-SIMS images of LAMS of silicon wet with 1-hexadecene.

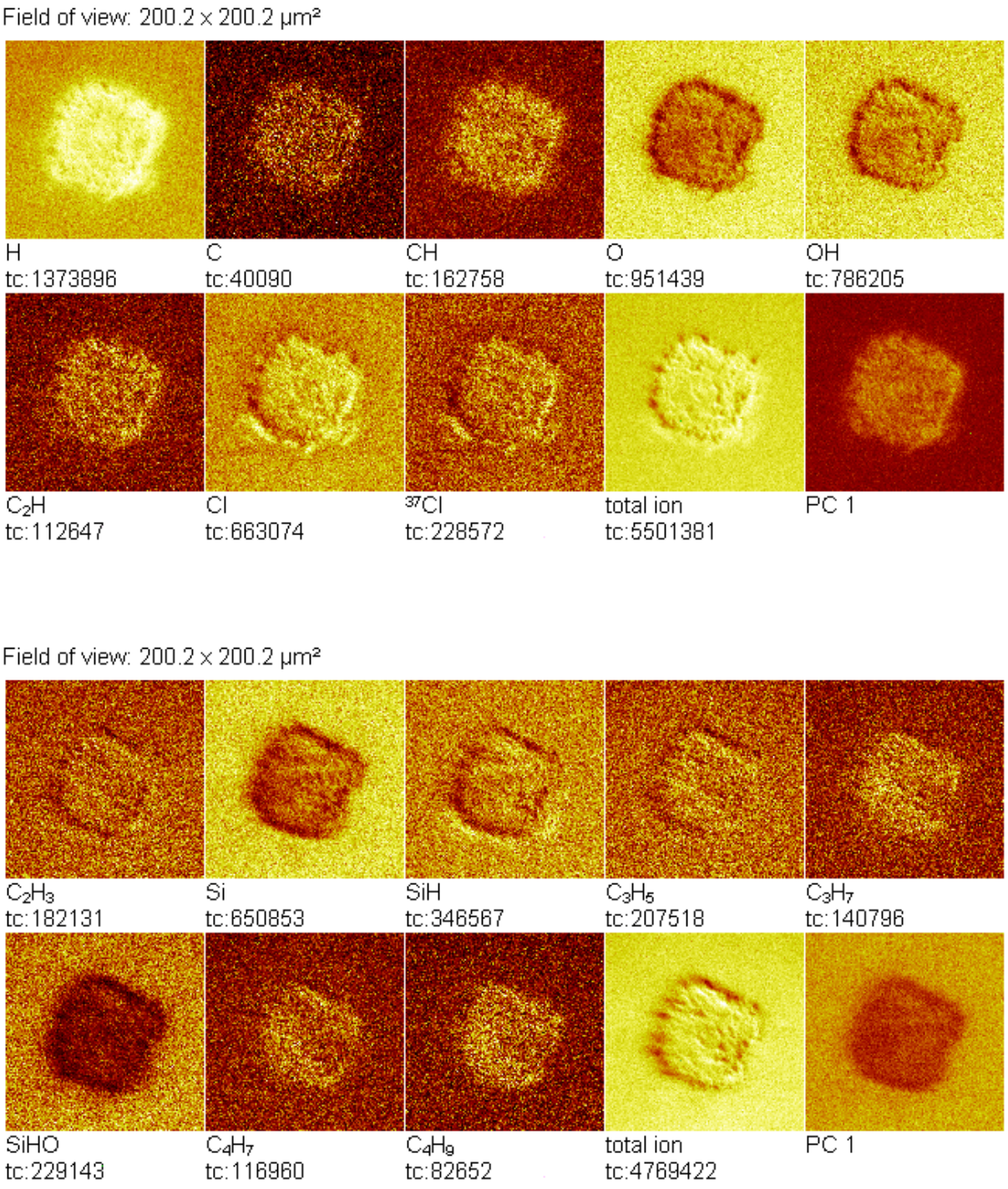

Figure 8. Negative- (upper) and positive- (lower) ion ToF-SIMS images of LAMS of silicon wet with 1-chlorooctane.

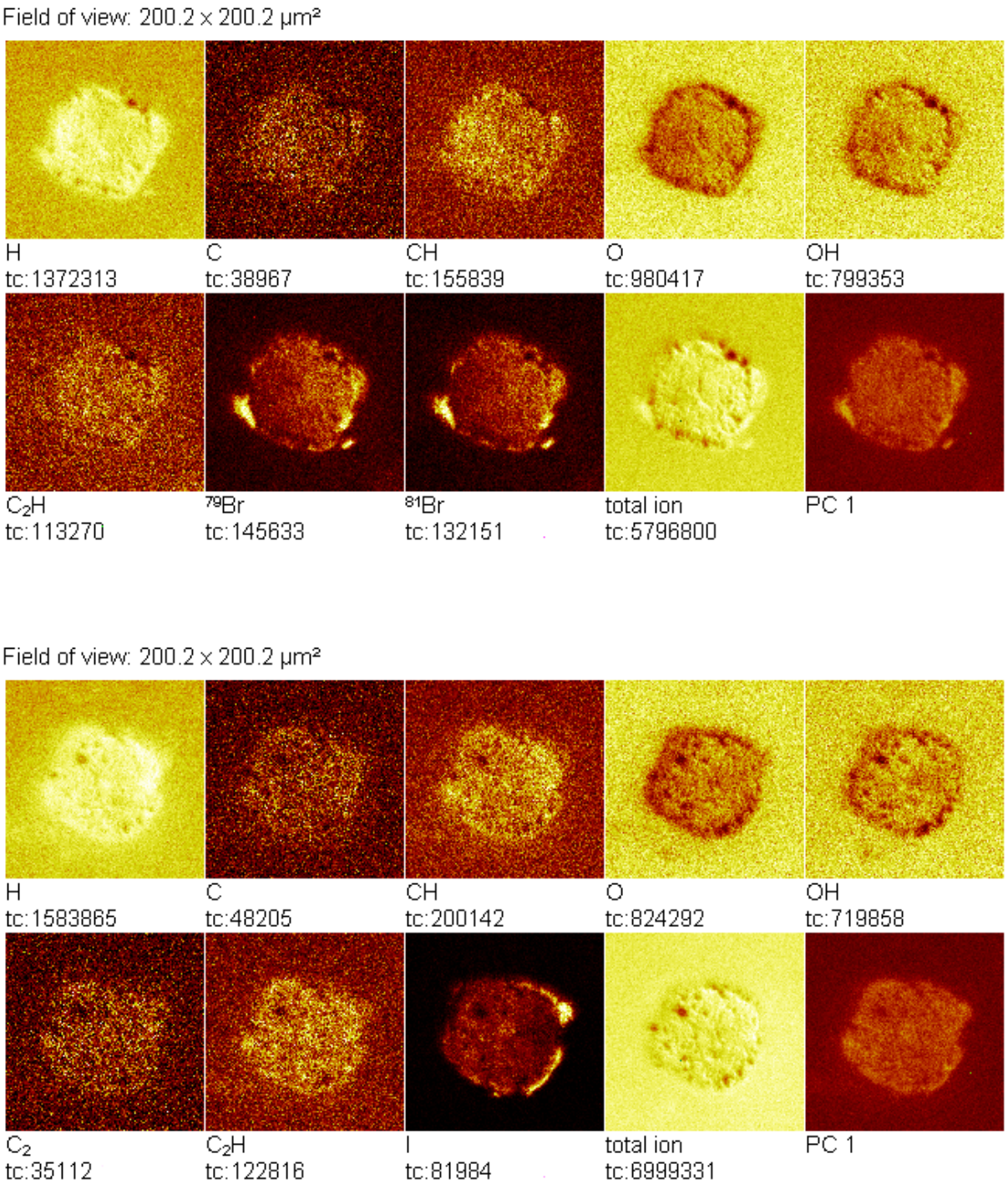

Figure 9. Negative-ion ToF-SIMS images of LAMS of silicon wet with 1-bromorooctane (upper) and 1-iodooctane (lower)

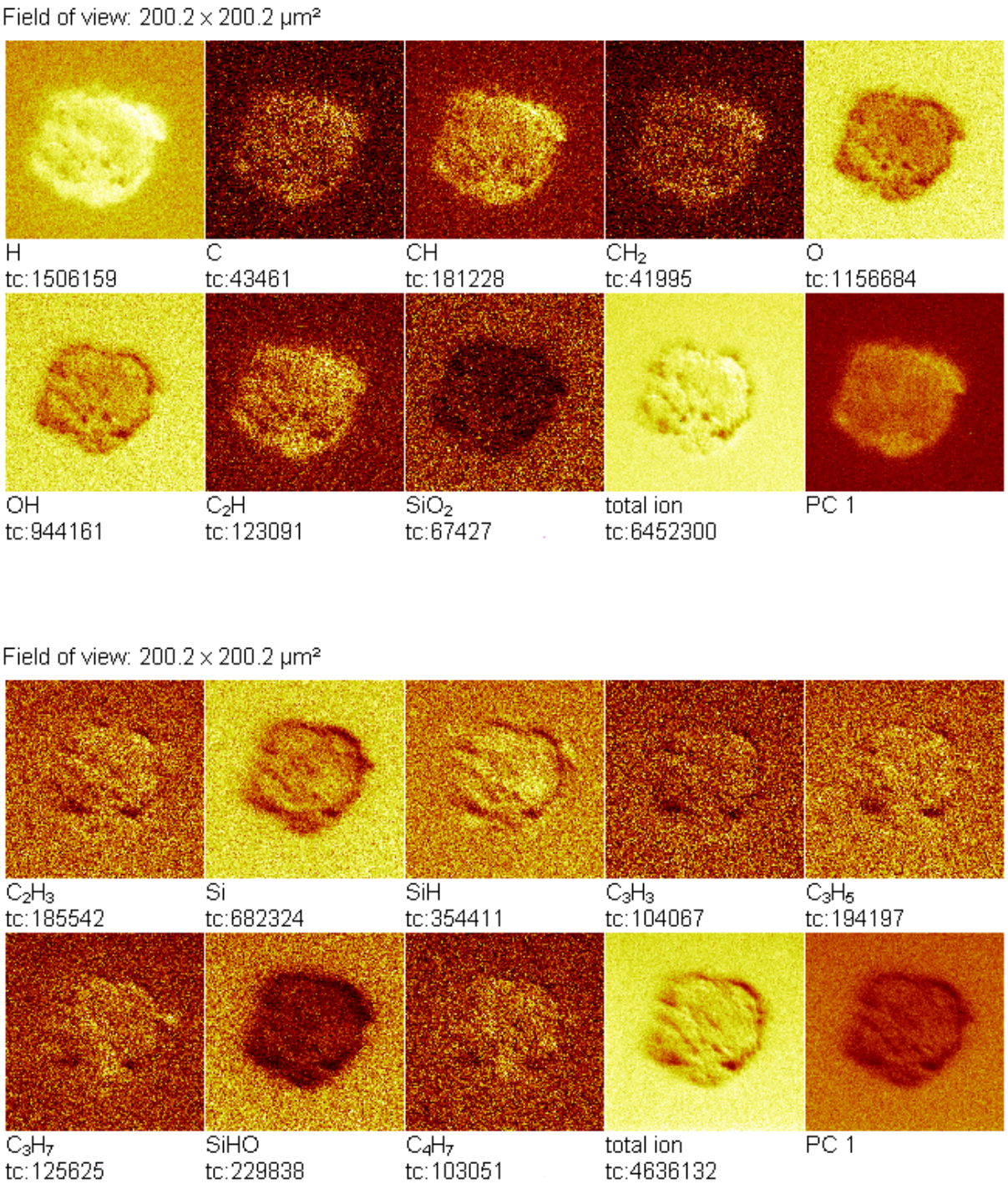

Figure 10. Negative- (upper) and positive- (lower) ion ToF-SIMS images of LAMS of silicon wet with 1,2-epoxyoctane.

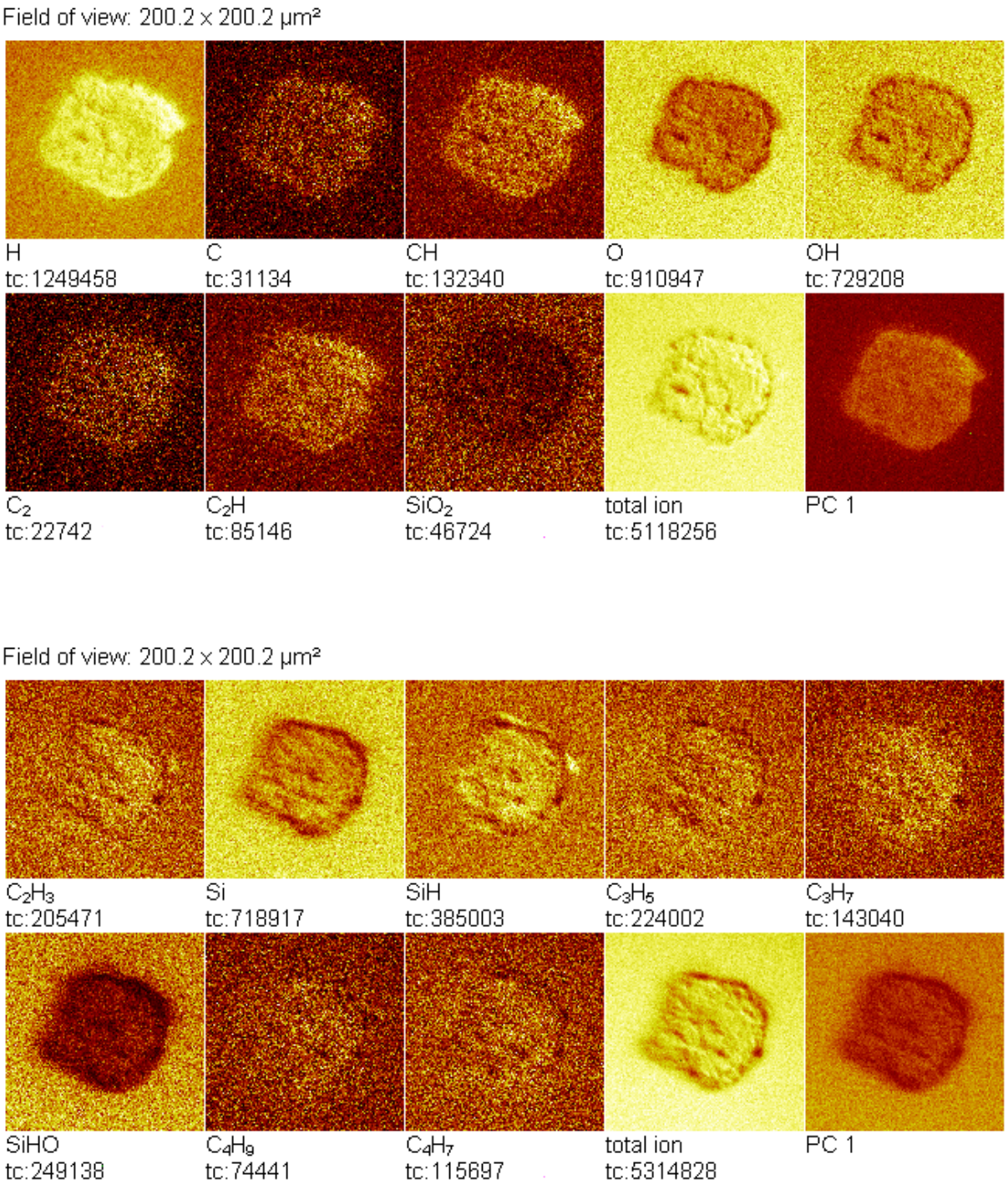

Figure 11. Negative- (upper) and positive- (lower) ion ToF-SIMS images of LAMS of silicon wet with 1-octanol.

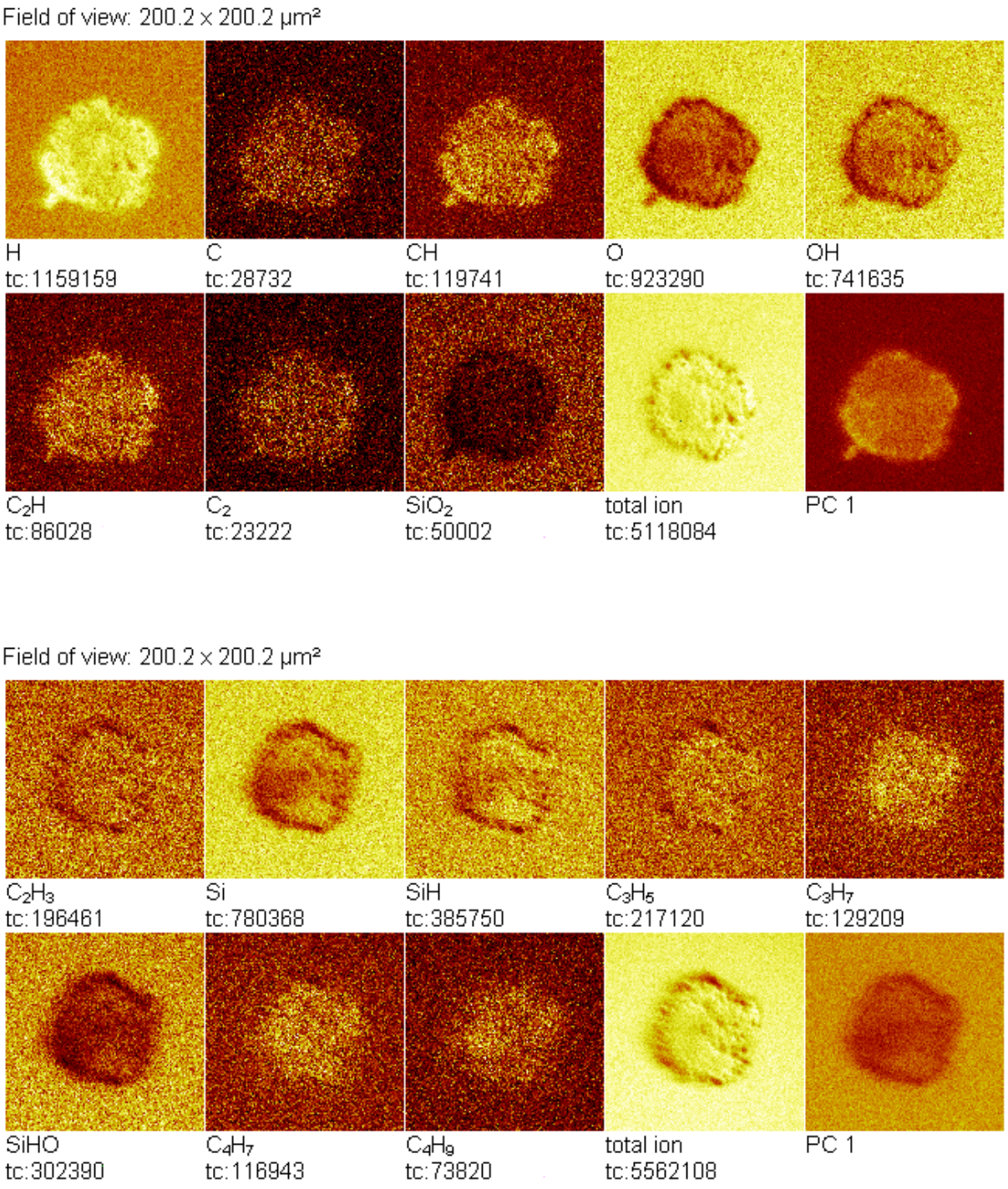

Figure 12. Negative- (upper) and positive- (lower) ion ToF-SIMS images of LAMS of silicon wet with octane. NOTE: The positive- and negative-ion images for the same reagents shown above are not necessarily from the same spot.

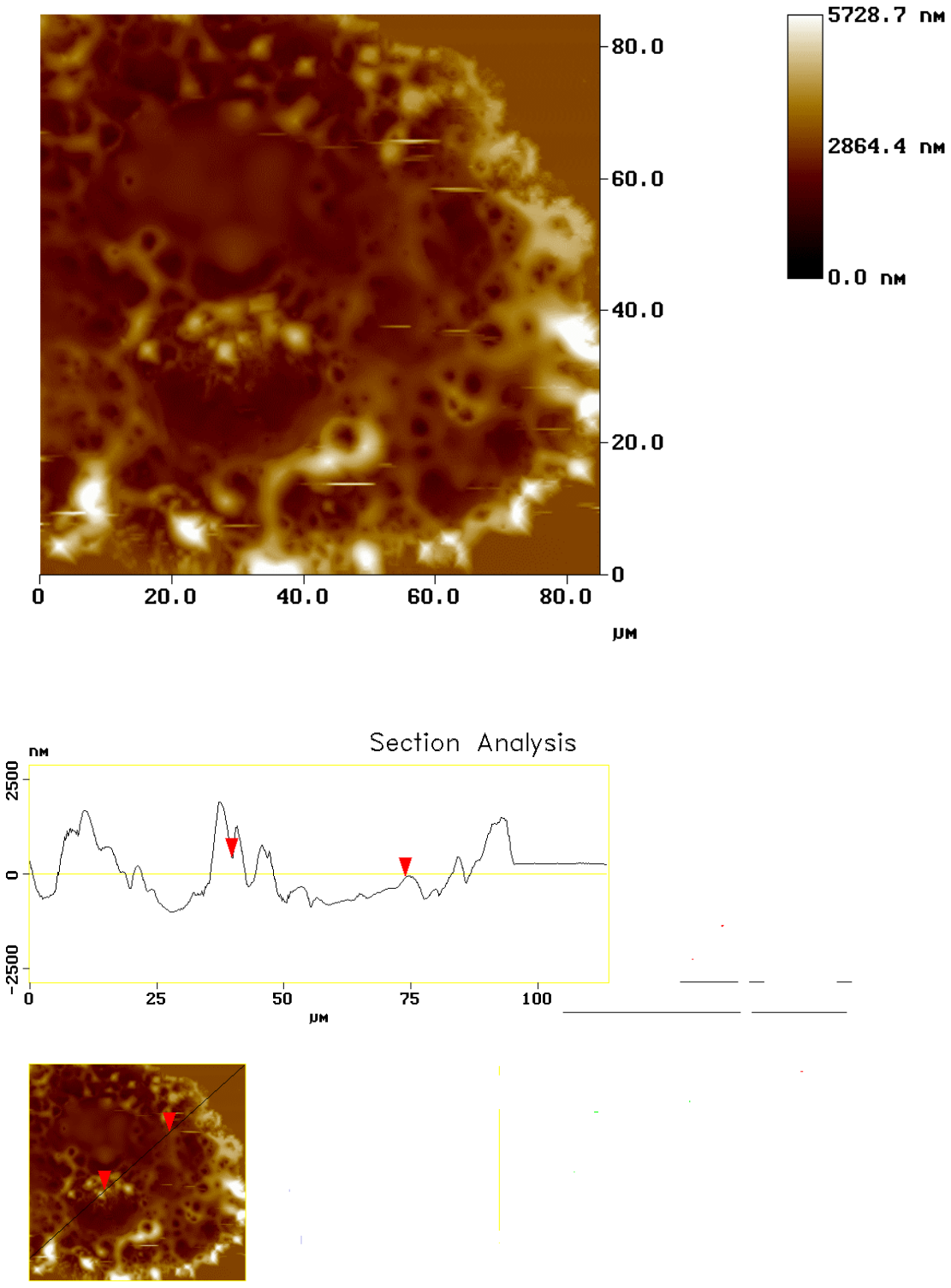

Figure 13. AFM contact mode height image of LAMS of silicon wet with 1-bromooctane.

Table 1: XPS Carbon curve fit summary (Data analysis by Greg Strossman at Charles Evans & Associates.).

	% Carbon seen as					
Sample	Si-C (carbide)	C-C, C-H	C-O	C=O	O-C=O	Si-C/ other C
1-Octene	34.5 ± 4.3	60.9 ± 3.0	3.9 ± 0.9	-	1.2 ± 0.2	0.52
1-Dodecene	33.9 ± 2.3	61.8 ± 2.5	4.2 ± 0.2	-	-	0.51
1-Hexadecene	26.4 ± 1.9	67.7 ± 2.4	4.4 ± 1.3	-	1.5 ± 0.4	0.36
1-Iodooctane	47.8 ± 1.2	46.3 ± 2.1	4.0 ± 0.6	-	1.9 ± 0.4	0.92
1-Hexadecene (blank)	-	83.7 ± 1.8	8.3 ± 0.1	1.7 ± 0.4	6.4 ± 1.6	0
1-Iodooctane (blank)	-	78.2 ± 1.3	10.3 ± 1.4	7.3 ± 0.8	4.2 ± 0.8	0

Table 2: XPS silicon curve fit summary

	% Silicon seen as			
Sample	Elemental Si	Si-C (carbide)	Silicone(?)	SiO_2
1-Octene	46.3 ± 4.9	30.7 ± 3.8	13.7 ± 1.4	9.4 ± 0.3
1-Dodecene	46.4 ± 1.5	31.4 ± 2.8	12.5 ± 2.5	9.7 ± 2.0
1-Hexadecene	47.7 ± 2.0	30.6 ± 1.5	16.0 ± 0.3	5.7 ± 1.2
1-Iodooctane	47.9 ± 3.0	28.3 ± 2.8	10.3 ± 0.3	13.6 ± 0.3
1-Hexadecene (blank)	75.3 ± 0.4	-	3.3 ± 0.1	21.5 ± 0.5
1-Iodooctane (blank)	75.7 ± 0.6	-	3.3 ± 0.8	21.1 ± 0.2